

Fallon, Ciara (2025) Estimating the glacial valley fill of the north-west Greater Caucasus Mountains using artificial neural networks. MSc(R) thesis.

https://theses.gla.ac.uk/85601/

Copyright and moral rights for this work are retained by the author

A copy can be downloaded for personal non-commercial research or study, without prior permission or charge

This work cannot be reproduced or quoted extensively from without first obtaining permission from the author

The content must not be changed in any way or sold commercially in any format or medium without the formal permission of the author

When referring to this work, full bibliographic details including the author, title, awarding institution and date of the thesis must be given

Enlighten: Theses
<a href="https://theses.gla.ac.uk/">https://theses.gla.ac.uk/</a>
research-enlighten@glasgow.ac.uk

# Estimating the Glacial Valley Fill of the North-West Greater Caucasus Mountains Using Artificial Neural Networks

### Ciara Fallon

Submitted in fulfilment of the requirements of the degree Master of Science (Research)

School of Geographical and Earth Sciences,

College of Science and Engineering,

**University of Glasgow** 

### **Abstract**

Glaciation and subsequent glacier retreat has resulted in unknown quantities of sediments being stored in valleys throughout the Greater Caucasus Mountains. It is difficult to estimate the quantity of this sediment fill as a result of there being no direct measurements of the thickness of these sediments. In this study, valley cross-sections are extracted from a catchment area in the western Caucasus using a DEM. Training data comprised of valley widths and sediment depth estimates is obtained from these cross-sections based on assumptions about the geometry of glacially eroded valleys. This training data is used to train an artificial neural network to create a model which can be used to estimate sediment depths and associated volumes in other valleys in the Caucasus. This model was then applied to other valleys that were found to show evidence of glacial sediment fill. A volume of  $42.05 \pm 1.01 \text{ km}^3$  is found from a combination of 7 valleys in the north-western and central part of the Caucasus which corresponds to a total mass of  $8.83 \times 10^{13} \pm 8.67 \times 10^{12}$  kg. The individual results from each valley showed that there is a relationship between the average width of the valleys and the maximum depth of sediment found within them. The results also highlighted that there are parts of the valleys that do not show evidence of glacial fill where they may be expected to. This presents implications for the glacial processes that impact the location of this sediment fill such as glacier motion and glacial erosion. The quantity and distribution of these sediments also have implications for isostatic adjustment associated with glacial retreat in the Caucasus as they demonstrate how mass has been transferred away from the mountains, which can contribute to the surface uplift resulting from ice mass loss.

## **Table of Contents**

Abstrac	et	2
List of	Tables	6
List of	Equations	7
List of	Figures	8
Acknow	wledgments	10
Author	Declaration	11
1. In	troduction	12
1.1.	Rationale and significance	13
1.2.	Aims and Objectives	14
1.3.	Methodology	14
1.4.	Glacial history	15
2. Back	kground	17
2.1.	Greater Caucasus Mountains	17
2.	1.1. Western Caucasus	17
2.	1.2. Central Caucasus	18
2.	1.3. Eastern Caucasus	18
2.	1.4. Climate	19
2.	1.5. Geomorphology	22
2.2.	Glaciation and Glacial History	23
2	2.1. Pleistocene	23
2	2.2. Holocene	24
2.2	2.3. Recent changes (LIA to present)	26
2.3.	Sediments and Glacial Processes	26
2	3.1. Overview	26
2	3.2. Glaciers and glacier motion	27
2	3.3. Glacial erosion	29
2	3.4. Sediment transport	30
2	3.5. Glacial sediments and deposition	31
2.4.	Alternative sediment sources	32
2.5.	Glacial Retreat and Isostasy	33
2.:	5.1. Glacial retreat	33
2.:	5.2. Isostasy	33

	2.6. Glacial valley fill prior research	35
3	. Methodology	38
	3.1. Artificial Neural Networks (ANNs)	38
	3.1.1. Background	38
	3.1.2. Training the ANN	39
	3.2. Study area	40
	3.3. Data collection	42
	3.3.1. Approach 1: parabola assumption	45
	3.3.2. Approach 2: artificial fill	47
	3.4. Linear regression.	48
	3.5. Model development and progression	49
	3.6. Model application and volume calculation	53
	3.6.1. Error calculations and propagation	56
4	. Results	59
	4.1. Conversion to sediment weight	63
5	. Discussion	64
	5.1. Key results and results context	64
	5.2. Uncertainties	66
	5.3. Result Implications	68
	5.3.1. Relationship between valley width and volume	68
	5.3.2. Valleys without evidence of glacial fill	68
	5.3.3. Exclusion of tributary valleys	70
	5.4. Formation of glacial eroded valleys	71
	5.5. Sediment origin assumption.	74
	5.6. Implications for glacial isostatic adjustment (GIA)	75
	5.6.1. Sediment mass estimate	75
	5.6.2. Weight distribution	76
6	. Conclusions and Future Work	78
	6.1. Conclusions	78
	6.2. Future work	78
A	ppendix A: Swath profiles	80
A	ppendix B: Hillslope distance and sediment depth tables	92
	Valley 1	92

Valley 2	93
Valley 3	94
Valley 4	95
Valley 5	96
Valley 6	98
Valley 7	
References	100

## **List of Tables**

Table 1 – showing valleys where method was applied to with their calculated volumes and	
corresponding geometries. NW refers to the valleys found in the north-western Caucasus, an	d
NC to valleys in the north-central Caucasus. $-6$	50
Table 2 - Showing sediment fill volumes for other glaciated regions with supporting data	
where applicable ( <sup>2</sup> Aarseth, 1997; <sup>3</sup> Hinderer, 2001 and Mey et al., 2015; <sup>4</sup> Syvitski et al.,	
2022; <sup>5</sup> Pomper et al., 2017)6	55

# **List of Equations**

Equation 1 – Adaptation of formula for the volume of a truncated ellipse	54
Equation 2 – Formula for propagating absolute error of a (distance from hillslope) and b	
(sediment thickness)	57
Equation 3 – Formula for calculating sediment weight from density and volume	57
Equation 4 – Formula for the calculation of error for mass estimation.	58

# **List of Figures**

Figure 1 - Map showing location of the GCM bounded by the Black Sea to the west and
Caspian Sea to the east
Figure 2 - Glacial extent in the Late Pleistocene (Gobejishvili et al., 2011). The darkest blue
colour indicating the 2011 extent of glaciation found in the Caucasus. Note key peaks (i.e. Mt
Elbrus) and altitude of maximum glacial extent down valley24
Figure 3 - Diagram illustrating the mechanism of GIA as ice retreats on a mountain range. Ice
cover over a mountainous region will contribute further to subsidence into the mantle,
resulting in subsequent uplift when this ice melts34
Figure 4 - Basic structure of an ANN comprising inputs, a hidden layer and an output adapted
from Mey et al., (2015)
Figure 5 - Workflow for training the ANN with reminder of simple ANN structure40
Figure 6 – Map showing location of study catchment area to the northwest of Mt Elbrus
within the GCM41
Figure 7 - a) NW Elbrus region and study catchment DEM – note red high elevation area to
be Mt Elbrus. b) NW Elbrus region and study catchment Satellite imagery41
Figure 8 - a) showing an example of a characteristic U-shaped glacially eroded valley in the
GCM (Potopalski, 2017) and b) showing an example of a characteristic V-shaped fluvially
eroded valley in the GCM (Fedorov, 2022). Note the more shallowly sloping valley walls and
broad flat valley floor in a) compared to the steep sided valley in b)42
Figure 9 - Showing location of swaths plotted throughout the principal valleys of the study
area
Figure 10 - Representative examples of swaths of varying shapes and their locations
throughout the study valley. Note c) Swath 65 being approximately V-shaped and its location
very high up in the valley. Note a) and b) having the characteristic sloping slides of a u-
shaped valley with a mostly flat and level valley bottom
Figure 11 - a) plot showing representative swath from study valley with a well-fit parabola
projection plotted and inferred valley fill shown shaded in purple and b) a representative
swath with a poorly fit parabola that does not project below the valley floor46
Figure 12 - Example swath showing artificial fill amount and positioning with respect to the
valley floor
Figure 13 - Plots of linear regression models produced from the parabola (left) and artificial
fill training data (right) approaches. Note variations in axis and therefore in gradient of
prediction line
Figure 14 - Plot showing ANN model prediction produced from parabola approach training
data, including training dataset, root mean square error (RMSE) window50
Figure 15 - Plot showing ANN model prediction produced from artificial fill approach
training data, including training dataset, root mean square error (RMSE) window51
Figure 16 - Plot showing ANN model prediction produced from the combination of training
data from the parabola and artificial fill approaches, including training dataset, root mean
square error (RMSE) window

Figure 17 - Plot showing 2 <sup>nd</sup> version of ANN model prediction using parabola approach
training data, including training dataset, root mean square error (RMSE) window53
Figure 18 - Diagram showing half ellipse formula applied in the context of the valley
structure with respective hillslope distance (a) and sediment thicknesses (b) shown54
Figure 19 - Flow chart showing workflow used to extract hillslope distance values from
valleys using ArcGIS55
Figure 20 - Map showing location of valleys extracted from the NW and NC Caucasus shown
as red polygons. Valleys used for training data (1 and 2) are shown outlined in the red box59
Figure 21 - Graph showing with volume of each transect and its corresponding valley width
for each valley, demonstrating that the transect volume increases linearly with valley width .
61
Figure 22 - Graph showing the total volume of each valley against average valley width 62
Figure 23 - Graph showing total volume of each valley against valley length62
Figure 24 - Showing locations of swaths throughout training catchment which did not show
evidence of glacial sediment fill. Note that there is a combination of swaths located high up
in the valley as well as further down the valley and at similar latitudes to swaths that did
display evidence of glacial sediment fill
Figure 25 - Map showing valleys used for volume calculation with some valleys not included
highlighted by blue boxes

## **Acknowledgments**

My first thanks go to my supervisor Dr Paul Eizenhöfer. His support and guidance throughout my Masters has been invaluable and it has been a privilege to work with him and learn from him. I have found this Masters incredibly rewarding but at times incredibly tough, facing challenges both academically and in my personal life, throughout which I have always been met with compassion and I thank Paul for bearing with me throughout this process. Thank you to my secondary supervisor Dr Iain Neill for his feedback on writing and his shared pain of researching an area that is relatively understudied compared to others. I am also very grateful for the Landscape Evolution group set up by Paul. Especially to Dr David Oakley for his assistance in all things coding and maths and for being patient with admittedly frequent need to repeated explanations. But also to Dr Sarah Falkowski, Dr James Gilgannon, and Chang Zhong for their advice and for always listening to my problems and presentation rehearsals in our meetings. On the same vein, I am grateful to all the other staff and researchers within the School of Geographical and Earth Sciences who made me feel welcome in the research clusters and were always enthusiastic about my research and contributions.

Thank you to my friends for their support throughout this process. To Kimberley, I am eternally grateful to you for having someone to share this process with, the occasional high and the many lows. To Sophie, Emma, Lisa, and Liv, thank you for putting up with both me and Kimberley throughout with our many rants and complaints and for always being a source of unwavering belief and encouragement. To Nat, Selena, Anna, Anna, and Abby, firstly apologies for hardly ever being available to last two years so thank you for being so understanding and for working around my schedule. To all my friends and colleagues at Costa, thank you for distracting me at work and always supporting me and making me laugh when I have been struggling.

I also need to thank my family; to my parents and Emily, I will never forget the love and support you have given me throughout, when this process has felt endless you have always been there for me in any way that I have needed. To Barbara and Tim, I am so grateful to your for the love and support and fun you bring to my life. To the many pets in my life who always provide a welcome distraction: Luigi, Pia, Jessie, Smilla, Snorri, Junie, Eddie, Lotte, Pablo and now Alice, Ladybug, Mo, and Lucy. To Else, I miss you.

Lastly, to Ben. I could not have done this without you so this is dedicated to you.

## **Author Declaration**

I declare that, except where explicit reference is made to the contribution of other authors, that this thesis is the result of my own work and does not include work submitted for any other degree at any institution.

Ciara Fallon

## 1. Introduction

Glacial retreat in mountainous regions has profound impacts on the local and wider geomorphology of the catchment area ranging over years to 10s of thousands of years. Intermontane valleys in presently or previously glaciated areas are often characterised by a 'Ushape' and are dominated with glacially eroded sediments (Anderson et al., 2006). Such intermontane valleys can be found in glaciated mountain regions worldwide. The Greater Caucasus Mountains (GCM) (see Figure 1) form the natural border between southern Russia and Georgia and Azerbaijan, stretching from the Black Sea in the west to the Caspian Sea in the east. This thesis will focus on the northern part of the GCM located wholly within Russia, with what will be referred to as the 'southern' GCM being the part of the mountain range within Georgia and Azerbaijan. As with other mountainous regions across Europe, they have hosted significant glaciation within the Holocene and ~1400 glaciers are still present at the highest altitudes, mostly between 3000 m and 4000 m (Solomina et al., 2024). This study aims to estimate the volume and distribution of glacial sediment fill in intermontane valleys within the GCM. This will be done by generating a data set of valley widths and estimated sediment fill from swath profiles throughout a chosen catchment area and then using this data to train an artificial neural network (ANN) to be applied to a larger area of the GCM.

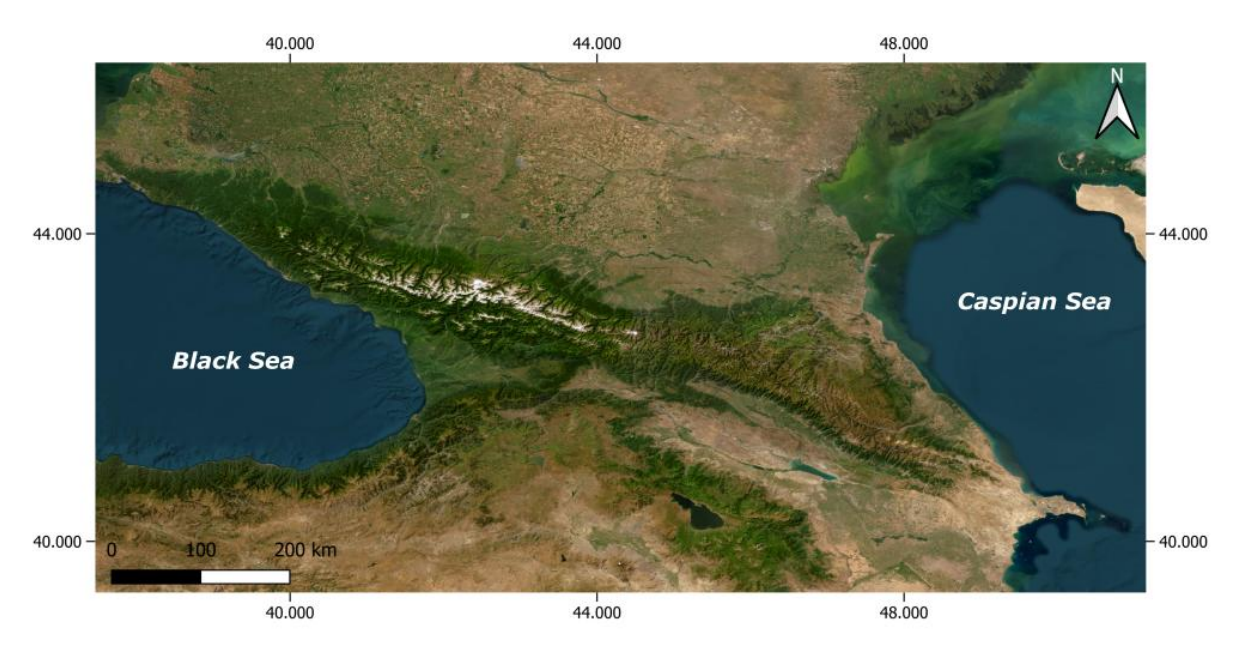


Figure 1 - Map showing location of the GCM bounded by the Black Sea to the west and Caspian Sea to the east.

#### 1.1. Rationale and significance

This research is significant for several reasons relating to both societal implications and the contribution to geomorphological research. Firstly, the populated areas of mountainous regions normally occupy the sediment-covered valley floors (Met et al., 2015); this is the case throughout the valleys of the GCM. The sediment fill distribution is therefore of relevance to the residents of these population centres due to the applications the sediments can have. For example, they can host aquifers and be necessary for agriculture (Margat and van der Gun, 2013). They can also be linked to extreme mass transport events such as debris flows and glacial lake outburst floods (GLOFs), where these sediments can be mobilised and swept through the valleys (Vezzoli et al., 2020). This is something of increasing relevance in the GCM where such events are increasing as a result of enhanced warming and glacial retreat (Seinova et al., 2007). This means that it is important to understand how sediment fill can be distributed throughout valleys in order to more accurately evaluate risk from mass transport events in the GCM and other similar regions globally. Part of the rationale behind this study was to work towards a larger research project aiming to gain insight into the isostatic rebound associated with glacial retreat in the Caucasus. However, in order to achieve this there is a significant amount of research needed into the geomorphology of the mountains since the Last Glacial Maximum (LGM) in order to begin to investigate any isostatic readjustment. This study will act as the first step within this bigger potential research project as it would be necessary to establish how much sediment has been eroded from the mountains. This would allow for the reconstruction of the mountains at the LGM so that their crustal load could be calculated prior to ice melt and rebound. It is important that the rate and impacts of this isostatic adjustment is understood as it can happen at rates of up to 10 mm a<sup>-1</sup> making it observable in human timescales (Whitehouse, 2018). The direct impacts include significant changes in relative sea level (up to around 100 m) and deformation of the surrounding crust occurring on the timescale of only tens of thousands of years (Whitehouse, 2018). Overall, this highlights how this study can contribute to a much greater, more significant piece of research, with much more farreaching impacts. Lastly, quantifying the sediment fill in mountain valleys contributes to the overall understanding of long-term sediment budgets and erosional changes over long-term geological timescales (Straumann and Korup, 2009).

#### 1.2. Aims and Objectives

The main aim of this study is to establish the quantity and distribution of valley sediment fill in the GCM. There are two primary research questions that will be addressed in this thesis:

- 1. What is the total quantity of glacially eroded sediments from the last glaciation filling an area of the GCM.
- 2. How does glacial sediment fill vary across valleys in the GCM?

These will be achieved by fulfilling three main objectives:

- 1. Undertake a thorough topographical analysis of a chosen valley extracted from DEM data in TopoToolbox.
- 2. Use the valley widths and sediment thicknesses obtained from this analysis to train an ANN to estimate valley sediment fill.
- 3. Use the trained ANN to estimate valley fill thicknesses across a wider area of the GCM.

#### 1.3. Methodology

There have been numerous attempts in previous studies to estimate sediment storage in mountain ranges using a variety of techniques. Blöthe and Korup (2013) used volume-area scaling in order to estimate sediment storage in the Himalayas. Similarly, Straumann and Korup (2009) established a method to quantify sediment storage and distribution over a large area of the Alps. These papers both apply methods utilising DEM-derived data with empirically based scaling in order to estimate sediment volumes on a large scale. There have also been numerous studies focused around obtaining sediment fill estimates on smaller scales which are supported by direct geophysical measurements such as seismic surveys or well data (e.g. Hinderer, 2001; Otto et al., 2008; Schrott et al., 2003). Problems with the oversimplification of natural systems and the inability to obtain accurate valley fill estimates without the input of direct measurements in previous studies were identified by Mey et al. (2015). From this, they applied a new method adapted from glacial bed topography and ice volume estimation using artificial neural networks (ANN) (Clarke et al., 2009). An ANN is a model containing inputs and outputs and a number of hidden layers containing nodes in between. They are trained using established data with a known input and output, so that they can be used to produce estimates for unknown outputs. Mey et al. (2015) applied this method of estimating fill thicknesses using ANNs in the Alps where the results could be validated and supported by direct fill measurements. Therefore,

having proven that this method works with good results, a similar approach was applied to the GCM where there are not direct measurements to use as a comparison.

The first part of this study involved the generation of a data set of valley geometries including maximum valley widths and estimated sediment depths from a principal catchment area within the GCM. This data set was comprised from swaths throughout the valley plotted from DEM data in the Matlab add-on, TopoToolbox. The catchment area was chosen based on its size and position in the centre of the GCM beside Mt Elbrus – the highest point of the mountain range at 5642m. This was to ensure that there would definitely be useable sediment fill data due to its proximity to still active glaciation and the highest altitudes where past ice accumulation has been the highest (Solomina et al., 2024). A data set of distance from hillslope and maximum sediment depth estimates were extracted from the swaths to be used to train the ANN as defined inputs and outputs respectively. Once trained, hillslope distance values from other valleys could then be inputted into the ANN model to produce sediment thickness estimates as outputs. These sediment thicknesses could then be used in conjunction with valley geometry data to estimate a volume and mass of sediment fill within valleys in the GCM. The execution of this method therefore comes with a reasonable level of uncertainty due to the assumptions and estimations involved in establishing the ANN which are then extrapolated across a larger area.

#### 1.4. Glacial history

Compared to other major European mountain ranges, such as the Alps, there is a significant lack of research relating to the glacial history and geomorphology of the Caucasus mountains. The increasing awareness globally of the rate of glacial retreat in mountainous regions and its implications has resulted in an uptick of research focused on more recent retreat in the GCM i.e. in the last several hundred years (e.g. Stokes et al., 2007; Shahgedanova et al., 2014; Tielidze et al., 2025). Several researchers have endeavoured to investigate the past glaciation in the GCM in more detail but poorly preserved glacial landforms often present challenges in clearly dating advance and retreat in this region. (e.g. Gobejishvili et al., 2011; Solomina et al., 2024). What is currently known about the glacial history of the northern part of the GCM (where the study area is located) mostly relies on dating from specific landforms and sediments within certain valleys such as <sup>14</sup>C dating of buried deposits or <sup>10</sup>Be dating of exposed sediments (Solomina et al., 2024). As with other regions, glaciation in the Caucasus has been following a general retreat trend throughout the Holocene with some more notable readvances 7.0-6.6 ka BP, and during the Little Ice Age (LIA) in the 13<sup>th</sup>-19<sup>th</sup> centuries (Solomina, 2000; Solomina et

al., 2024). Since the end of the LIA, glaciers in the GCM have been retreating with an average observed ice loss of ~50% (Tielidze et al., 2025).

Across the entirety of the Caucasus, more than 2000 glaciers still remain, of which ~1400 are in the northern Caucasus but they are in steady decline (Stokes et al., 2007; Solomina, 2000; Solomina et al., 2024). The glacial retreat in the GCM has left significant quantities of glacial sediments and landforms within the valley networks (Gobejishvili et al., 2011). Glacial retreat is still occurring on a large scale here and on average, the area of glaciers in the GCM decreased by 18% between 1986 and 2014 (Solomina et al., 2024). Mountain glaciers are known to have strong erosional power and can be seen to overprint previously fluvially-dominated erosional regimes with glacially eroded valleys (Anderson et al., 2006). This erosion produces the characteristic 'U-shape' valley associated with formerly glaciated regions worldwide. Where there is especially high levels of glacial erosion, overdeepened troughs can form in these valleys which are usually filled with water or sediments as ice retreats (Benn and Evans, 2010). An assumption from this overfilling and overprinting is that the majority of valley fill in glaciated mountain regions has glacially eroded origins. This is the case for many valleys in the Alps, and the majority of this valley fill is thought to originate mostly from the most recent glaciation (Schlunegger and Norton, 2013). The Alps and GCM share several similarities in their geomorphology, climate, and glacial extent. Both ranges have similar maximum elevations: 5642 m for Mt Elbrus in the GCM and 4809 m for Mt Blanc in the Alps. They similarly both experience strong precipitation gradients influencing contrasting weather patterns throughout each mountain range. One of the main differences between the two is in the main form and shape of the mountains. Where the GCM is comprised of one main chain, the Alps have a more complex structure consisting of several parallel chains. In terms of their glacial history, both ranges have experienced extensive glaciation throughout the quaternary with multiple phases of advance and retreat (Fitzsimons and Veit, 2001; Solomina et al., 2024). This glaciation has resulted in similar glacial geomorphology with characteristic erosional landforms such as troughs and cirques throughout the Alps and GCM (Fitzsimons and Veit, 2001; Koronovskii, 2016). The lack of similar research conducted in the GCM itself means that comparisons from the Alps are a good analogue that can be used.

## 2. Background

#### 2.1. Greater Caucasus Mountains

The Greater Caucasus Mountains (GCM) form a natural border between Russia to the north and Georgia and Azerbaijan to the south (west and east respectively) across 1200 km between the Black and Caspian Sea. It is the tallest mountain range in Europe with peaks reaching over 5000m, most notably Mt Elbrus (5642 m a.s.l.) and Mt Kazbek (5064 m a.s.l.). The mountain range is commonly split into 3 distinct sections: the western Caucasus bound by the Black Sea and Mt Elbrus; the central Caucasus between Mt Elbrus and Mt Kazbek; the eastern Caucasus from Mt Kazbek to the Caspian Sea (see Figure 2). Further to the south of the Greater Caucasus is the Lesser Caucasus, a smaller mountain range. Both ranges formation can be attributed to the continental collision between the Eurasian and Africa-Arabian plates resulting in a series of platform and fold-thrust units (Adamia et al., 2011).

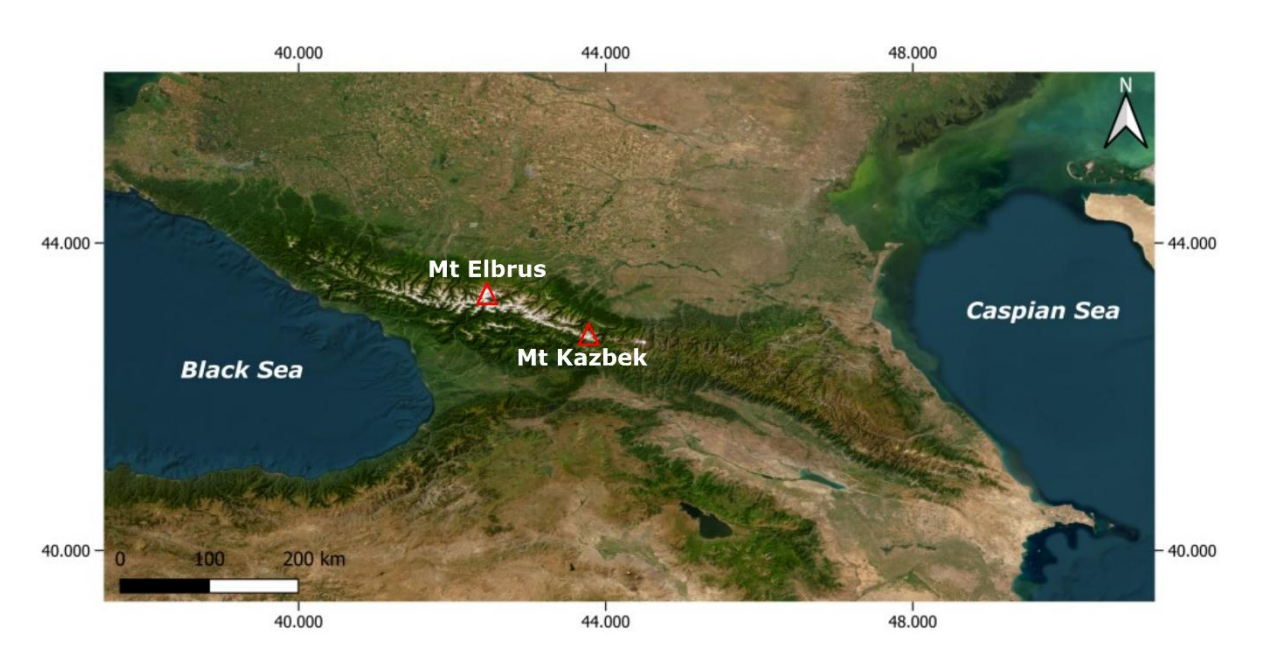


Figure 3 – Map of the GCM showing the locations of Mt Elbrus and Mt Kazbek which mark the boundaries between the western, central, and eastern Caucasus.

#### 2.1.1. Western Caucasus

The western Caucasus is generally characterised by metamorphic (Proterozoic and Palaeozoic age) and sedimentary (Mesozoic age) rocks such as schists, gneisses, shales, sandstones, and limestones. These oldest metamorphic rocks having been brought to the surface by extensive tectonic uplift (Adamia et al., 1981).

#### 2.1.2. Central Caucasus

Similar to the western side, the central Caucasus also has a suite of core Proterozoic and Palaeozoic age metamorphic rocks such as slate, marble, chert, and phyllite, as well as volcaniclastic rocks. The sedimentary cover – again similar to the western Caucasus – is mainly limestone, sandstone, and shale (Adamia et al., 2011).

#### 2.1.3. Eastern Caucasus

The eastern reach of the mountain range differs the most geologically from the more similar western and central Caucasus. Here there lacks a core crystalline element and is mostly dominated by shales and sandstones of Jurassic age coupled with high levels of deformation that has resulted in a range of complex structural components (Adamia et al., 1981; Adamia et al., 2011).

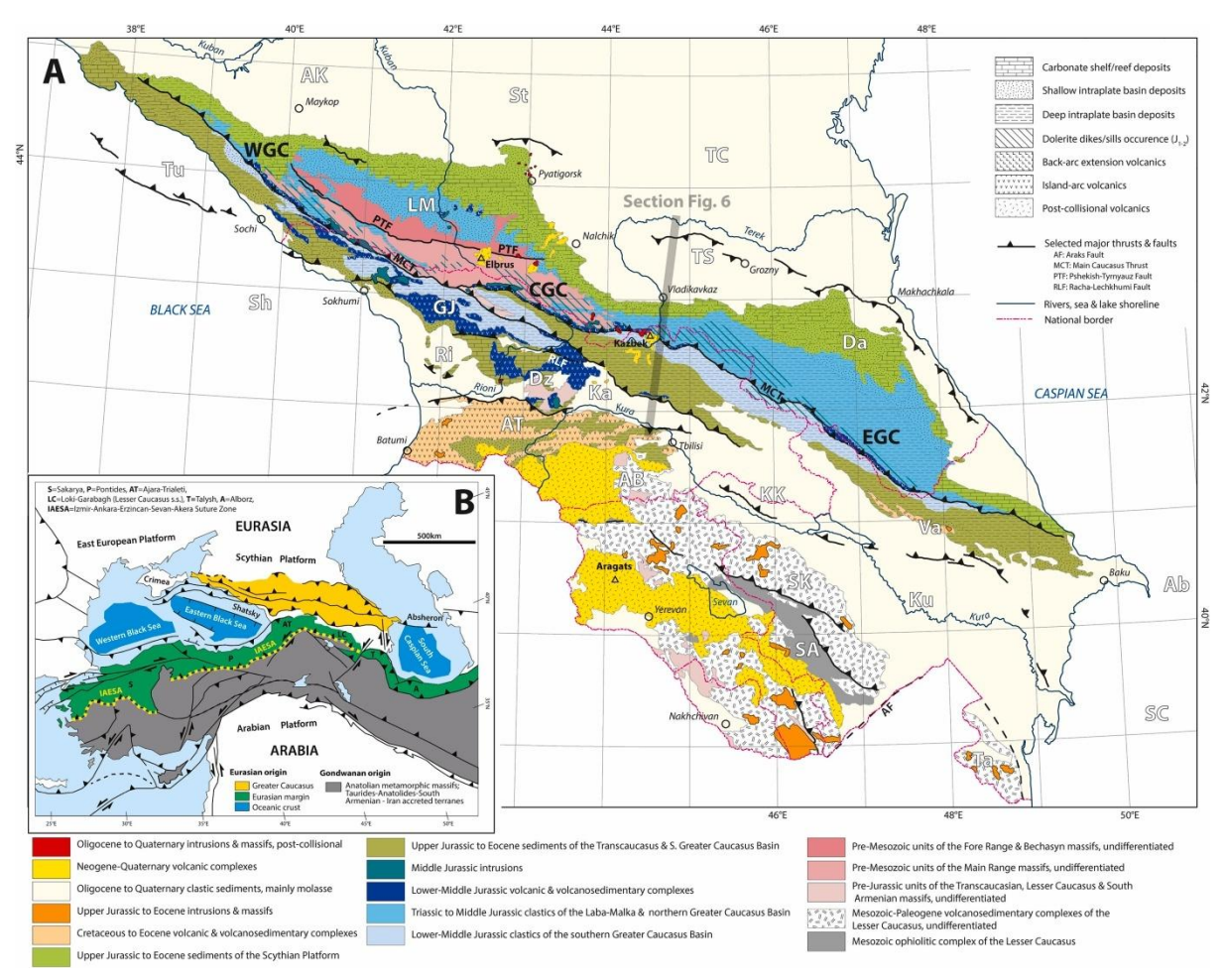


Figure 4 – Tectonostratigraphic map pf the Greater Caucasus (compiled by Mosar et al., 2022). Key aspects to note for this study are the volcanic complexes (yellow) surrounding Mt Elbrus, the fault marked 'PTF' running through the north-western Caucasus close to Mt Elbrus, and the contrasting lithologies in this area of pre-Mesozoic basement massifs (pink) and Triassic to Middle Jurassic clastics (blue).

Figure 4 shows the main lithologies and structural features of the GCM and how they fit into the wider tectonic setting of the region (map compiled by Mosar et al., 2022). This highlights the aforementioned similarities in geology between the western and central Caucasus where there are more volcanics and older basement lithologies.

#### 2.1.4. Climate

The GCM have a relatively unique climate based on a variety of factors such as geographical position, range in minimum and maximum altitude, and influence of nearby water bodies (Tashilova et al., 2019). These characteristics results in a moderate continental climate with more local variations due to altitudinal and positional zones throughout the region (Tashilova et al., 2019). There is generally a key difference in climate and weather conditions between the northern and southern slopes of the mountains as they act as a climate divide between the northern temperate zone and the southern subtropical zone (Tashilova et al., 2019) (see Figure

5)The northern slopes – the more heavily glaciated region situated mostly in Russia – have a more continental climate characterised by cold winters and milder summers (Tielidze et al., 2015). In contrast, on the southern slopes – mostly in Georgia – there is a greater impact from the Black Sea causing milder winters and warm summers (Tielidze et al., 2025). Similarly, this also causes variations in the precipitation on the northern and southern slopes. The southern slopes are significantly wetter due to the orographic influence of the GCM, whereas the northern slopes are much drier and can be classified as 'semi-arid' (Tashilova et al., 2019). In addition to this north to south variation in climate there is also a west to east variation for similar reasons. The proximity of the Black Sea to the mountainous topography results in orographic rainfall concentrated on the western Caucasus compared to the much more arid eastern Caucasus (Forte et al., 2016). In the east, annual rainfall ranges from 600-1800 mm compared to 1000-4000 mm annually in the west (Vezzoli et al., 2014). This contributes to there being a greater concentration of glaciation in the western and central GCM compared to in the east.

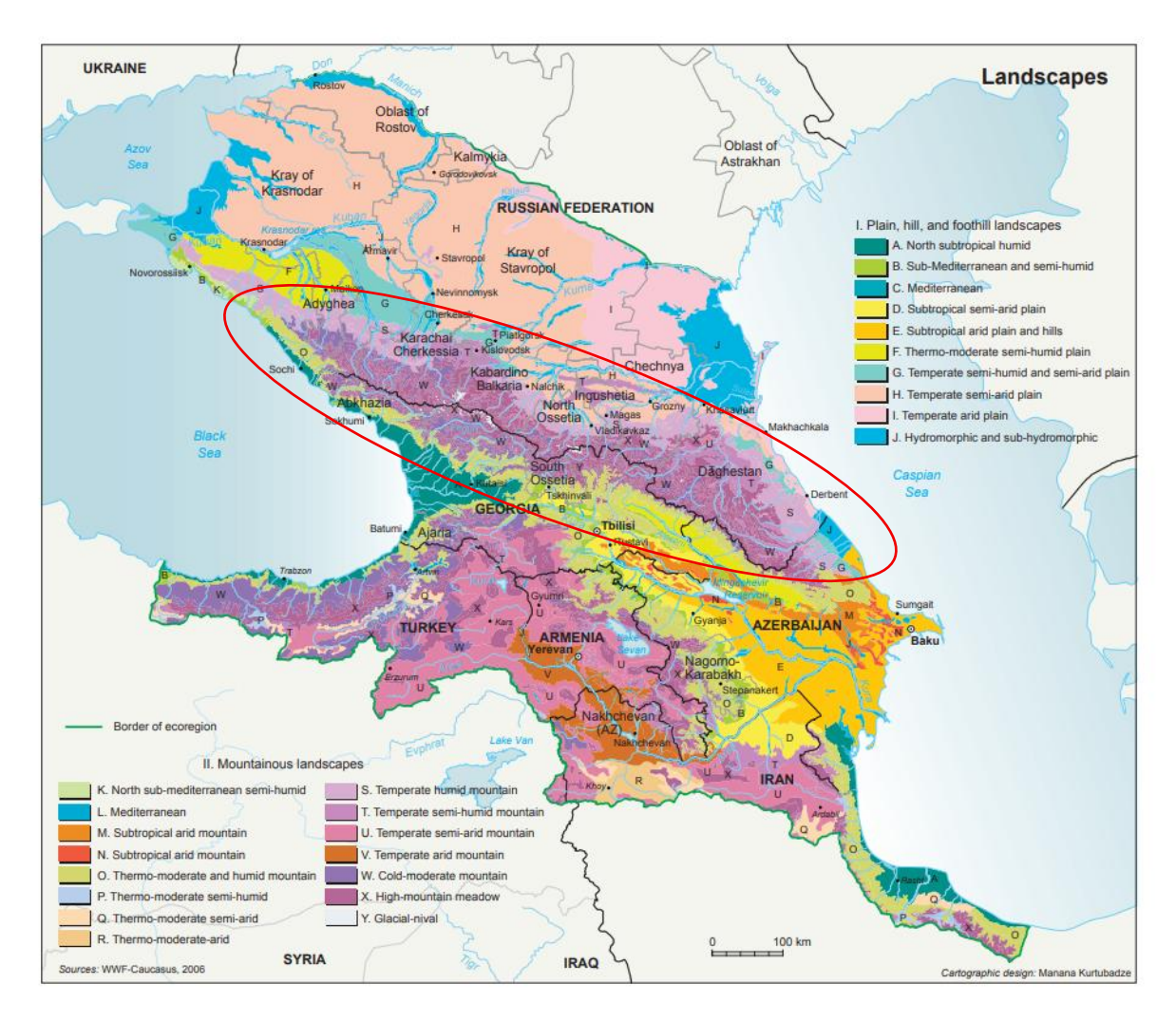


Figure 5 – Climate zone map of the GCM and wider geographical area. Note the general transition from the temperate zones in the plains and foothills to the north of the mountain range (approximate area shown by the red outline) to the humid, sub-tropical, and Mediterranean zones to the south (WWF-Caucasus, 2006).

In general, the climate in the GCM is following the global warming trend with temperatures found to be rising at a higher rate than the global average at 0.46°C/10 years from 1976-2017 (Tashilova et al., 2019). This has implications for a mountainous and glaciated region like the GCM due to accelerated glacier melting as air temperatures rise, leading to higher flow volumes in rivers and slope instability (Tielidze et al., 2022). Meteorological observations have only been continuously monitored for just over 100 years in the Caucasus region from 20 weather stations located in the northern Caucasus (Brugnoli et al., 2010). Tashilova et al. (2019) used these weather stations to track the annual mean precipitation and temperature for 50 years 1961-2011 (see Figure 6). Key observations from this figure are that while temperature variations are typically in phase across each zone, there is significantly less consistency in precipitation variations between the zones. This recent improvement in meteorological

monitoring means that past climate insight therefore relies on more indirect methods such as dendrology (e.g. Tashilova et al., 2019); Brugnoli et al., 2010), and seasonal glacier mass balance variations evident in ice cores (e.g. Mikhalenko et al., 2015).

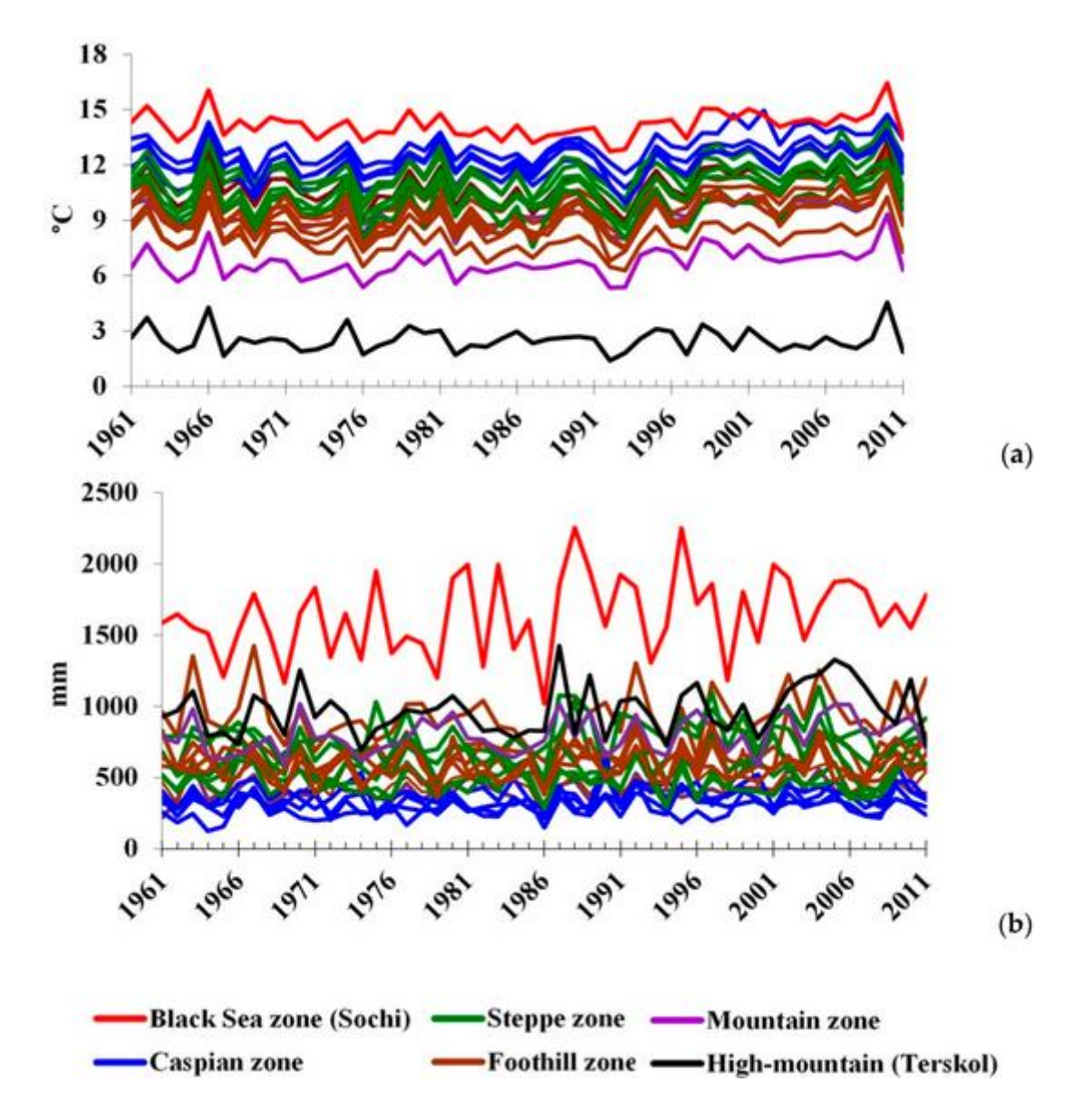


Figure 6 – graphs showing a) mean annual temperature and b) mean annual precipitation across zones in the northern Caucasus. Note the high mountain station Terksol which is located close to the study area of this research.

#### 2.1.5. Geomorphology

The GCM has an interesting geomorphological character as despite having clear variations in metrics such as convergence rate and climates from west to east, the mountain range is topographically relatively homogenous, with little variation in relief and mean elevation (Forte et al., 2016). The average elevation across the whole region is ~2500 m with the highest points being found in the central Caucasus where there are many peaks exceeded 5000 m elevation

(Vezzoli et al., 2020). The GCM is has an alpine-valley glacier system, particularly in the western and central zones with the central Caucasus being home to the most glaciers with approximately half the total glacier area of range being located here (Seinova et al., 2007). There are many large rivers throughout with their main source of water being snow and ice melt such as the Terek and Kuban with lengths of 623 km and 870 km respectively (Vezzoli et al., 2020). Valleys throughout the GCM are characterised by a mix of landforms related to glacial, fluvial, and glacifluvial processes, as well as from mass transport events such as mudflows (Gobejishvili et al., 2011).

#### 2.2. Glaciation and Glacial History

The GCM hosts 98% of the glaciers in the Greater and Lesser ranges combined (Solomina et al., 2024). In 2020, there were >2000 glaciers still present occupying an area of ~1000 km<sup>2</sup> across the GCM (Tielidze et al., 2022). Glacial extent and retreat over the past century has been generally well studied (e.g. Tielidze, 2016; Tielidze et al., 2022) but there is more discourse over the understanding of past glaciations. This is due to many of the glacially derived landforms that indicate glacial advance, retreat and maximum extent – such as moraines – are not that well preserved in many areas due to reworking of these sediments post-deposition as a result of non-glacial processes (Gobejishvili et al., 2011).

#### 2.2.1. Pleistocene

The Pleistocene is the first epoch of the Quaternary, running from ~2.6 Ma to 11.7 ka BP (Walker and Geissman, 2022) and covers the most recent period in Earth's history of repeated glaciations. Due it's length, the most recent part of the Pleistocene is often referred to in literature as the 'late' or 'upper' which generally covers from ~129 ka BP to the start of the Holocene at 11.7 ka BP. The boundary between the Pleistocene and Holocene is marked by an abrupt cooling event known as the Younger Dryas occurring from 12.9-11.7 ka BP. As previously established, due to the preservation of glacial landforms in the valleys in the GCM, it can be very difficult to resolve accurate dates for glacier variations, even for more recent fluctuations within the Holocene. As a result of this, reconstructing glacial extents into the Pleistocene becomes very difficult. One well-defined landform in the GCM are cirques. Cirques are a type of erosional landform that are common in mountainous glaciated regions, and it has been proven that cirque area at the head of a glacier can be used to estimate previous glacier length (Gobejishvili et al., 2011). This relationship was used and applied to cirque areas

across the entirety of the GCM in order to reconstruct maximum glacier extent in the Late Pleistocene. This has created a fairly comprehensive and solid estimate of glacial extent which can be seen in Figure 3.

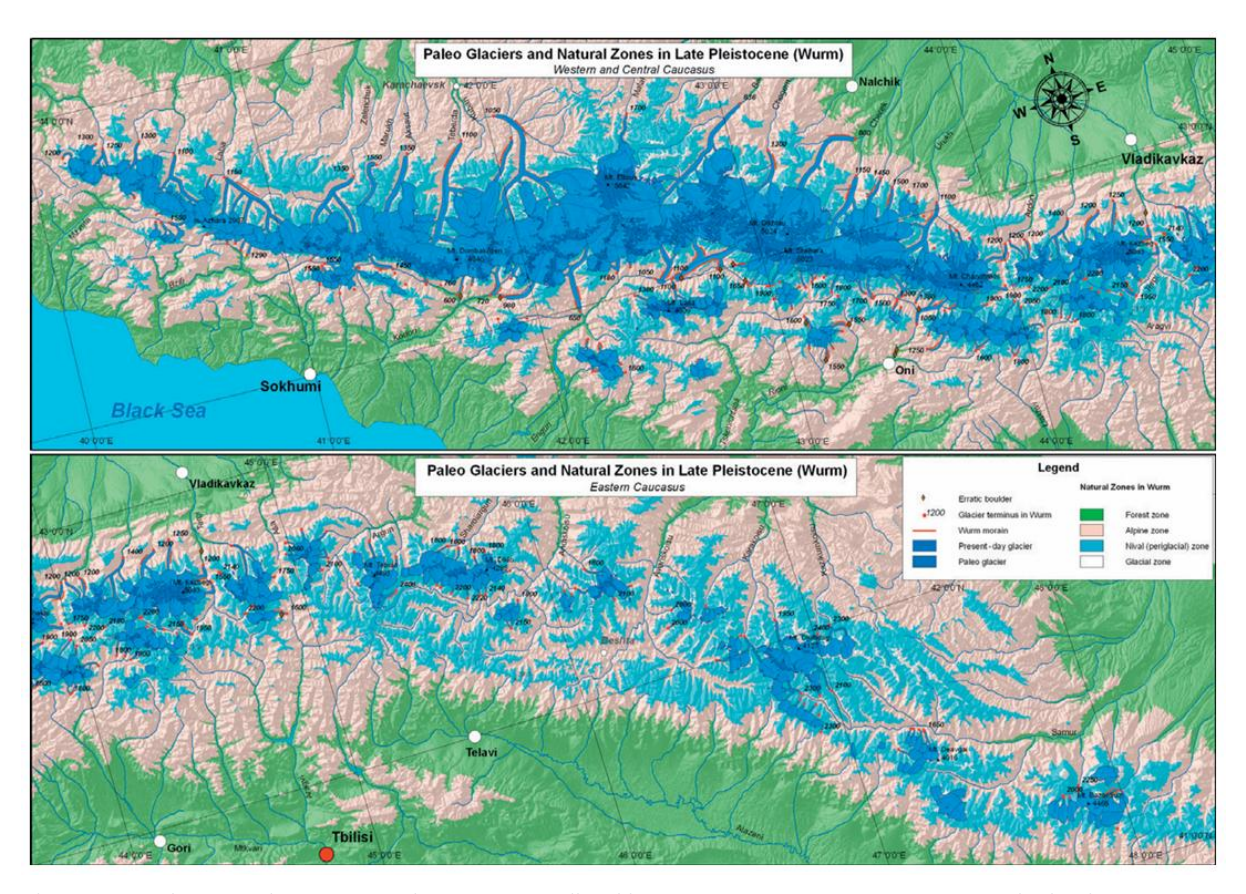


Figure 2 - Glacial extent in the Late Pleistocene (Gobejishvili et al., 2011). The darkest blue colour indicating the 2011 extent of glaciation found in the Caucasus. Note key peaks (i.e. Mt Elbrus) and altitude of maximum glacial extent down valley.

Such a full picture of past glacial extent in the GCM is unique for studies in the region both due to lack of research or it not being possible to perform research on this scale. This leads on to the point that lack of supporting research means that such full reconstructions should be viewed with the knowledge that there are not any available studies to either confirm or contradict their accuracy. Despite this, based on the method used in this example, this glacial extent reconstruction is known to be an estimate and still provides valuable insight into the glacial history of this region.

#### 2.2.2. Holocene

The Holocene is the most recent epoch of geological time within the Quaternary period, directly succeeding the Pleistocene from ~11.7 ka BP to present (Walker and Geissman, 2022). It marks

the beginning of the current interglacial period and therefore an overall stage of glacial retreat (Wanner et al., 2008). In the GCM, direct methods of dating and correlating glacial extents are often difficult to apply. This is due to key landforms linked to glacial advances and retreats such as moraines are typically not well-preserved (Gobejishvili et al., 2011). In the northern Caucasus, some sets of frontal moraines from individual glaciers are in good states of preservation and can be dated only back to the beginning of the Holocene (Solomina et al., 2024). In the case where there is little to no preservation of glacial landforms, other indirect methods are applied to give dating estimates of glacier fluctuations. A key example of this is the <sup>14</sup>C dating of palaeosols within valley or lake sediments to indicate distinctive periods of advance and retreat (e.g. Solomina et al., 2022). The same methods can also be applied to date soil horizons that indicate certain climatic conditions i.e. warmer or cooler periods that consequently have glacial implications (Solomina et al., 2024).

Glacial landscapes from the early Holocene (11.7-8.2 ka BP) have been found to be very difficult to reconstruct (Solomina et al., 2024). Any moraines found to be dated close to this time are typically from the latest advance in the Younger Dryas that occurred shortly before the beginning of the Holocene at the end of the Pleistocene. Some moraines could be successfully dated using cosmogenic 10Be exposure dating which found that the extent of glaciers in the early Holocene may have been similar to the maximum extent during the LIA (Solomina et al., 2024). There is some evidence that there may have been an advance during the early Holocene but the timing seems to coincide with a time when the Caucasus climate was particularly warm (Solomina et al., 2024). Without further work attempting to date more landforms from this time this can only be speculated. Fortunately, there is much better moraine preservation in some valleys from the mid-Holocene (8.2-4.2 ka BP). A series of well-preserved moraines located in the Bezengi valley in the central Caucasus indicate a noteworthy and clearly established advance ~ 7.0-6.6 ka (Solomina et al., 2024). Similar, to in the early Holocene, the climate in the Caucasus was thought to be warm at this time, therefore contradicting this advance. No further investigations have been done to establish a cause therefore for this advance, but it is hypothesised to have been caused by increased winter precipitation patterns (Serebryanny et al., 1984). Mostly due to their age, moraines and other glacial landforms from the late Holocene (4.2 ka BP – present), are generally in a much better state of preservation than many of their predecessors. Similarly to their predecessors however, they do also indicate periods of glacier advance throughout this time. This period coincides with the previously discussed LIA and more recent glacier advancements and retreats.

### 2.2.3. Recent changes (LIA to present)

Despite still being within the Holocene, acceleration of glacier loss globally means it is important to discuss more recent fluctuations in glaciation in the GCM. Due to global climate change, as with most other glaciated areas globally, glaciers in the Caucasus have been retreating since the Little Ice Age (LIA) (Solomina, 2000). The LIA was a period of cooler climate conditions from the 13<sup>th</sup>-19<sup>th</sup> centuries that resulted in the expansion and readvance of glaciers (Grove, 2004). This expansion was significantly smaller than maximum ice extents at the LGM but before the LIA and then since there has been an overall trend of glacial retreat throughout the latter part of the Holocene with only minor readvances at points (Tielidze et al., 2025). A selection of glaciers in the GCM were studied to compare their equilibrium line altitudes (ELA) from their most recent maximum extent towards the end of the LIA to 2020 to compare total area loss (Tielidze et al., 2025). The ELA of a glacier is the altitude marking where there is a change from net ice accumulation to net ice ablation (Armstrong et al., 1973). The lower the ELA, the greater the accumulation area above it and therefore the glacier typically advances, and the higher the ELA, the greater the ablation area below it, normally resulting in glacier retreat. It is therefore a good metric to use to understand and compare past and present glacier dynamics. In their study, Tielidze et al. (2025) took 12 representative glaciers to study and found that from the 1820s to 2020 there was an overall ice area loss of 51% with the rate of decrease increasing throughout that time period. Coupled with this were also increases in the mean elevation at which these glaciers were found, and a reduction in their maximum and minimum extent and terminus elevations. All of these metrics indicate a clear retreating trend across the GCM. The main cause for this recession can be accredited to increasing air temperatures throughout this time period (Toropov et al., 2019). This continued and rapid retreat has implications for water resources in the GCM as the glaciers are important sources of fresh water for people living in the region and increased melt and runoff has implications for the reliability and consistency of this water supply (Tielidze et al., 2022).

#### 2.3. Sediments and Glacial Processes

#### 2.3.1. Overview

Glacially carved valleys have a clearly distinct shape compared to valleys and landforms derived from other natural processes such as fluvial and aeolian. It has long been established that glacially eroded valleys have a diagnostic general 'U-shape' (e.g. Grotzinger and Jordan,

2014). Conversely, fluvial valleys are generally described to have more of a 'V-shape' where they have eroded mostly vertically down into the valley (Montgomery, 2002). Glaciers erode significantly more efficiently than rivers and therefore result in deep erosional features, a process known as glacial overdeepening (Montgomery, 2002; Preusser et al., 2010). Such overdeepened valleys typically end up being filled by lakes or sediments as the glaciers that formed them retreat (Anderson et al., 2006).

The mechanisms of glacial erosion and generation of sediments are something that has long been studied within glaciology and geomorphology (e.g. Forbes, 1846; Chamberlin, 1888). From a culmination of research, two main erosional processes are considered to occur at the erosional base and sides of glaciers: abrasion and quarrying (Iverson, 2002). Coupled with this erosion are the processes of glacial deposition. There are also three main categories of glacial deposition: the release of sediments held within the ice (englacial) to either the top or base of the glacier (supra- and subglacial respectively); sediments being carried in either a supra- or subglacial position that are deposited in situ beneath the or in front of the ice (proglacial); and a final category of water sorted sediments (glaciofluvial) (Whiteman, 2002). The combination of these erosional and depositional processes results in a variety of glacial sediments and landforms. Examples of erosional landforms are striations, cirques, and U-shaped valleys. Examples of depositional landforms are eskers, moraines, drumlins, and outwash fans.

#### 2.3.2. Glaciers and glacier motion

To investigate these processes in more detail, it is first necessary to understand basic concepts of how glaciers form and flow. The movement of glaciers is ultimately controlled by their mass balance. This is the function of a glacier that describes it's gain (accumulation) and loss (ablation) of ice. As previously explained (2.2.3.), glaciers have an equilibrium line altitude (ELA) with the areas above and below being known as the accumulation and ablation zone respectively. Glacier motion is controls the transfer of ice and snow from the accumulation down valley into the ablation zone (Benn and Evans, 2010). When a glacier has more accumulation that ablation, it advances, and in the reverse it will retreat. Three main processes dictate the mechanisms of glacier flow: sliding, deformation of the ice, and deformation of the glacier bed (Benn and Evans, 2010). There are many factors that control the dominance of each of these processes within a glacial environment but overall, they are heavily influenced by the glacial classification. Glaciers are typically split into three classifications related to their

thermal properties. In order to distinguish between these categories, it is necessary to understand the concept of pressure-melting. This is where the melting point of ice decreases with increasing pressure applied to it and has been found to be at a rate of 0.072°C/MPa in usual cases without heavy influence of impurities (Benn and Evans, 2010). As a result of this, as the maximum depth of a glacier increases, the melting point of the ice throughout decreases. The three classifications informed by this concept are as follows:

- 1) Temperate glaciers where the majority of the glacier sits at pressure-melting point.

  Typically found in regions such as southern Iceland, New Zealand, and western Norway.
- Cold glaciers which are normally frozen to their base and below pressure-melting point.
   Typically found in regions such as Antarctica and other more localised cold desert environments
- 3) Polythermal glaciers are a blend of the two and can vary from predominantly 'warm' to predominantly 'cold'. Most widely distributed classification found in regions such as the European Alps and Svalbard.

Glacier sliding directly on bedrock is a process of glacier flow that relies on a localised pressure-melting around obstacles on the rock bed (regelation) or the local deformation of basal ice (enhanced creep) (Benn and Evans, 2010). Regelation describes how when a glacier reaches an obstacle at its base, one of the ways in which it 'slides' over it is by the melting and refreezing of basal ice around the obstacle. As it approaches a barrier to flow, the pressure upslope from the obstacle increases resulting in local pressure-melting. The thin layer of water produced by this melting reduces the friction between the ice and surface and therefore allows the ice to slip over the obstacle and as this pressure reduces again, the ice refreezes on the downslope side. The importance of pressure-melting in this process means that it is typically found more at temperate or polythermal glaciers where this point is more easily reached. Enhanced creep is the sliding mechanism more commonly found at the base of cold glaciers. This is because it allows for flow without the need for ice to be at or close to its pressure melting point (Benn and Evans, 2010). This flow process works by deformation of the ice based of changing stresses as opposed to the frictional changes involved in regelation creep. In this case, as the glacier approaches an obstacle, the ice experiences a higher strain rate as the stress on the ice increases. This allows the ice the deform around the obstacle and alter its shape to allow movement between the glacier and bedrock (Benn and Evans, 2010).

The processes of regelation and enhanced creep are the main two mechanism that dictate ice flow over bedrock. However, many glaciers flow over unlithified sediments and in these conditions, the ice flow operates differently therefore also resulting in different methods of glacial erosion and depositional of glacial landforms (Boulton, 1979). Studies of some such glaciers (e.g. Breiðamerkujökull, Iceland) have shown that as much as 88% of movement is caused by deformation of the unconsolidated sediments in the glacial bed (Boulton and Jones, 1979). This highlights how variations in the glacial bed type from lithified to unlithified has profound impacts on glacier flow which has further implications for the types of sediments and landforms which may be observed.

#### 2.3.3. Glacial erosion

As previously established, there are two main agents of glacial erosion: abrasion and quarrying (see section 2.3.1.). Abrasion is the action of rock fragments being dragged along the glacier bed and wearing it down by either polishing the surface or scoring the bedrock and creating striations (Hallet, 1979; Benn and Evans, 2010). Striations are formed by sharp and irregularly shaped parts of rock fragments that under the intense pressure at the glacier bed are able to score grooves into the bedrock (Benn and Evans, 2010). Polishing and striations are linked concepts as the more the rock fragments abrade and score the rock surface, the smoother both the fragments and any asperities on the bedrock become, leaving a polished surface (Benn and Evans, 2010). Quarrying is an erosional process that operates by stresses exploiting existing cracks in rocks resulting in widening and eventually complete separation from the original rock (Benn and Evans, 2010). These two processes are responsible for a variety of erosional landforms on a range of scales. On the smallest scale ( $\sim 10^{-2} - 10$  m), these features include striations, polished surfaces, chattermarks, and gouges. On an intermediate scale ( $\sim 10 - 10^3$  m), landforms include roche moutonnées, whalebacks, and rock drumlins. Large scale erosional forms ( $\sim 10^3 - 10^7$ m) covers features on a landscape scale such as rock basins, overdeepened valleys, troughs, fjords, and cirques. Such geomorphological landforms are typically the most easily identifiable in past glacial landscapes and best highlight the significance of a glaciers erosional power. It is these signature landscapes that appear as glaciers retreat that are the most necessary to understand and identify for the purpose of this research. Overdeepened glacial valleys are formed by a combination of abrasion and quarrying over significant spatial and temporal scales (Benn and Evans, 2010). Such levels of these erosional forces require water at the ice base in order to accelerate these processes and therefore predominantly occurs at wetbased temperate glaciers. Additionally, as well has having water present from pressure melting at the glacier base, large water pressure variations have been shown to increase the effectiveness of quarrying (Iverson, 1991). In practice, this results in rapid erosion around fractures in the bedrock thus causing overdeepening of the bed (Hooke, 1991).

#### 2.3.4. Sediment transport

Following on from erosion, any sediments that are produced are often then entrained and transported elsewhere by the glacier. Debris entrainment will always occur either from the top (supraglacial) of ice surface or from the glacier bed (subglacial) (Benn and Evans, 2010). The biggest contributor to supraglacial sediments is via gravitational processes where there are rock surfaces above the ice cover for example valley walls or nunataks (individual peaks that extend above the ice). In valley glaciers, this is one of the biggest contributors to sediment entrainment due to weathering and mass movement processes releasing debris from the rock slopes above the ice (Benn and Evans, 2010). In other glaciers that do not sit within the influence of supraglacial sediment sources, the biggest supplier of debris is from the glacier base through subglacial entrainment. As previously explained, basal ice sits at very high pressures resulting in a variety of erosional and deformative processes which can often then result in sediments being incorporated into the ice. In some cases, it has been shown that basal ice is comprised of up to 75% sediments and debris (Benn and Evans, 2010). This entrainment has implications beyond sediment transport as it also influences the way glaciers flow and erode over their beds. A high concentration of sediment being carried in the basal ice increases the friction between the glacier and underlying bedrock or sediments therefore impacting glacier motion. These sediments can also increase subglacial erosion rate due to enhanced abrasion and increased pressure at the glacier bed as a result of the increased friction. Once sediments have been incorporated into the glacier ice, either supra- or sub-glacially, they can then be transported significant distances in a supra-, sub-, or englacial position due to dynamics within the ice. For example, subglacially entrained sediments can be brought up to within or even to the ice surface through folding and thrusting of ice due to compressive stresses in basal ice (Benn and Evans, 2010). Significant proportions of glacial sediments are transported within the ice but there are also very large quantities of sediment transported by water flow associated with the glacier through to glacifluvial systems. It has been shown that in most temperate glaciers meltwater transports the most sediment in the system, more than the ice itself (e.g. Kirkbride and Spedding, 1996). The way in which sediments are transported also has a strong influence on

the morphology of individual sediments, more specifically on their texture, shape, and roundness (Boulton, 1979). The way in which a clast has been transported is often clearly reflected in its morphological characteristics. This as a result of the glacial erosional processes that continue to occur during transport. An actively transported clast within the glacier ice may end up being very angular due to quarrying and fracturing processes whereas clasts undergoing glacifluvial transportation become more well-rounded with travel due to abrasion (Benn and Evans, 2010). The textures of glacially transported clasts are also unique for the same reasons. As with erosion directly on the bedrock and obstacles overridden by the ice, striations and polished surfaces are also common on individual clasts picked up by the glacier. Such features are important as it allows for clear identification of glacially influenced sediments compared to fluvial and coastal sediments which may have similar shapes or roundness.

#### 2.3.5. Glacial sediments and deposition

The varied and unique erosional processes that occur in glaciated environments consequently results in a range of unique sediments and landforms. The term typically used to refer to unconsolidated glacial sediment is 'till' and it is used widely within glacial research to describe all kinds of glacially related sediments (Menzies et al., 2006). The deposition of glacial sediments across all glacial environments can be very complex and therefore for the purpose of this thesis and the detail needed will be investigated and explained as a broad overview. From this, two main categories of sediment deposition will be investigated: subglacial till formation and glacifluvial deposits. This is because these are the most relevant to the sediments found at the base and fronts of ice margins and therefore comprise the majority of valley floor sediments.

Subglacial till formation occurs through four main processes: lodgement, melt out, deposition by gravity, and friction retardation (Benn and Evans, 2010). Lodgement and frictional retardation are both related to the variations in friction at the basal ice margin. Lodgement occurs due to imbalances between friction and shear stress between sliding ice and the bed resulting clasts becoming lodged or fixed into the bed (Dreimanis, 1989). This can occur on a variety of scales from single clasts to large volumes of debris-laden ice (Benn and Evans, 2010). Frictional retardation occurs where the substrate layer beneath the ice is deforming as the ice slides over it. In this case, subglacial sediments are deposited when this layer stops deforming resulting in the sediments being unloaded (Benn and Evans, 2010). Melt out and gravitational

deposition are the simpler processes where till is deposited either from being melted out of the ice directly at the ice margin or within a cavity in the ice where it falls to the floor through gravity.

Glacifluvial sediment deposits are a significant source of sediments and deposition within glacial systems like those found in the Caucasus due to seasonal melt periods where high volumes of water are flowing through and out of the glaciers. The sediments produced from this process can be formed both in the proglacial area from meltwater channels after retreat or within the glacier ice and at the glacier base due to streams and conduits that travel through the ice (Benn and Evans, 2010). Such deposits typically resemble fluvial deposits and may contain features such as dunes, ripple cross-laminations, and channel fills (Benn and Evans, 2010) but often with the distinctions found in glacial till described in section 2.3.4. helping to define these sediments as glacially derived.

#### 2.4. Alternative sediment sources

Glaciation has a significant erosional and depositional impact on landscapes and has been proven to overprint existing sediments and landforms originating from other sources such as rivers (Schlunegger and Norton, 2013). However, it is important to consider that as glaciers retreat, fluvial regimes and other sources of sediments such as from mass transport events will become more prominent. This is an aspect to be examined in the Caucasus as much of the glaciation is now limited to mountain tops with an increasingly small proportion of valley glaciers throughout the GCM (Shahgedanova et al., 2014). One of the most significant sources of large volumes of sediment in the GCM are from mass transport events such as mudflows which are becoming increasingly common in the region (Aleinikova et al., 2020). In the northern Caucasus, ~950 mudflow basins have been identified which were responsible for 1810 flows from 1900-2010 (Karavaev and Seminozhenko, 2019). However, the dynamics and frequency of these events are increasing, and this can be mostly attributed to climate warming which is consequently accelerating glacier retreat in the region (Aleinikova et al., 2020). This is typically as a result of outbursts from glacial lakes or the melting of ice within moraine deposits. This highlights how the presence of mudflow deposits within the GCM are intrinsically linked to the glaciation present and particularly the impacts of rapid glacial retreat as proglacial lakes are increasing in frequency and volume (Shahgedanova et al., 2009). This could suggest that although large volumes of sediments may be being mobilised and redistributed by other processes, they are still likely to be glacially derived sediments.

#### 2.5. Glacial Retreat and Isostasy

#### 2.5.1. Glacial retreat

It has clearly been established in the above sections that glaciers are experiencing a global decline with examples from the Caucasus indicating that retreat is happening on a rapid, measurable scale. As glaciers are the main source of water in the Caucasus and with many other regions globally this retreat can have significant impacts on local geomorphology and consequently any local populations. As explained in section 2.3.2. glaciers gain ice through accumulation and lose ice through ablation and the balance between these two processes controls whether the ice will advance and retreat. Most glaciers naturally switch between a period of advance and retreat throughout the year due to seasonality but in a stable glacier these two periods balance out. What is becoming increasingly common especially in glaciated mountain regions is much higher rates of ablation due to milder summers which is not being balanced out by winter accumulation. For example, in the GCM, from 1985-2000 94% of a selection of measured glaciers in the central Caucasus were found to have retreated (Stokes et al., 2006).

More generally and for the purpose of this thesis, it is important to understand how glaciers retreat, whether it be rapidly or otherwise due to the impact this has on the sediments and landforms within valleys. Retreat of glaciers often results in the formation of lakes at the glacier snout, and this is something that is becoming common in the GCM (Shahgedanova et al., 2009). This is an important aspect of glacial retreat as ice that terminates into water often melts at a higher rate due to warmer water than air temperatures (Sutherland et al., 2020). Glacial lakes are also of significance in the Caucasus as they pose an increased hazard from the glaciers due to flooding events (Stokes et al., 2007).

#### 2.5.2. *Isostasy*

The retreat of glaciers globally has been shown to have a variety impacts and implications both in a social and geomorphological contexts. Isostasy is the concept in earth science describing the equilibrium between the more buoyant crust 'floating' on the denser mantle beneath (Watts, 2023). This means that any change in mass of the crust disrupts this equilibrium and causes the

crust to either depress into the mantle with the addition of mass or uplift with any reduction in mass. This is relevant in a glacial context as ice sheets at a significant load onto the lithosphere causing subsidence and when they retreat and the ice mass reduces the lithosphere then rebounds (see Figure 8). This occurs over some time lag due to the time it takes the mantle to respond to these mass variations (Benn and Evans, 2010). The process is referred to as glacial isostatic adjustment (GIA) and due to this time lag is being readily observed on human timescales across the northern hemisphere as a result of ice retreat since the LGM. Uplift of the crust can also be caused by denudation isostasy. This is where continued erosion of a landscape over time causes uplift as the overall weight of the area is reduced (Gilchrist and Summerfield, 1991). This differs from GIA as this is directly reducing the overall load by eroding from the mass of the crust, compared to the load being reduced by the removal of mass from ice. However, the combination of denudation isostasy and GIA will result in a further increased uplift as it there will be both unloading from ice retreat, as well as from mass loss from intense erosion as a result of the glaciation.

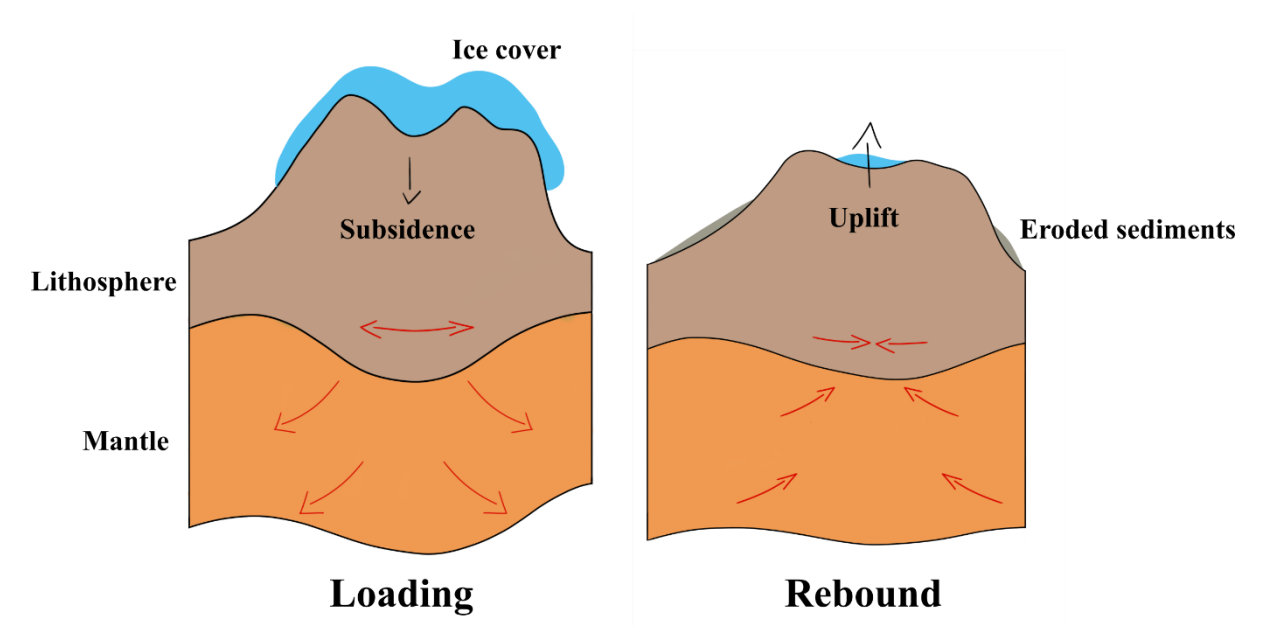


Figure 3 - Diagram illustrating the mechanism of GIA as ice retreats on a mountain range. Ice cover over a mountainous region will contribute further to subsidence into the mantle, resulting in subsequent uplift when this ice melts.

It is possible and necessary to quantify GIA as the subsiding or uplift of the lithosphere has significant implications for relative sea level change (Whitehouse, 2018). In order to do this, several metrics need to be quantified so that the lithospheric load can be estimated. In the

context of a mountain range such as the Caucasus, it is necessary to know the initial load of the mountains and the current or projected load. As clarified in section 2.3.3., glaciers have significant erosional power and erode large volumes of sediments as they carve through valleys. This means that during the glaciation of the Caucasus, an amount of the mountain range would have been eroded and redistributed in the form of sediments on a large scale. The first step in this GIA estimation would be to establish the quantity of these sediments in order to reconstruct what the initial size of the mountain range would have been. The next step would be to estimate the maximum extent of the ice sheet and the load this was bearing on the lithosphere. Finally, with an estimation of the current known load that the Caucasus has, these metrics can be combined together to model the GIA associated with the ice retreat.

#### 2.6. Glacial valley fill prior research

There have been many studies in multiple aspects of geomorphology attempting to quantify unknown thickness of land cover such as ice and sediments of various origins. Such studies typically involve a measure of direct investigative methods such as ice or rock core drilling, and air- or ground-borne geophysical surveys (e.g.Buechi et al., 2016; Pomper et al., 2017). These approaches are often used in conjunction with more indirect methods and data sources such as aerial imagery and DEMs. Much of the research around attempting to quantify glacial sediments has relied upon being either fully or partially informed by direct measurements from cores or geophysical methods. However, this is not always financially, politically, or practically possible. For many researchers, the funding and/or materials are not available to pursue direct measuring methods such as rock core drilling and extensive geophysical surveys. There are also many areas which may not be accessible for research due to political reasons, or that are simply inaccessible due to their geographical remoteness. This has led to some research attempting to move away from these direct methods and attempt to find a way to conduct the same research using more indirect methods with varying degrees of success and accuracy.

An example of one of these methods is a study by Otto et al. (2009) which used a combination of direct and indirect methods to quantify the sediments stored in the Turtmanntal valley in the Swiss Alps. A distinction in this study compared to some others including the research of this thesis is that includes an estimation of sediments stored throughout the valley including the

hanging valleys and trough slopes. Comparatively, in this thesis and other similar studies (to be discussed in this section), sediment storage quantification is limited to the valley floor (e.g. Blöthe and Korup, 2013; Mey et al., 2015). The methodology of this study was split into two main parts. Firstly, data from a geophysical study on one of the hanging valleys was used to establish its sediment thickness which was then used to estimate the sediment volume found in all 7 of the hanging valleys of the Turtmanntal catchment. Secondly, the sediment stored in the main valley trough was quantified using an approach of deepening the DEM to the estimated valley shape pre-sediment deposition using parabolas plotted against the profile curvature. The study found that over 60% of the total sediment volume stored in the valley is found in the hanging valleys and is comprised predominantly of moraine and slope deposits. This suggests that in certain regions, there may be significant stores of sediments beyond the main valley floor. One of the main strengths of this study is showing the ability to distinguish between and quantify different types of sediments within the valley, without solely using geophysical methods. In terms of the geophysical data used in this study, only a data for one hanging valley was needed, with the estimates for the remaining ones scaled up from this. This demonstrates how very little direct data can be needed in order to quantify volumes over a larger scale, although this does come with higher uncertainty.

In contrast to the study by Otto et al. (2009), which quantifies sediment storage on the single valley scale, there have also been attempts to scale this up onto a much larger scale. Blöthe and Korup (2013) present an approach of quanitfiying sediment fill volumes over the mountain belt extent (>38,000 valley fills) in the Himalayas. This research was based on establishing sediment routing systems in this region from the major drainage basins of the Indus and Ganges-Brahmaputra. The valleys identified as having sediment fill were judged to mostly all be of postglacial origin. The scale of this study area meant it was necessary to establish a method to quantify the volumes of valley sediments throughout these basins as sediment fill will act as a buffer to sediment yields. This was done by extracting the outlines of filled valleys from a DEM and applying an empirical volume-area scaling method founded upon some known published volumetric data for valleys in the Himalayas. However, the availability of this data is quite limited. The implications of this were that some valleys were consequently excluded for their lack of conformity with typical V- and U-shape valley morphologies. The result of this is that the total volume is most likely to be an underestimate but ensured that the data was as reliable as possible for the valleys included. The total volume projected for the ~38,000 valleys was ~690 km<sup>3</sup> but with a variation of up to 30% depending on the approach used to extract valley fill areas. The principal advantage of this method is that it provides a way

to estimate sediment fill volumes over mountain-range scales. However, this does unsurprisingly come with high uncertainties as demonstrated by the error margin generated by applying different methods of valley outline extraction. The execution of the study was overall limited by lack of direct measurements from which to apply the volume-area scaling method, which resulted both in the high error margin and the necessary exclusion of some valley types. Despite this, it has therefore been demonstrated that it is possible to reasonably quantify sediment volumes in valleys with very little direct data with which to support it.

A final example of one of these studies is by Mey et al. (2015) titled 'Estimating the fill thickness and bedrock topography in intermontane valleys using artificial neural networks'. The aim of this study was to test a method of quantifying the thickness of sediment in the Rhône Valley in the Alps based on valley geometry. In this study, Mey et al. (2015) identified that there is a lack of middle ground in methods that avoid the use of direct geophysical methods whilst still producing reasonable predictions of buried valley topography that have not been overly simplified. They also identified that there was a lack of methodologies that can predict and reconstruct V-shaped valleys. From the identification of these knowledge and methodology gaps, they generated a method adapted from Clark et al., (2009) where ANNs were used to project subglacial bed geometries and ice volumes. In this new method, valley geometries were used to train artificial neural networks to estimate fill thickness throughout both the U- and V- shaped valleys using artificial fills. This produced a model that can estimate sediment fill thicknesses based on valley geometries which was then used to generate a volume estimate for the glacial fill within alpine valleys such as the Rhône Valley. The estimate of sediment volume in the Rhône Valley produced from this method closely matched other estimates from previous studies based on direct measurements (e.g. Hinderer, 2001). This therefore highlights the success of this method as it has been shown to predict sediment volumes within the error margins of estimates founded on direct measurements. It similarly highlights the merits of using ANNs for the purpose of estimating sediment fill thicknesses, based upon readily accessible and available data such as DEMs, meaning a similar method could be applied to most areas worldwide.

## 3. Methodology

## 3.1. Artificial Neural Networks (ANNs)

#### 3.1.1. Background

Artificial neural networks (ANNs) are a type of computational model based on and inspired by biological concepts, more specifically the electrical activity and communication between the brain and nervous system (Walczak and Cerpa, 2003). ANNs can be used and have applications across a wide variety of research topics from other scientific disciplines to business with the main benefit being their ability to deal with non-linear predictions with little known prior knowledge. The basic architecture of a neural network comprises inputs followed by a number of hidden layers within which are nodes, followed by outputs – a simple structure of an ANN can be seen in Figure 9.

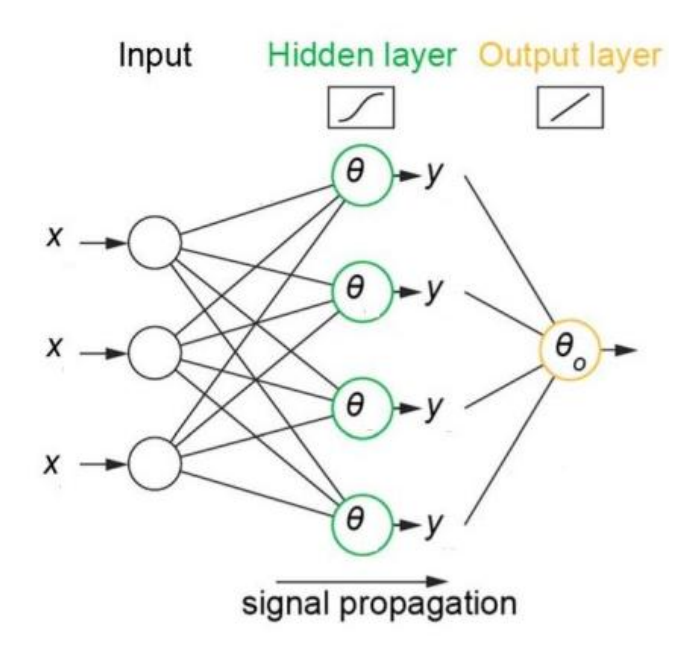


Figure 4 - Basic structure of an ANN comprising inputs, a hidden layer and an output adapted from Mey et al., (2015).

The number of hidden layers and nodes are predetermined when setting up the network structure. As shown in the figure there are connections between the inputs and nodes within the hidden layer which each have a specific weighting between 0 and 1. This weighting can also be predetermined but as part of the training phase, the ANN itself alters the weighting in order to find the best fit for the outputs. This is done in the hidden layer of the neural network where

the training process occurs. It is within the hidden layer that the network learns to recognise patterns between the inputs and outputs and consequently alters the weighting between each node accordingly. In order to train the network, once the network structure has been set up, it is given a set of inputs and their known outputs which are used to train it to identify and recognise the pattern in this data and therefore predict new outputs.

It has previously been established that ANNs were used by Mey et al. (2015) to estimate sediment fill thickness of valleys in the Alps (see section 2.6). The methodology used in this thesis is influenced by the approach used by Mey et al. (2015) in that an ANN based method will be used to estimate sediment fill thicknesses and volumes in the GCM. Their results showed that such a method could be successfully applied in glaciated mountain regions. This helped to justify producing a new model specific for the GCM. A new model was created using a set of training data from a study area in the Caucasus in order to account for variations in valley morphologies in the Alps compared to the GCM. The nature of this method already included larger uncertainties due to the estimations involved as well as the intention to upscale the model for application in other valleys. This meant that it was important to mitigate and reduce as much as possible for any known sources of uncertainty, such as applying an Alpine specific model to the GCM.

#### 3.1.2. Training the ANN

In this research, the ANN model was set up and run in MATLAB using the Netlab toolbox designed for neural network algorithms (Nabney, 2002).

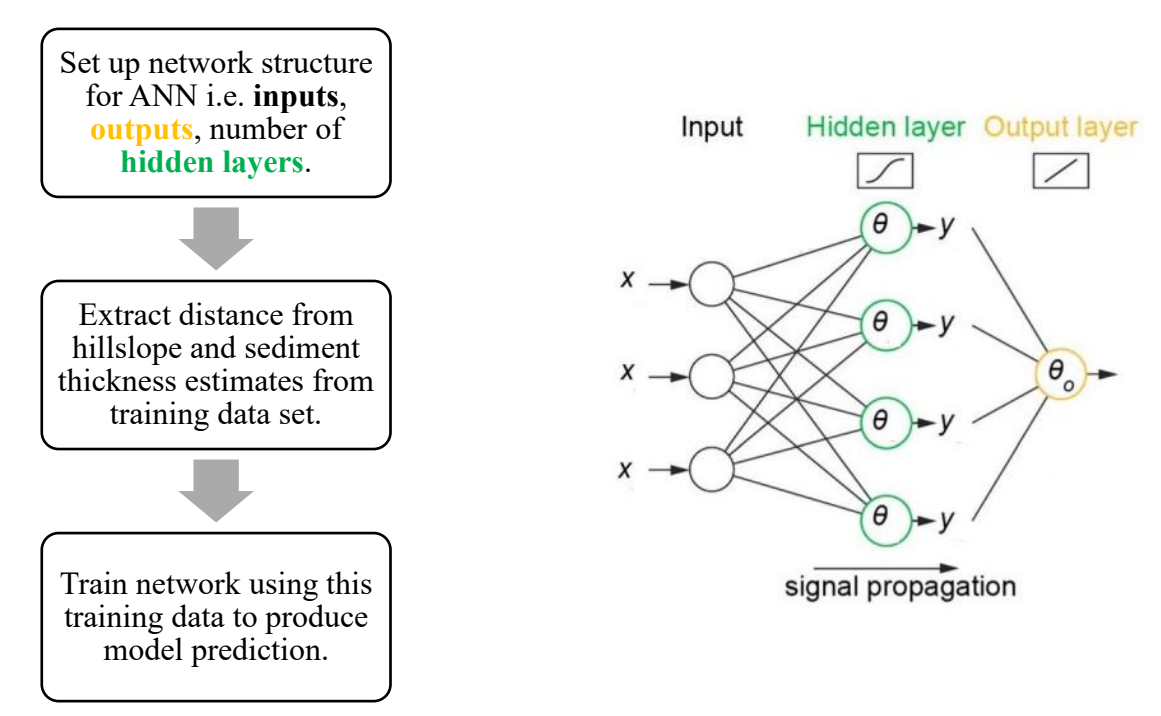


Figure 5 - Workflow for training the ANN with reminder of simple ANN structure.

## 3.2. Study area

The first starting point for this research was to establish a focal valley or catchment area that would be used to obtain training data and provide a representative view of glacially influenced valleys in the north-western Caucasus. There were several criteria to be met in order to select a sample valley:

- 1. Size: ideally it needs to contain some of the wider and deeper valleys in the region that has clearly experienced glacial overdeepening and therefore houses glacially eroded sediments.
- 2. Shape: in order to generate a representative selection of training data, the catchment area needs to have variation of valley widths throughout so that there is a variety of valley geometries being accounted for.
- 3. Glacial influence: at first level investigations, in order to ensure that there has been a clear and continued glacial influence on the valleys, there would ideally still be existing glaciers present within catchment.

As the initial focus of this research was in the western Caucasus, this led to the selection of a catchment area in the Elbrus region (see Figures 11 and 12). This catchment covers an area of

~2500 km² encompassing a drainage area which feeds into the Kuban River, the largest river in the northern Caucasus. Within the catchment, drainage flows northwards before the Kuban River drains to the Sea of Azov, connected to the Black Sea in the west.



Figure 6 – Map showing location of study catchment area to the northwest of Mt Elbrus within the GCM

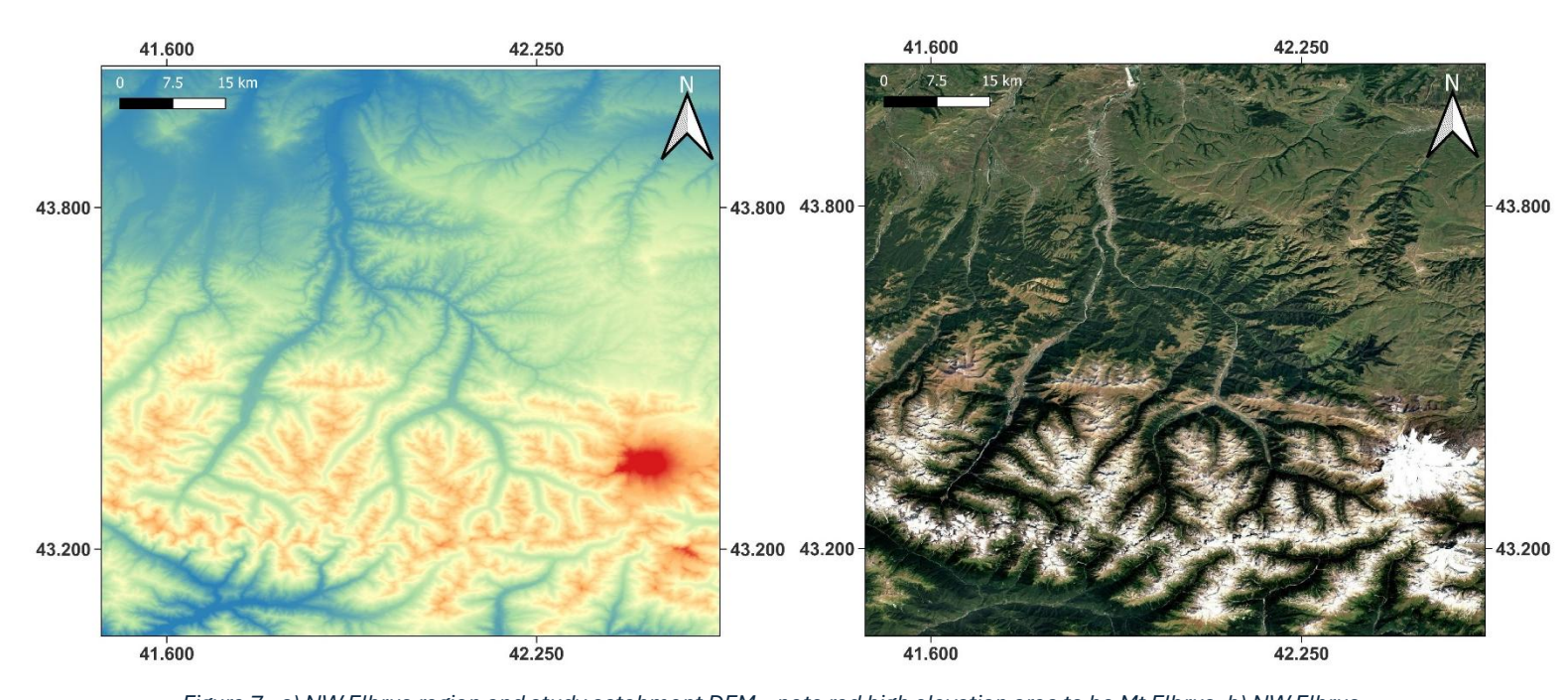


Figure 7 - a) NW Elbrus region and study catchment DEM – note red high elevation area to be Mt Elbrus. b) NW Elbrus region and study catchment Satellite imagery.

This catchment area clearly meets these criteria due to its size and shape with a variety of channel widths and upon further investigation (using satellite imagery to check valley features) a mix of U-shaped glacially eroded valleys and some V-shaped fluvially dominated valleys demonstrating a general variation in sediment origin. These valleys range from ~150 m at their narrowest and ~2100 m at their broadest throughout the training catchment. The valley floors elevations range from ~1000-2000 m.a.s.l. with the surrounding mountains at an elevation of 3000-4000 m.a.s.l. with the exception of Mt. Elbrus at >5000 m.a.s.l.. The glacial influence is also evident from surrounding glaciation. Having selected a study area, the next step was to establish how to collect meaningful data from it to use as training data. Figure 13 below shows example U- and V-shaped valleys located within the drainage area of the selected valley.





Figure 8 - a) showing an example of a characteristic U-shaped glacially eroded valley in the GCM (Potopalski, 2017) and b) showing an example of a characteristic V-shaped fluvially eroded valley in the GCM (Fedorov, 2022). Note the more shallowly sloping valley walls and broad flat valley floor in a) compared to the steep sided valley in b).

#### 3.3. Data collection

The data collection for this research was done using the MATLAB programming and computing environment and predominantly the TopoToolbox analysis add-on (The MathWorks inc, (2024); Schwanghart and Scherler, 2014). The purpose of collecting this data was to use it to train an ANN to estimate sediment thickness based on valley geometry. This meant that from the study catchment area, valley widths and sediment depth estimates needed to be extracted to be used as training data. In order to extract valley geometry data from the selected valley a series of swaths were plotted throughout the valley at approximately 500 m intervals. The start and end point of each swath were manually selected at the valley edges to produce a plot of the

valley profile. 'Valley edges' refers to the highest topography on either side of the valleys. This level of coverage was picked in order to give a full representation of the valleys shape and size. In total, 67 swaths were plotted and their locations throughout the valley can be seen in Figure 14 below. The selection of this valley was partly informed by the fact that it contains both Ushaped and V-shaped valleys indicating glacially and fluvially dominated environments. These contrasting morphologies were therefore reflected in the plotted valley profiles as can be seen in a selection of representative swaths in Figure 15. Plots a) and c) show the characteristic Ushaped, sediment filled valleys in the region. They have sloped sides and a broad flat valley bottom. The main difference between these two cross-sections is the valley floor width where a) has a total width of ~1000 m compared to ~1500 m in c). In contrast, plot b) shows the other main valley shape that can be found in the study catchment. It has steep valley walls and a Vshape, so it does not have the same flat valley floor as the other two cross sections. It is also much narrower, with the valley bottom occupying only ~200-300 m. It is important to note that the swath plotting was stopped at the point where the cross-sections were displaying more Vshapes than U-shapes, namely that there was no longer clear evidence of glacial valley fill. This data set then needed to be processed in MATLAB so that specific training data could be extracted from it. The training data was comprised both of distances from hillslope and the corresponding estimated sediment thicknesses. Distance from hillslope refers to the length from the edge of the valley floor to any point between this edge and the centre of the valley, i.e. the maximum distance from hillslope will be half of the total valley width. Sediment thickness estimates based on the valley widths extracted using the above method were found using 2 approaches which will be explained in the following section.

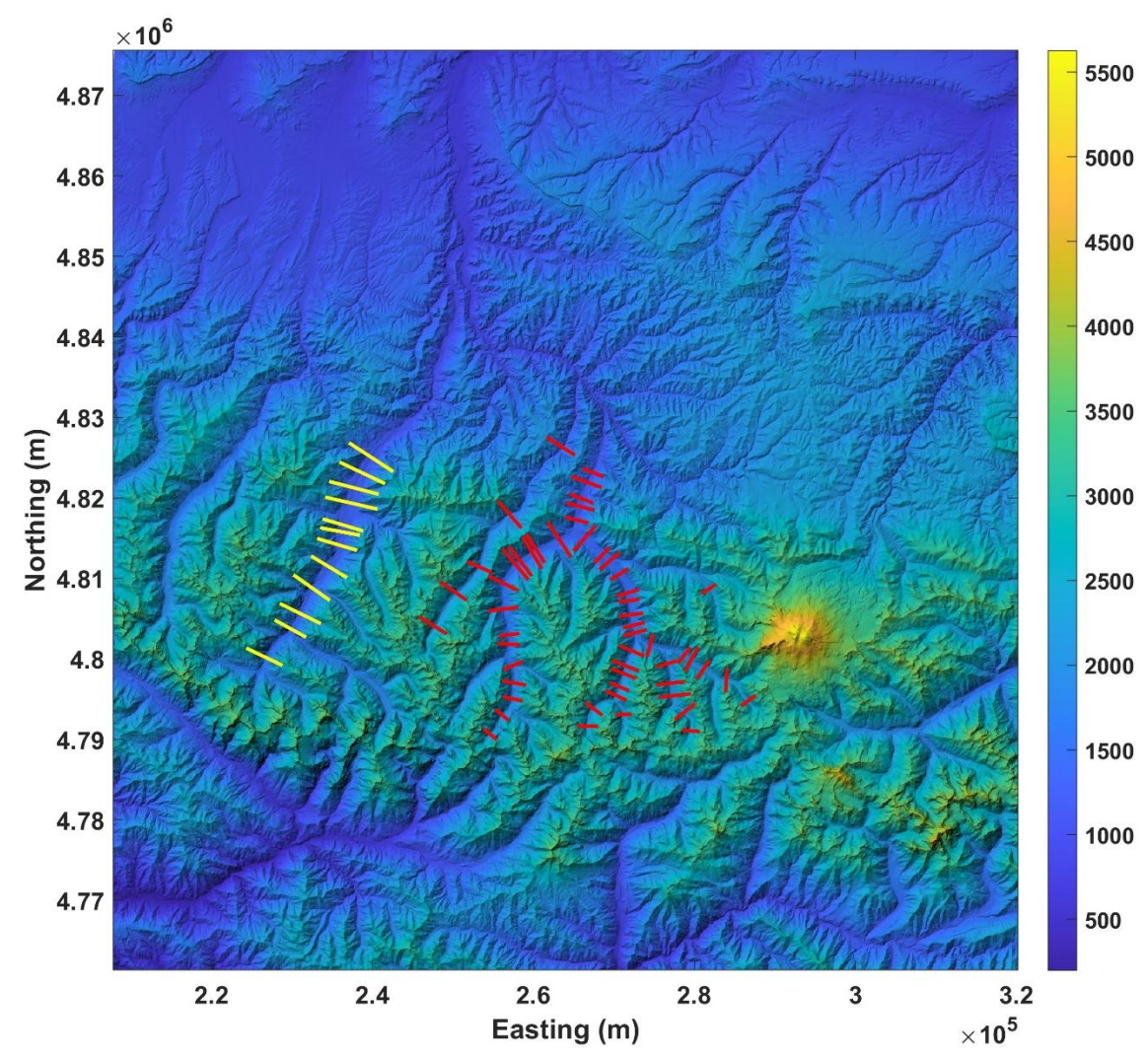


Figure 9 - Showing location of swaths plotted throughout the principal valleys of the study area.

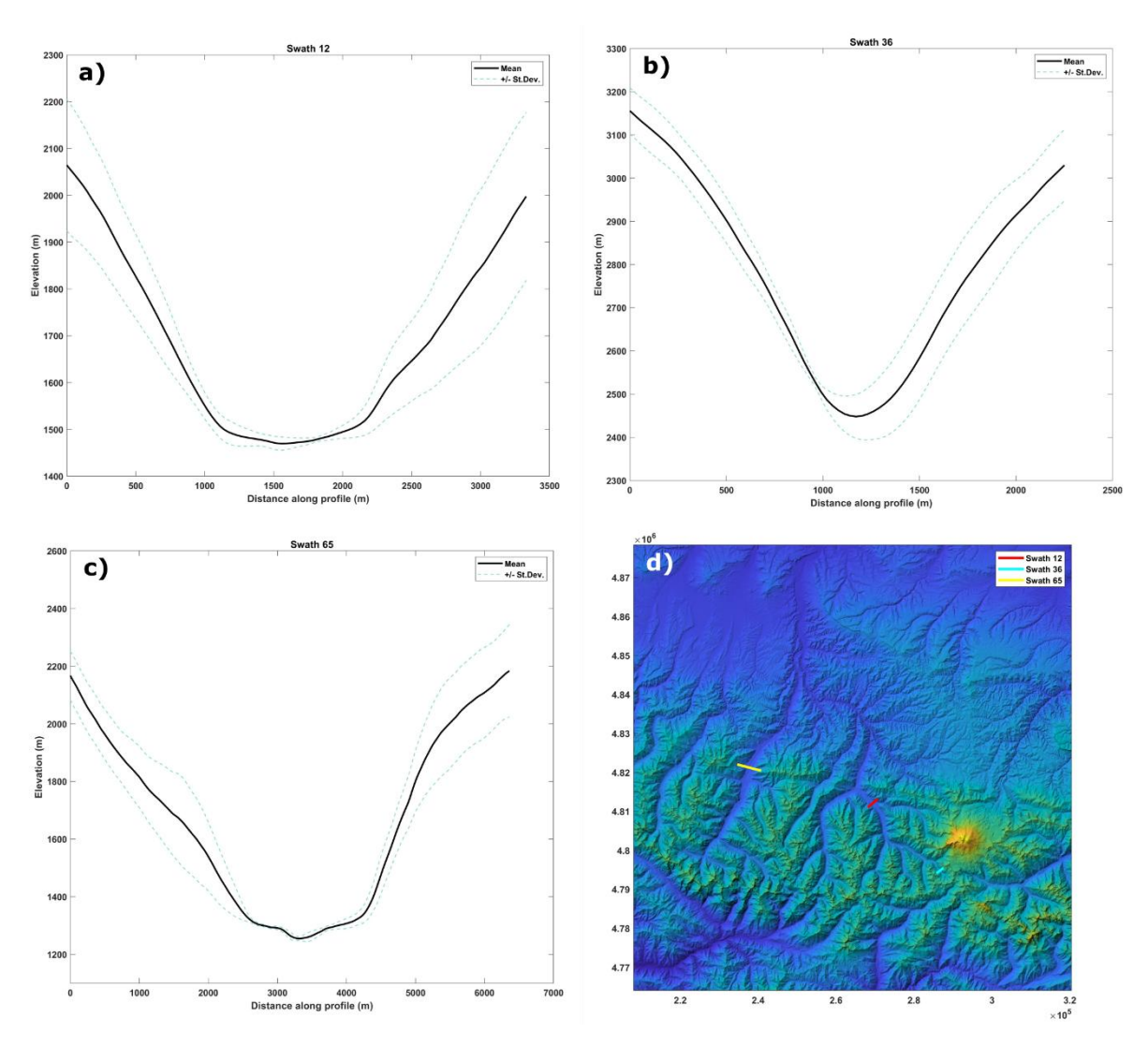


Figure 10 - Representative examples of swaths of varying shapes and their locations throughout the study valley. Note c) Swath 65 being approximately V-shaped and its location very high up in the valley. Note a) and b) having the characteristic sloping slides of a u-shaped valley with a mostly flat and level valley bottom.

## 3.3.1. Approach 1: parabola assumption

It has been clearly established that glacially eroded valleys have a characteristic U-shape. Svensson (1959) proved that this U-shape very closely matches a mathematical parabola just with some minor symmetry issues. This assumption was used to inform the methods used by Mey et al. (2015) and the same assumption has been used in this research. Due to the glacial overdeepening that has occurred in valleys in the GCM, the U-shaped valleys typically have a flattened valley floor where glacially eroded sediments have filled and levelled the base of the valley (see example in Figure 15). Without drilling or geophysical investigation, there is no clear direct way of knowing how deep this sediment fill is. However, based on the assumption

that these valleys are shaped like parabolas, the equation  $y = ax^2 + bx + c$  can be used to describe their shape where x and y represent the valley widths and resulting elevations associated with these widths respectively. This means that if the shape of the valley before it was filled with sediment can be projected using this equation, the depth of sediment filling the valley floor can then be estimated by comparing the actual valley shape to the projected valley shape. As a result of the variety of valley morphologies in the study area, this approach could not be applied to all of the swaths. Each swath was assessed individually to determine if there was enough glacial influence to plot a parabola. If there was any evidence of glacially related sediment fill, such as a U-shape and/or flat valley bottom, then a parabola was plotted. In the absence of these two criteria, the swath profile was typically clearly V-shaped with steep sides and a very narrow valley base and so no parabola was plotted. Following these criteria resulted in 54 parabolas being plotted out of the 67 swaths in total.

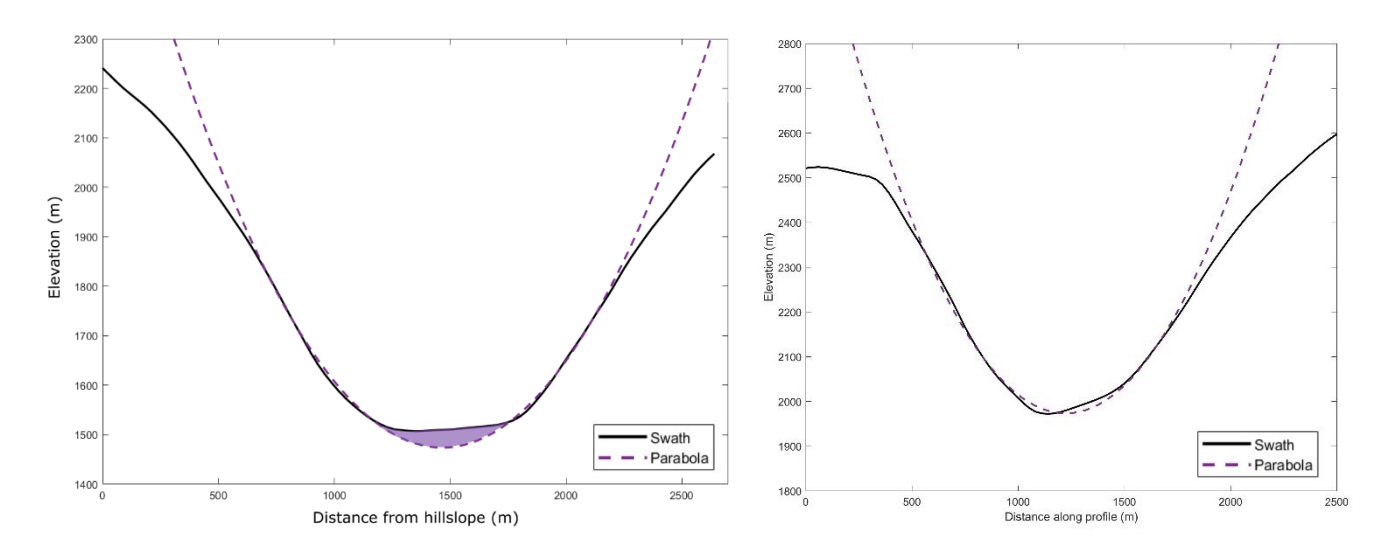


Figure 11 - a) plot showing representative swath from study valley with a well-fit parabola projection plotted and inferred valley fill shown shaded in purple and b) a representative swath with a poorly fit parabola that does not project below the valley floor.

In order to extract meaningful data for the ANN, the parabolas needed to extend below the real valley surface in order to predict any sediment fill. These parabolas were plotted by first filtering out all points along the swath apart from the steepest and straightest parts of the slopes. This was done so that the majority of the parabola would closely match the existing valley walls and therefore project the most accurate prediction of filled valley floor. The filtered-out data was used to then plot the parabola using the polyfit function in MATLAB. The ideal example of this is shown above in Figure 16a but the useable swaths were then further filtered to exclude any where the parabola did not extend below the valley profile (Figure 16b). This

left a final number of 27 swaths that could be used for training data using this approach. These swaths were then processed in MATLAB in order to extract the hillslope distances from the swath profile and projected sediment dept from the plotted parabola.

## 3.3.2. Approach 2: artificial fill

In order to generate as much data as possible to train the ANN, some of the valleys were 'artificially filled'. A similar approach was used by Mey et al. (2015) in order to validate and support their model. Adding this training data can make a model more robust as unlike the estimates of sediment depth being used from the parabola approach, the sediment depths being inputted to train the model from artificial fill are known values. The parameters for this data set were informed from preliminary results from the ANN model produced by the parabola assumption in approach one. Although the data from this approach was initially going to be used separately to train and produce a separate model, the end goal was to combine it for the final model. This meant that the sediment fill depths needed to be within the same range as what was found using approach 1. Initial sediment thickness estimates from the parabola approach yielded depths of up to ~50 m which consequently informed a maximum artificial fill depth of 50 m. Additionally, the artificial fill was applied only to the same 27 valleys which were identified to have clear evidence of glacial sediments. This is to ensure that the hillslope distances used in the ANN training data are only those associated with glacial valleys and not fluvial ones. Figure 17 below shows an example of how artificial fill was added.

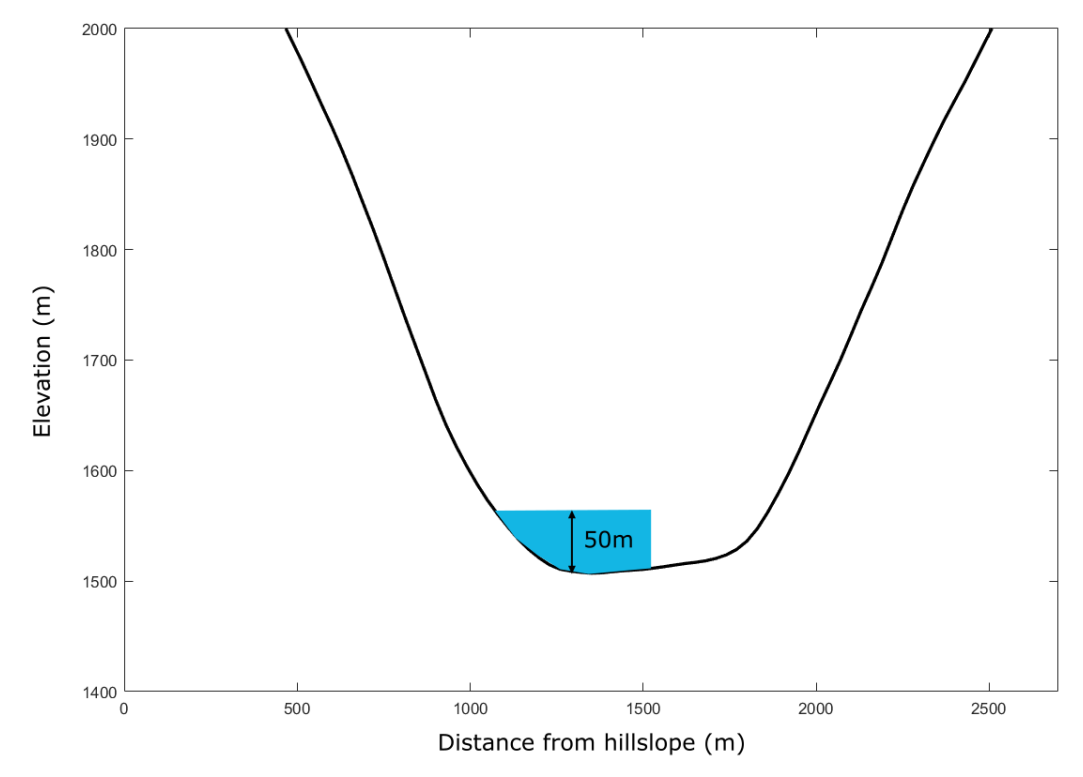


Figure 12 - Example swath showing artificial fill amount and positioning with respect to the valley floor.

Training data was obtained from these 'filled' valleys by extracting the hillslope distance values that corresponded to the first 50 m of elevation up the valley wall. As a result of the DEM resolution of 30 m, this could be done only at 30 m intervals which consequently limited the amount of data that could be manually extracted.

#### 3.4. Linear regression

One of the benefits to the ANN approach is the model's ability to predict patterns for non-linear data sets. It can be shown that the relationship between sediment thickness and distance from hillslope is approximately linear which presents the question of whether or not a more complex model such as an ANN is necessary or if a simple linear regression model would be sufficient. For this reason, the same training data used in the neural network model from both approach 1 and 2 were put through linear regression analysis in order to provide a comparison. This was done using the regression learner app in MATLAB and was applied using both approaches to produce the plots shown below in Figure 18.

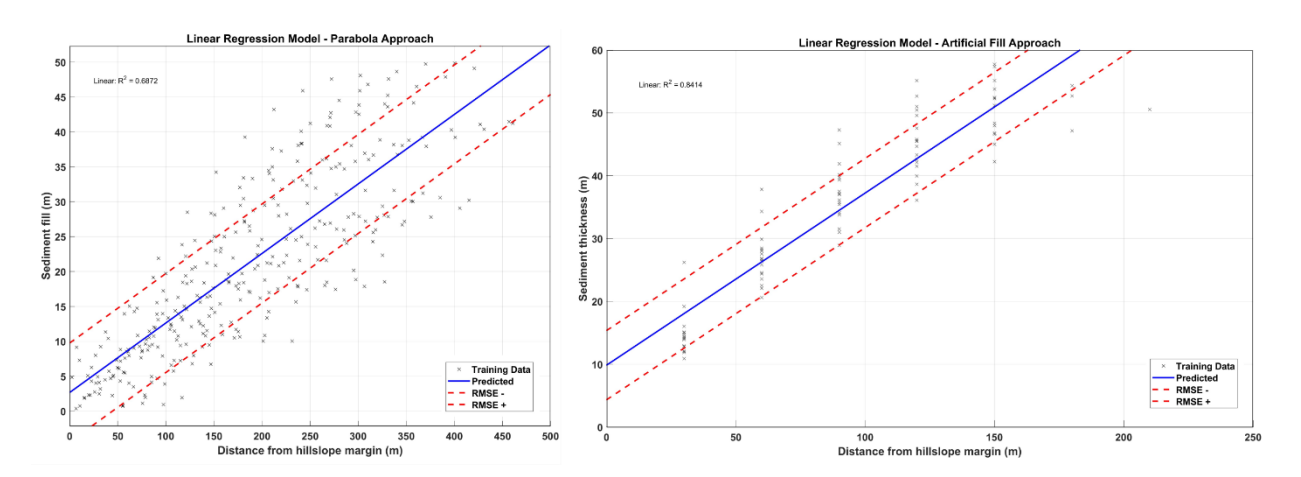


Figure 13 - Plots of linear regression models produced from the parabola (left) and artificial fill training data (right) approaches. Note variations in axis and therefore in gradient of prediction line.

The focus of this research was to estimate sediment fill using ANNs and therefore the inclusion of these simple regression models was solely for the purpose of assessing the effectiveness of the ANN in this context. This will be discussed in further detail in Chapter 5.

## 3.5. Model development and progression

Section 3.1.2. explained the process for training the ANN model which was then applied to both approach 1 and approach 2 both explained above in sections 3.3.1. and 3.3.2. respectively. As previously established, 67 swaths were plotted and used to generate training data for the ANN model. However, initially only 55 swaths were plotted and used. The initial focus of data collection was on the eastern set of valleys within the study area (see Figure 14), so that the remaining valleys within the locality of the study area could be used for testing the resulting model. The model from approach 1 generated from this training data can be seen in Figure 19 below. The axis on the produced models show sediment thickness i.e. the depth of sediment fill at the deepest point which is assumed to be in the centre of the valley, and distance from hillslope i.e. the distance from the edge of the valley to the valley centre point. This means that it can be assumed that if the maximum distance from hillslope in part of a valley is 300 m, then the valley is 600 m wide. The model shows that based on this training data, sediment thicknesses of up to ~40 m can be predicted for valleys with a maximum width of ~900 m.

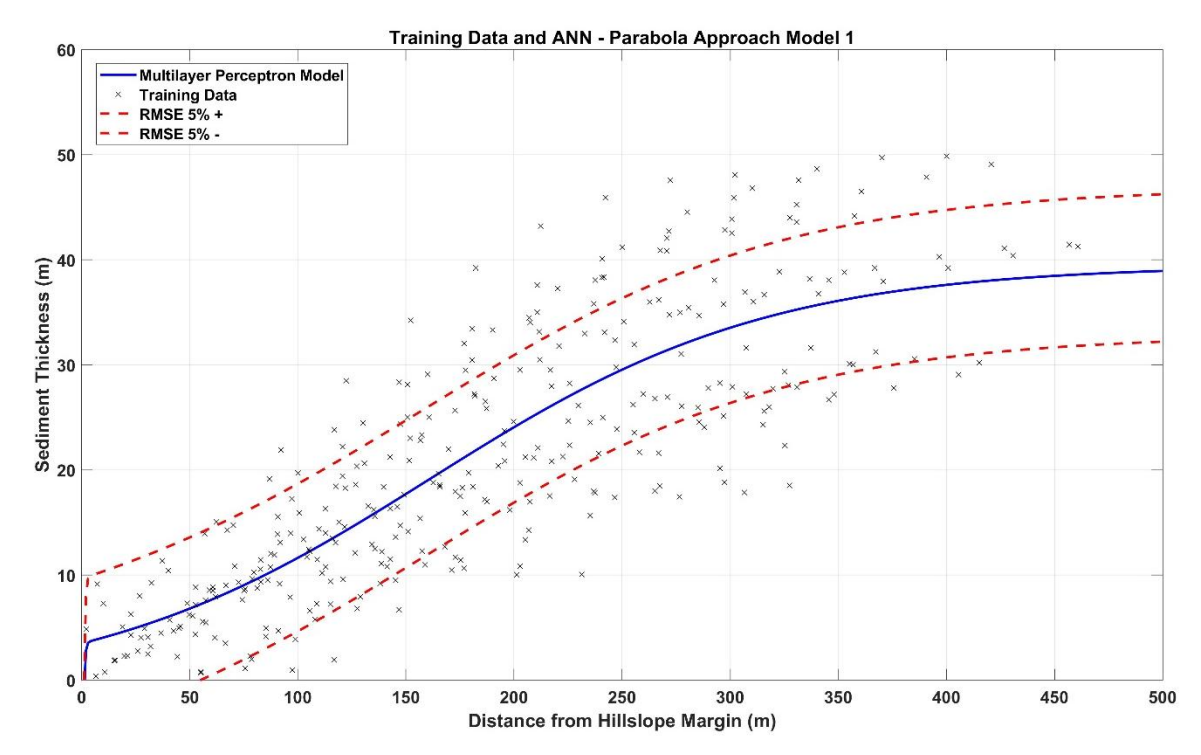


Figure 14 - Plot showing ANN model prediction produced from parabola approach training data, including training dataset, root mean square error (RMSE) window.

The model was then reproduced using the artificial fill training data from approach 2 which can be seen below in Figure 20.

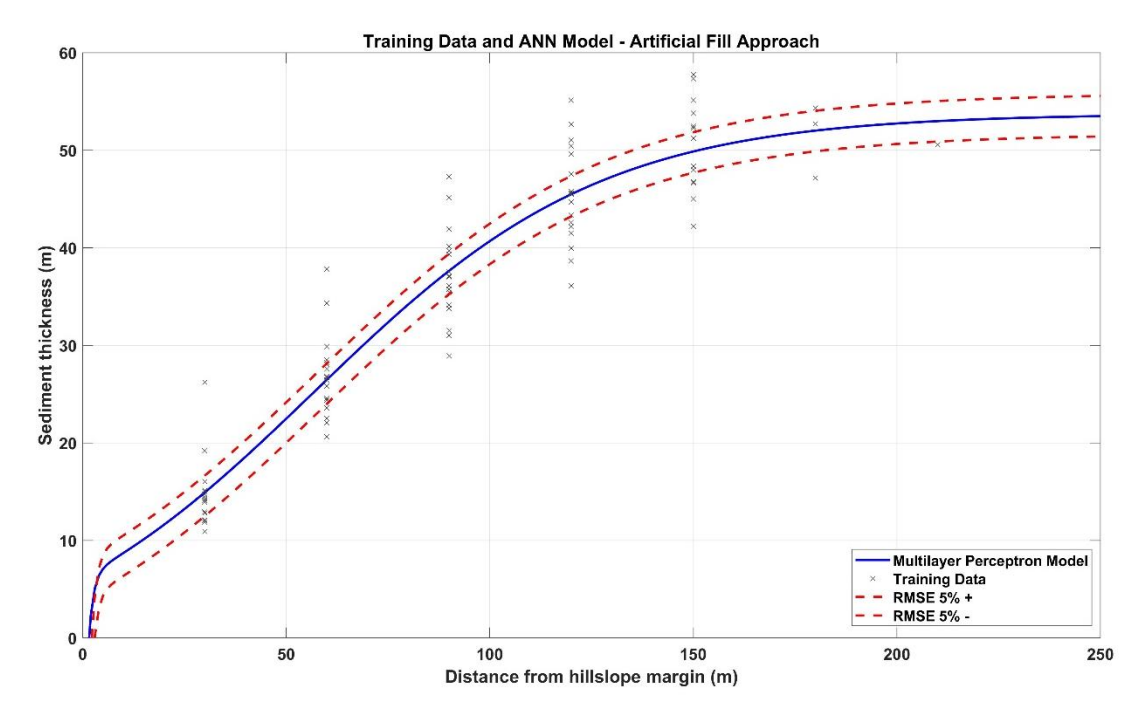


Figure 15 - Plot showing ANN model prediction produced from artificial fill approach training data, including training dataset, root mean square error (RMSE) window.

One of the key observations from this model is that although there is a much smaller RMS error attached to the prediction, the majority of the training data does not sit within this error window. This is likely due to the concentration of data points as the resolution issue that came with this approach is also very apparent with the 30m gaps between sets of data points. Additionally, in comparison with the parabola approach, the predictive power of this model in terms of range of valley widths is significantly lower as that distance from hillslope data reaches a maximum of ~200 m. This data was then combined with the data from approach 1 to produce a combined model prediction. This can be seen in Figure 21 below.

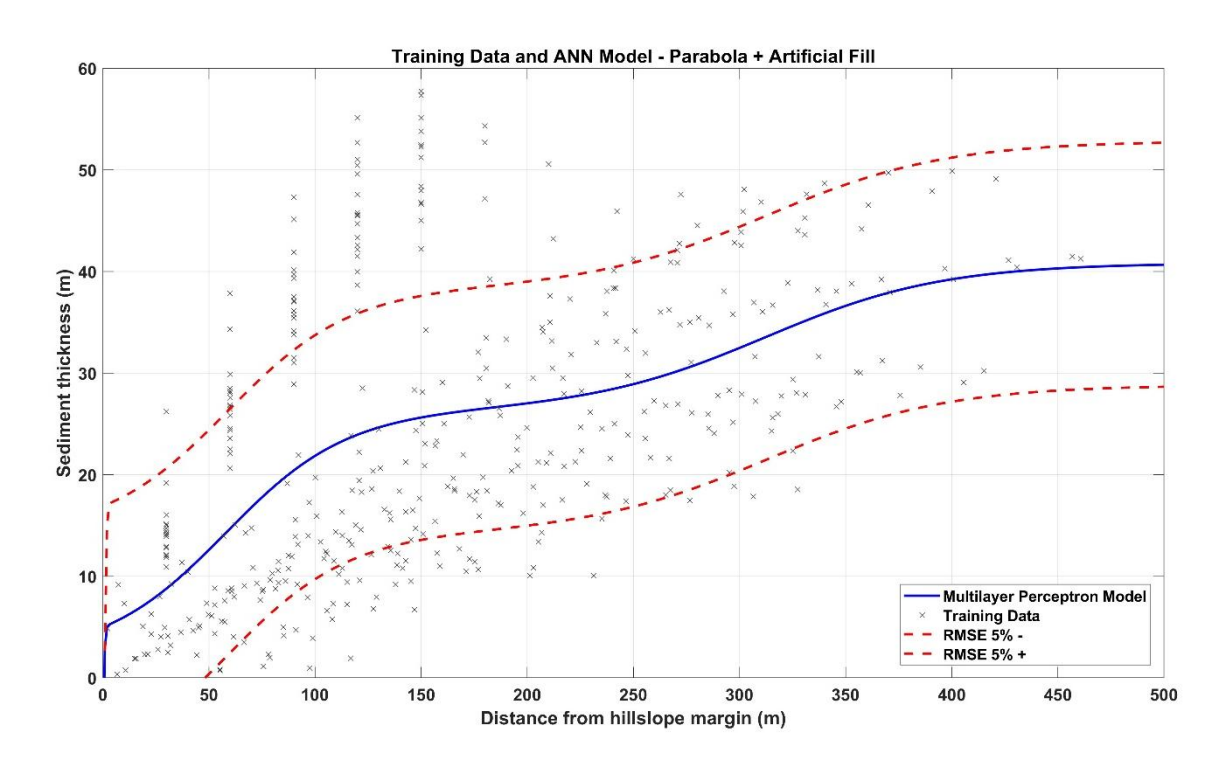


Figure 16 - Plot showing ANN model prediction produced from the combination of training data from the parabola and artificial fill approaches, including training dataset, root mean square error (RMSE) window.

It is clear from Figure 21 that the two data sets do not combine well, with the sediment thicknesses increasing with hillslope distance at a much steeper gradient than the parabola assumption training data. This is likely due to the part of the valley which has been artificially filled. The fill thicknesses found from the parabola approach are estimated from the parabola extension beneath the valley floor. This means that they are associated with the hillslope distances where the valley bottom is at its flattest point with the lowest slope values. The fill thickness from the artificial fill approach sit above the valley floor. This means that the same hillslope distance values are corresponding to fill thickness at points where the valley slides begin to increase in slope as seen in Figure 17. Consequently, the gradient at which the thicknesses increase with hillslope distance are much steeper compared to with the parabola assumption, causing the two data sets to not combine. As a result of the failure of the model combination, the model development was then focused solely on approach one, bringing the focus back to the parabola approach model 1 in Figure 19 and how it could be improved.

The final model produced can be seen in Figure 22. This model has an improved predictive power, where it can predict sediment thicknesses up to ~140 m corresponding to valleys with

a maximum width of ~2000 m. The training data set includes all hillslope distances and sediment thickness estimates found from the parabola approach from all the swaths plotted in Figure 14. The yellow swaths seen in this figure plotted in the westernmost valley of the study area contributed larger valley widths thus expanding this data set. This meant that the model could better satisfy the goal of applying it across other valleys in the GCM as more valley widths and variations in valley width could be included.

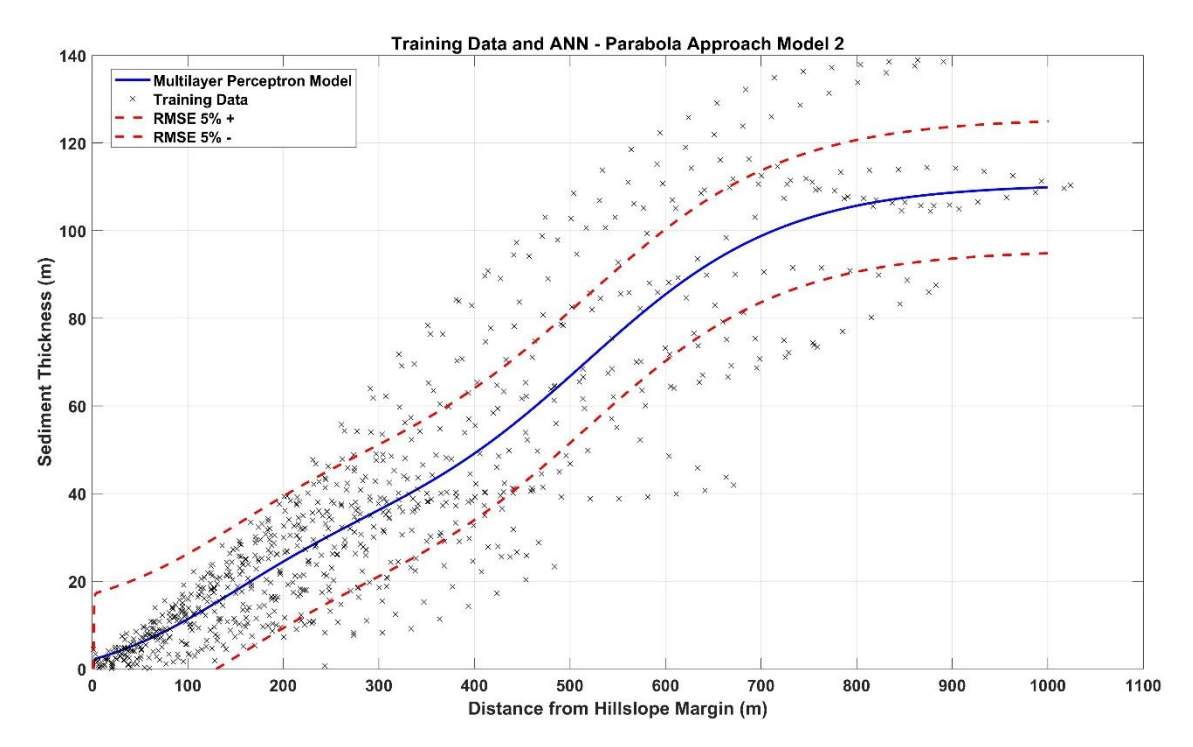


Figure 17 - Plot showing  $2^{nd}$  version of ANN model prediction using parabola approach training data, including training dataset, root mean square error (RMSE) window.

#### 3.6. Model application and volume calculation

The main aim of this research was to estimate a total volume of glacial sediment within valleys in the north-western Caucasus. In order to do this, there were two main challenges: first was to find a way to translate the valley geometry data and estimated sediment thicknesses into a volume calculation, and second to scale this method up across other valleys in the Caucasus. Distance from hillslope values and sediment estimates had already been extracted from the study valley for training data so this was the starting point for a volume calculation. It was necessary to consider that the sediment thickness and valley width are changing throughout the valley and therefore the calculation needed to account for this in order to get the most accurate

volume calculation possible. This led to using the formula for the volume of a truncated ellipse which can be seen below.

Equation 1 – Adaptation of formula for the volume of a truncated ellipse.

$$2V = \frac{1}{3}\pi h(a_1^2 + a_2^2 + b_1^2 + b_2^2 + a_1a_2 + b_1b_2)$$

Where:

a = distance from hillslope

b = sediment thickness

h = distance between transects

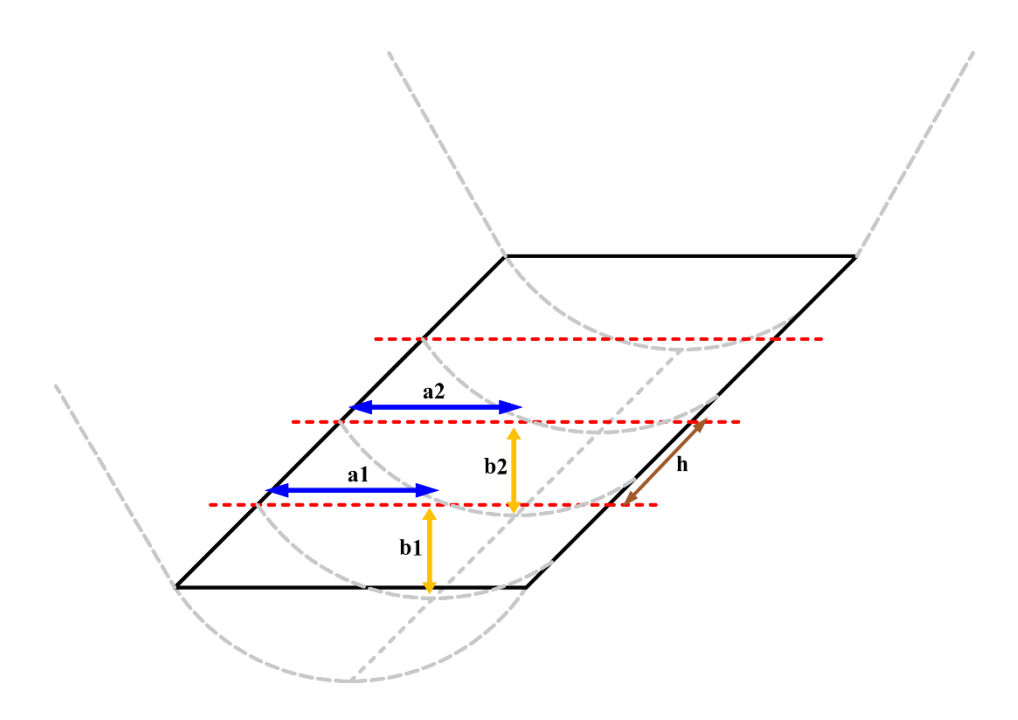


Figure 18 - Diagram showing half ellipse formula applied in the context of the valley structure with respective hillslope distance (a) and sediment thicknesses (b) shown.

To find the volume for the whole valley, the formula above was applied to each of the 500 m sections divided by the transects and each of these individual section volumes summed together to find the total valley volume. In order to scale this up across other valleys in the GCM, it was necessary to establish a method to obtain distance from hillslope values (i.e. the ANN inputs)

from other valleys in order to run them in the ANN model to get sediment depth estimates. This was done using ArcGIS where areas of the valley floors that showed sediment fill were mapped.

The criteria for determining whether or not there was glacial sediment fill present were based on a combination of satellite imagery and elevation data. Firstly, a topographic map was filtered based on slope angle to try to isolate the mostly flat valley floor. This was done in combination with looking at satellite images in order to ensure that the slope range included encompassed the full valley floor. This resulted in a range of slopes from 0-14° which included all of the valley floors. However, due to the nature of the local geomorphology, this also included many areas of the Caucasus where the slope angles can still be low but are beyond the valley floor such as small plateaus and ice-covered surfaces. As a result of this, once the topographic map had been filtered down to the shallowest slopes, polygons of the outline of the valley floor were plotted using a combination of this filtered map and the satellite imagery which had helped inform it. The distance from hillslope data from the training data was a measure from the edge of the valley floor i.e. beginning of change in slope to the valley walls, to the centre point of the valley. The process then followed in order to extract the data needed for the volume calculation can be seen below.

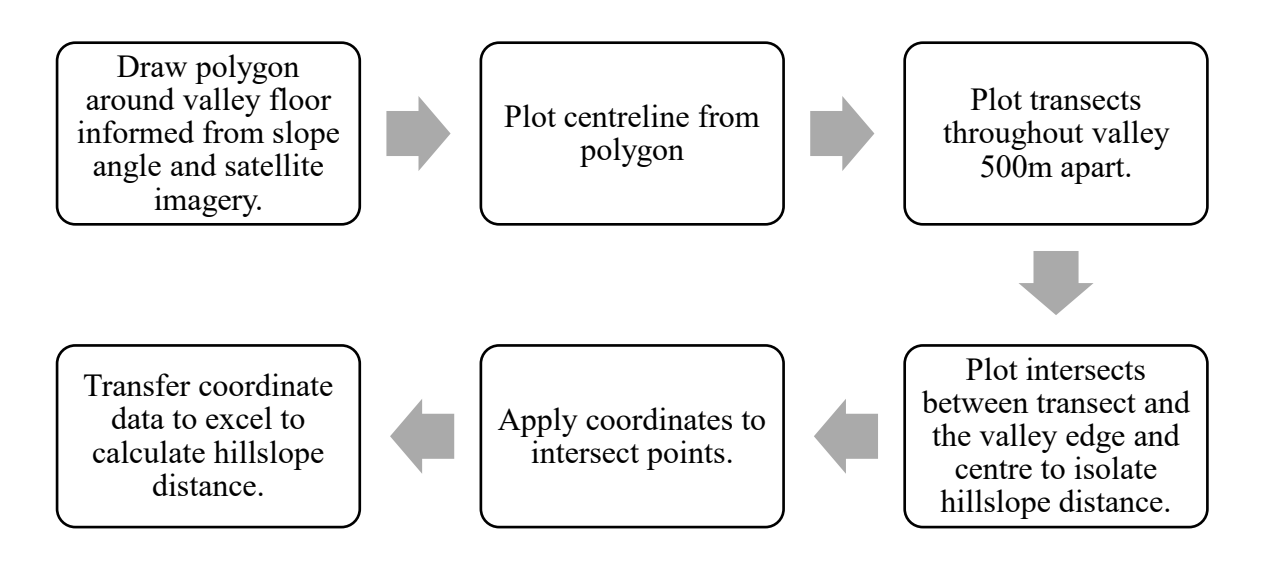


Figure 19 - Flow chart showing workflow used to extract hillslope distance values from valleys using ArcGIS.

Once this process had been followed, the calculated hillslope distances were then run through the trained ANN model to produce sediment thickness estimates for each valley and this combination of data could then be fed into the formula above to generate a volume estimate.

#### 3.6.1. Error calculations and propagation

Once a volume had been estimated for each individual valley, the model was applied to (including the training catchment), the next step was to calculate an error for the volume calculation. The sediment thickness estimate error is based on the accuracy of the predictions in the ANN model. As shown in Figure 22 this was a root mean square error (RMSE) founded on a 95% prediction interval. A range of prediction intervals from 5-20% were tested to see how well the model performed. This involved using a random sample selector function in MATLAB to randomly select and remove 5%, 10%, 15%, or 20% of the data and calculate the RMSE based on the remaining values. Increasing the percentage of data removed did not have a significant impact on the calculated error and so the RMSE including 95% of original data was used so the most amount of data was still represented. The distance from hillslope data was generated by drawing polygons around the valley floor area and therefore the error from this data should be based on the accuracy of this selection. In order to calculate this, the widest valley (the western valley within the training data catchment area) was selected to have the valley floor area polygon replotted 10 times. From this, 3 of the transects throughout the valley were picked from south to north with varying widths and the distance between the intersect point from the original polygon and each of the 10 polygons was measured on both ends of the transect. The mean of the difference between these points was first calculated for each of the 3 transects per polygon, with the final absolute error calculated from the mean of those 10 values.

Following on from finding the absolute error of the sediment thickness estimates and distance from hillslope, the overall error was then found for the volume calculation by propagating these two errors through the volume formula. This was done by using the general formula of error propagation by finding the derivatives of each value in respect to the volume and combining these to find the total absolute error for V or  $\sigma V$ . This followed the same process used for the initial volume calculation, with  $\sigma V$  found for each 500m transect then combined together for the whole valley following the rules of error propagation (i.e.  $\sigma V = \sqrt{(\sigma_a^2 + \sigma_b^2...)}$ ). The resulting formula for calculating the absolute error for each transect was as follows:

Equation 2 – Formula for propagating absolute error of a (distance from hillslope) and b (sediment thickness)

$$\sigma V = \sqrt{(\sigma_{a1} * dV da_1)^2} + (\sigma_{a2} * dV da_2)^2 + (\sigma_{b1} * dV db_1)^2 + (\sigma_{b2} * dV db_2)^2$$

Where:

$$dVda_1 = \frac{h * \pi * (2a_1 + a_2)}{6}$$

$$dVda_2 = \frac{h * \pi * (a_1 + 2a_2)}{6}$$

$$dVdb_1 = \frac{h * \pi * (2b_1 + b_2)}{6}$$

$$dVdb_2 = \frac{h * \pi * (b_1 + 2b_2)}{6}$$

V = Volume

 $h = distance\ between\ transects$ 

a = distance from hillslope

b = sediment thickness

#### 2.1.1. Volume to weight conversion

Part of the background context behind this project was to consider the magnitude of glacial isostatic adjustment as a result of glaciation and glacial retreat in the Caucasus. With an estimate sediment volume, it is simple to estimate a total weight associated with this quantity of sediments. This can be done using the simple formula shown below.

Equation 3 – Formula for calculating sediment weight from density and volume.

$$m = \rho * V$$

Where:

m = mass

 $\rho = \text{density}$ 

V = volume

This requires an estimating of the density of the glacial sediments found in the valley. In order to do this, it is necessary to establish a density for glacial sediments. Clarke (2018) found that the density of glacial till ranges from  $\sim 1.9 - 2.3$  g/cm<sup>3</sup>. These values vary as a result of differing levels of water saturation of the sediments. As water saturation is not a constant throughout sediments, both spatially and temporally, for the purpose of this thesis the median density will be used with the range of other possible densities taken into account for the overall error of the weight. The median density value is 2.1 g/cm<sup>3</sup> so from the range of other possible values the error margin is  $\pm 0.2$  g/cm<sup>3</sup>. The units used to report the depths and distances in this thesis have been reported in metres, so the literature reported density value are converted into kg/m<sup>3</sup> using a conversion factor of 1000. The density value therefore used in the below formula is 2100 kg/m<sup>3</sup>. This is a simple multiplication calculation, so the error was calculated as follows:

Equation 4 – Formula for the calculation of error for mass estimation.

$$\frac{\delta m}{m} = \sqrt{\left(\frac{\delta \rho}{\rho}\right)^2 + \left(\frac{\delta V}{V}\right)^2}$$

# 4. Results

The aim of this research was to calculate a volume of glacial sediments for as much of the north-western Caucasus as possible. As explained in the methodology, this involved applying the established process across the training catchment area and then onto other valleys. In total, this method was applied to 7 valleys (inclusive of the training catchment) which can be seen in Figure 25 below.

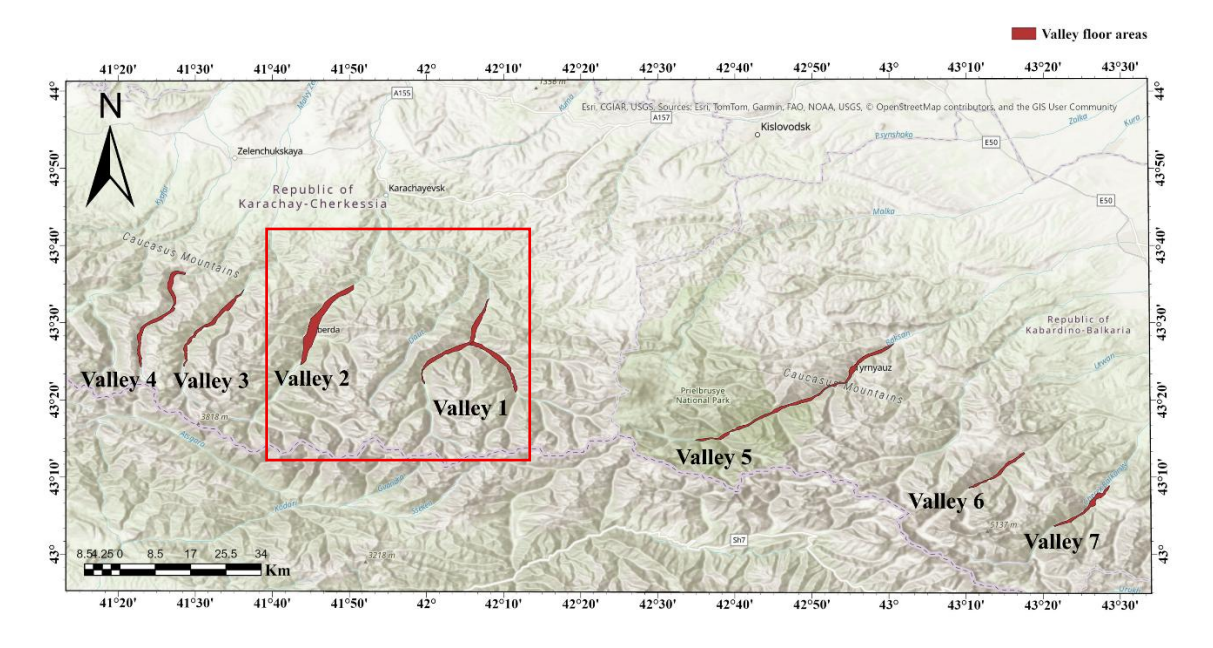


Figure 20 - Map showing location of valleys extracted from the NW and NC Caucasus shown as red polygons. Valleys used for training data (1 and 2) are shown outlined in the red box.

Figure 25 shows valleys 1-7 split by two groups. Valleys 1-4 are all within the north-western (NW) Caucasus and valleys 5-7 within the north-central (NC) Caucasus. The calculated volumes of each of these valleys can be seen below.

Table 1 – showing valleys where method was applied to with their calculated volumes and corresponding geometries. NW refers to the valleys found in the north-western Caucasus, and NC to valleys in the north-central Caucasus.

Valley Number	Length (km)	Average width	Volume (km³)
		(km)	
1 (NW)	40.9	0.77	$8.83 \pm 0.46$
2 (NW)	22.2	1.39	$14.97 \pm 0.60$
3 (NW)	22.7	0.65	$3.54 \pm 0.29$
4 (NW)	27.6	0.66	$4.05 \pm 0.31$
5 (NC)	44.1	0.61	$6.50 \pm 0.40$
6 (NC)	13.3	0.54	$1.37 \pm 0.18$
7 (NC)	14.4	0.69	$2.79 \pm 0.26$

These results show that there is a significant quantity of glacial sediments being stored in valleys in the GCM both in parts of the NW and NC GCM, with the valley with the greatest fill being found in the NW Caucasus. The total volume of sediments in all of these valleys combined is  $42.05 \pm 1.01$  km<sup>3</sup>. Figure 21 shows that there are some valleys and some parts of the chosen valleys where there are not any plotted polygons. This is due to there not being sufficient evidence – based on the workflow established in the methodology – to definitively say that there was glacial sediment fill within these valleys. For example, there were many parts that were clearly V-shaped and therefore fluvially dominated, meaning that it was not possible to attribute sediment formation to glacial processes. It was established in Chapter 2 that there are clear differences between the western and central, and eastern Caucasus in its climate, geology, and glacial history. The plotted valleys are therefore limited only to the NW and NC Caucasus due to limited confidence in there being enough robust similarities between this part of the GCM and the eastern Caucasus to apply the model there.

In addition, these results show that there is the strongest correlation between the average valley width and sediment fill volume which has an R-value of 0.91, corresponding to a p-value of 0.001 (see Figures 26 and 27). In comparison to this, there is a very weak correlation between

the valley lengths and sediment fill volume with an R-value between these two metrics of 0.35, corresponding to a p-value of 0.217 (See Figure 28). This therefore highlights how the valley width has the greatest influence on the volume of glacial sediments found in valleys in the GCM.

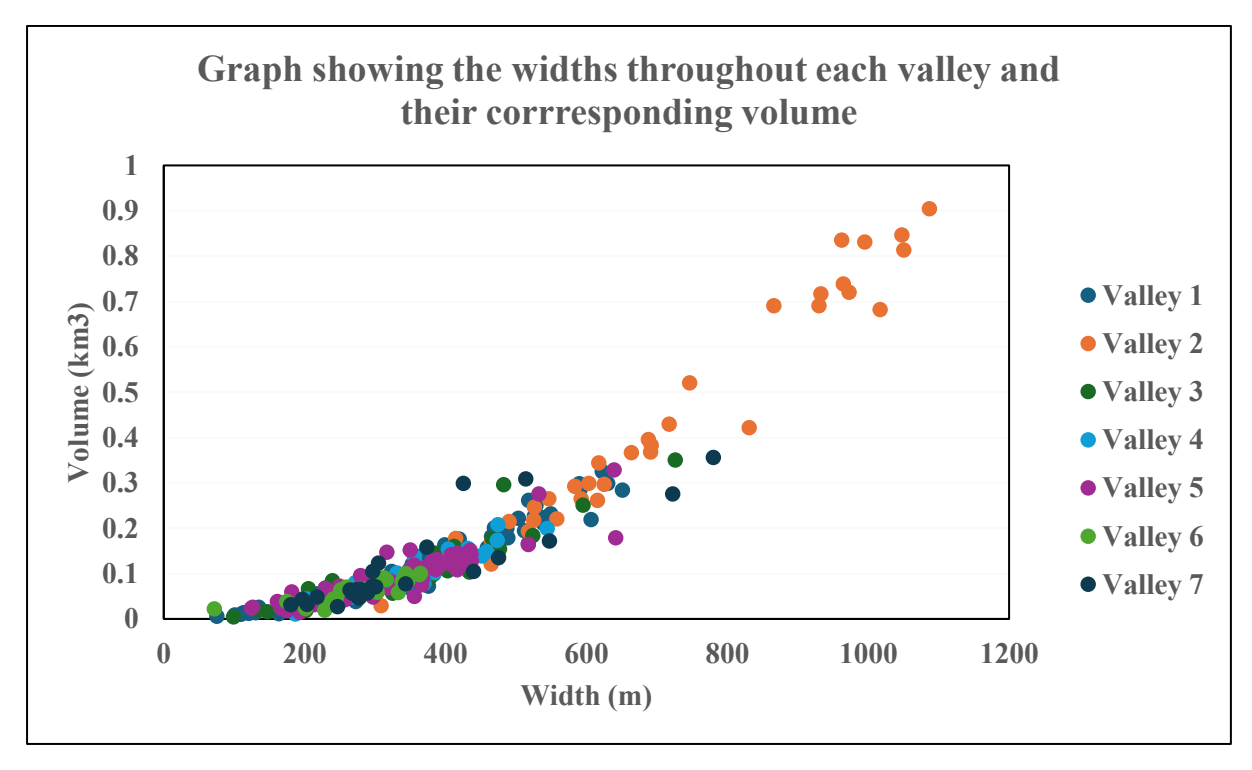


Figure 21 - Graph showing with volume of each transect and its corresponding valley width for each valley, demonstrating that the transect volume increases linearly with valley width.

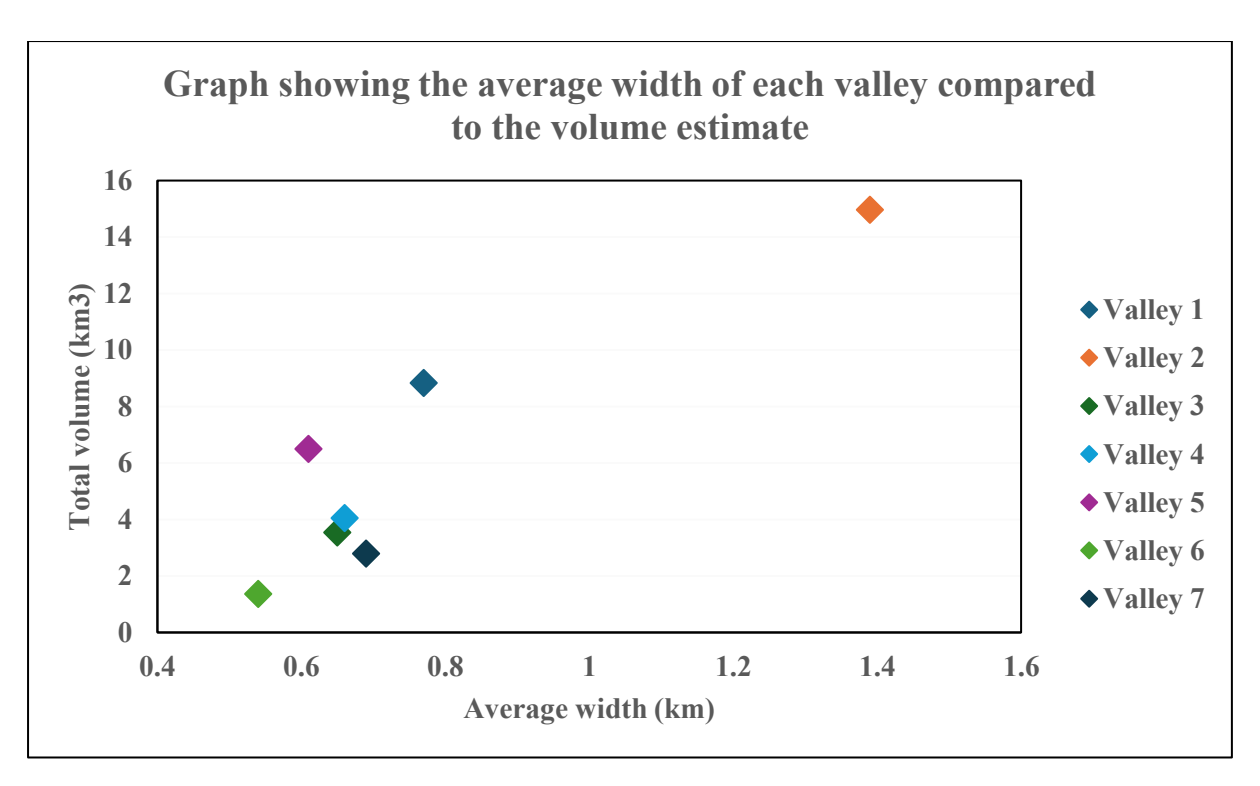


Figure 22 - Graph showing the total volume of each valley against average valley width.

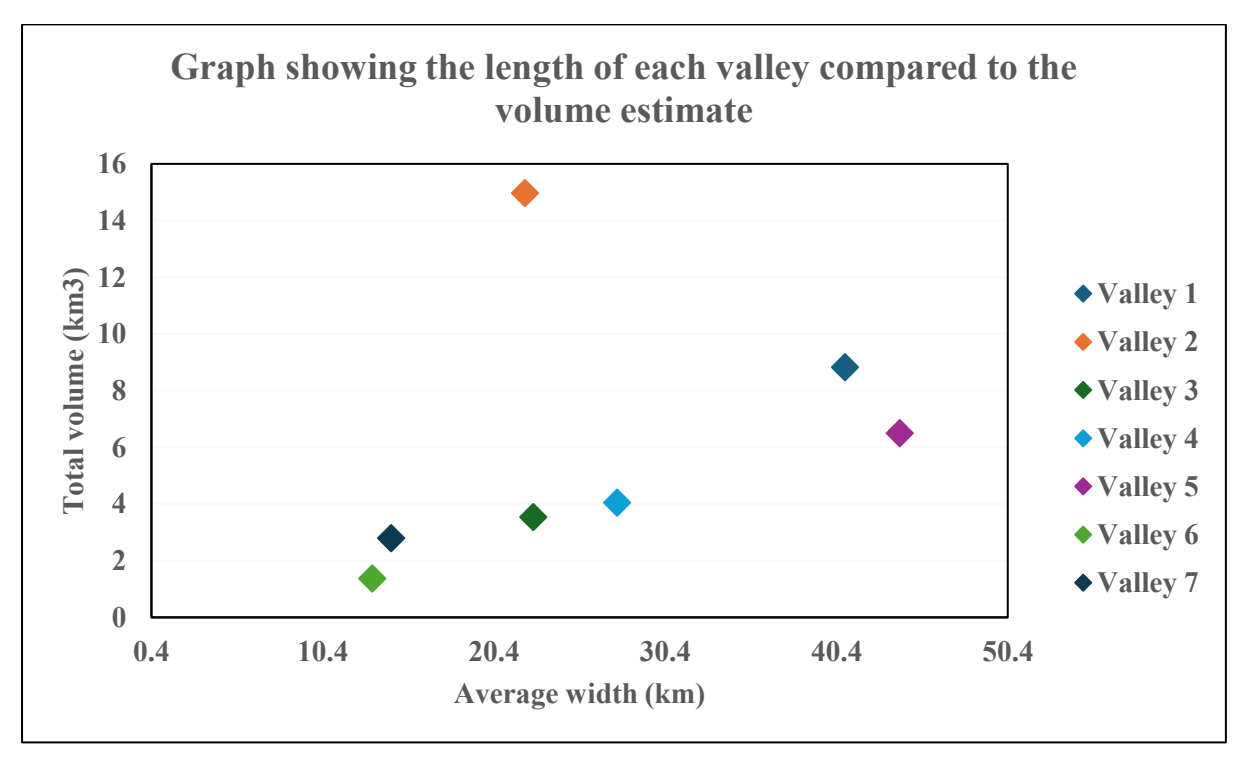


Figure 23 - Graph showing total volume of each valley against valley length.

## 4.1. Conversion to sediment weight

Section 3.6. explained how this volume would be used to estimate a total mass of these sediments in order to consider the isostatic impact. This found a total sediment mass for the 7 valleys of  $8.83 \times 10^{13} \pm 8.67 \times 10^{12}$  kg. As this calculation is directly based on the valley volumes, the same relationships between this mass and the valley geometries applies. The implications of this result will be discussed in the following chapter.

## 5. Discussion

### 5.1. Key results and results context

To summarise, the results showed that there are large quantities of sediments within valleys in the GCM, totalling  $42.05 \pm 1.01 \text{ km}^3$  across a selection of valleys in the north-western and north-central Caucasus. As this is an estimate which has been produced without validation or support from direct measurements, it is important to establish whether or not this volume estimate fits in with other glacial sediment volume calculations. There is limited access to volume estimates or calculations for glacial sediment fill in other regions that can contextualise these results either due to lack of similar research or estimates not being done over the same scale. Another challenge is finding published estimates that may have all of the same metrics to compare, namely the valley widths or lengths associated with a volume or the associated maximum sediment thicknesses. This is due to this being a fairly novel approach and so other methods have either been supported by direct measurements or are based on scaling methods. Table 2 below shows a compilation of examples of sediment volume with the available supporting data in order to contextualise the results of this research.

Table 2 - Showing sediment fill volumes for other glaciated regions with supporting data where applicable (<sup>2</sup>Aarseth, 1997; <sup>3</sup>Hinderer, 2001 and Mey et al., 2015; <sup>4</sup>Syvitski et al., 2022; <sup>5</sup>Pomper et al., 2017)

Location	Avg. Valley length (km)	Avg. Valley width (km)	Maximum sediment depth (m)	Sediment fill volume (km³)	Direct measurements (Y/N)	Notes
Russia						
<sup>2</sup> Western	90	N/A	430	150	Y	All fjords between
Norwegian Fjords						59-63° latitude
<sup>3</sup> Rhone basin,	120	6	N/A*	$106 \pm 15$	Y	*Mean depth of
Swiss Alps						360m
<sup>4</sup> Baffin Fjords,	57	3.6	26	38.1	Y	
Canada						
<sup>5</sup> Lower Salzach	25	4 <sup>†</sup>	338	17	Y	1 valley
Valley, Austria						†Maximum width

It is important to note the variation in location and type of glacial environment involved in these examples. For example, the studies 2 and 4 relate to glacial sediment fill found in fjords environments, rather than mountainous valleys like those in the GCM or Alps. As explained in section 2.3., intense glacial erosion can result in valley overdeepening and the formation of troughs which are then infilled with water or sediments as the ice retreats. This highlights how similar processes have occurred to result in fjords and sediment fill. However, this is also an important distinction as it means the sediments found in fjords are additionally under the influence of lacustrine and marine processes. The result of this can been seen in the example of the western Norwegian fjords seen in table 2. Aarseth, (1997) identified a maximum depth of the sediment fill in this region of 430 m, highlighting the stark difference in the extent of overdeepening found here compared to in the GCM. Conversely, the Baffin fjords in Canada were found to have a significantly shallower maximum fill depth of 26m (Syvitski et al., 2022). This is also the region with the most similar value of reported sediment fill volume, although the geometries of the Baffin fjords are notably different, with the troughs on average being approximately double the length and triple the width of the valleys in the GCM. As some of these examples are missing parts of the contextual data that accompanies the Caucasus such as the associated sediment depths and widths, it can be difficult to provide a good comparison of volume estimate. This is further hampered by the variations in locations and therefore geomorphologies and glacial histories that have influenced the volumes of sediments infilling valleys. Nevertheless, these examples show that the valley fill volume estimate found for this study for the GCM sits within the same order of magnitude as in other regions globally. Additionally, one important similarity between each of these data sets is that they are all in areas that have experienced significant glacial retreat but still with some glaciation present.

## 5.2. Uncertainties

The nature of the approach used in this thesis means that there are reasonably high levels of uncertainty associated with the results. This uncertainty originates from several places. In the methodology, there were three main assumptions made concerning valley morphologies in the Caucasus and the sediments found within them. The first of these assumptions was that glacially derived sediments would be found mostly in U-shaped valleys, as these are valleys characteristic of intense glacial erosion (e.g. Grotzinger and Jordan, 2014). This was a justifiable assumption as there needed to be a starting point in establishing the location of

glacial sediment fill within the GCM in order to generate training data for the ANN, and the concept of U-shaped valleys being of glacial origin has been thoroughly demonstrated (e.g. Svensson, 1958; Graf, 1970). However, despite being justifiable, this assumption is a still a source of uncertainty in the results. Assuming that the bulk of glacial sediments are only found in these U-shape valleys has likely excluded a proportion of sediments found in other (i.e. V-shape) valleys from the sediment volume, meaning that the total volumes quoted in the results is potentially an underestimate.

The second assumption is that the sediments found within these U-shape valleys are of glacial origin. This is one of the biggest assumptions that has been made as there are limited direct published observations of the nature of sediments within the GCM from which to rely upon. Consequently, this assumption was based upon research from other regions such as the Alps where it has been demonstrated that glaciation overprints the past landscapes (Schlunegger and Norton, 2013). Although founded on research from similar areas, this is a weighty assumption as there will not necessarily be the exact same conditions in the GCM as in certain valleys in the Alps. The consequence of this assumption is that there may be sediments being included in the fill thickness and thus volume estimates that are not of glacial origin.

The final main source of uncertainty in this thesis is sourced from limitations of the parabola approach to generate training data. As explained in section 3.3.1., this approach was used in order to estimate the thickness of glacial sediments stored within overdeepened valleys without the need for direct measurements. This proved to produce estimates of valley fill thickness and consequently fill volumes comparable to in other glaciated regions, showing this to be an effective method. However, as this is an estimate, and one from which results have been upscaled, any inconsistencies or issues in this method could be amplified. For example, there may be uncertainties stemming from the method used to fit the parabolas to the swaths. They were plotted based on an extrapolation from the steepest and straightest parts of the valley wall in order to project below the valley floor. The parabolas were judged to have a good fit based upon how closely the shape matched the existing valley wall shape, and how well they projected below the valley floor (see explanation and examples in section 3.3.1). The limitation of this is that there are likely to be variations in valley geometries throughout the study area due to influences such as slope processes. These variations in valley geometries can be as a result of slope failures such as mudflows and landslide, events that have increased in the GCM and continue to increase with glacial retreat (Kos et al., 2016). As a result of this, the valley

cross-sectional profiles may begin to deviate from the characteristic U-shape associated with glacial landscapes. This could mean that there are swaths which were excluded from the training data set due to having a poor parabola fit but may still have had quantifiable sediment fill. The impact of this on the results of this thesis is that the volume estimate could be an underestimate, and perhaps if a more statistically based method had been used to determine parabola fit, more swath profiles could have been included with the benefit of both increasing the training data set and making the total volume estimate potentially more accurate.

It is important to note that as explained in section 3.6.1., the final error calculation is based upon the absolute errors that originated from the method used to find sediment thickness and valley width, the two metrics used in the final volume estimate. This means that these errors may not the perfect reflection of the approximation involved in the derivation of these numbers and instead reflect the precision of the ANN model approach rather than its accuracy. In the absence of having direct measurements as a measure of the accuracy of the findings of this thesis, this was the alternative that could be used in order to provide some judgment of the estimate.

## 5.3. Result Implications

#### 5.3.1. Relationship between valley width and volume

The results identified that there is a clear relationship between the valley width and sediment volume. As the volume is calculated from the hillslope distance (half valley width) and sediment depth this is therefore directly related to the link between the valley width and maximum sediment thickness. Coupled with this relationship shown in the results is the flattening observed in the ANN model prediction shown in Figure 22 in section 3.5.. Throughout most of the model prediction, sediment thickness increased with hillslope distance whereas once the hillslope distances reached ~750 m, the sediment thickness prediction curve began to flatten. The implications of these results is that there appears to be a limiting factor on either the maximum depth of overdeepened valleys, or the maximum amount of sediment that can be stored within them. This in turn therefore has implications for the erosional and depositional processes that occur in glaciated valleys, as well as the processes of erosion and sediment reworking that occur in postglacial environments.

#### 5.3.2. Valleys without evidence of glacial fill

One of the other key observations from the results was that there are several valleys and parts of valleys throughout the GCM where the sediment volume estimation method was not applied due to a lack of evidence of glacial sediments. The training data selection process was outlined

in section 3.3.1. which included a set of criteria that needed to be met in order to only use the parts of the valleys containing glacial sediments. This meant that only valleys which demonstrated a U-shape in combination with a well-fitting parabola that extends below the existing valley floor to indicate sediment fill. This highlighted that there were a number of valleys which did not show evidence of glacial valley fill. This was something that had already become clear during the initial data collection phase where many of the swaths were not included in the training data as they displayed more fluvially-dominated features than glacial. More specifically, many of the valley cross sections throughout the catchment area were either mostly V-shaped, or very closely matched the parabola shape meaning it was not possible to extract sediment depth estimates from them. Figure 29 below shows the locations of these swaths throughout the training catchment area.

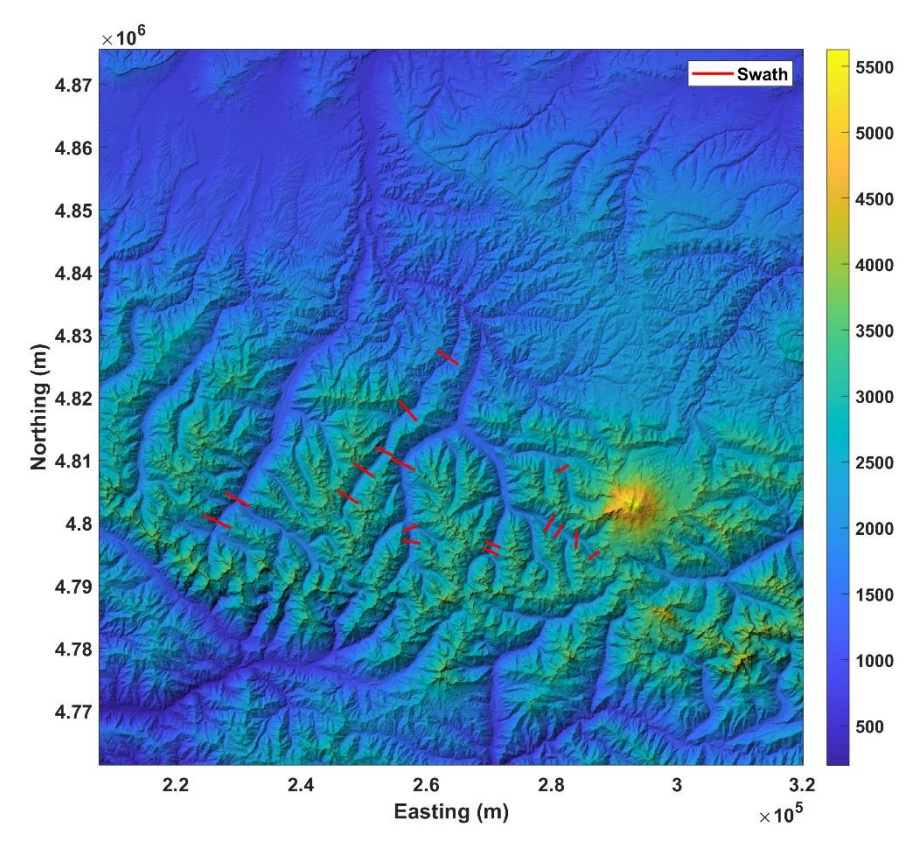


Figure 24 - Showing locations of swaths throughout training catchment which did not show evidence of glacial sediment fill. Note that there is a combination of swaths located high up in the valley as well as further down the valley and at similar latitudes to swaths that did display evidence of glacial sediment fill.

One of the key observations from Figure 29 above is that these swaths are located at the beginning of the valleys. As explained in section 3.3., data collection was stopped where the swaths were producing more V-shaped cross sections; from this it can be assumed that the bottom parts of the valleys are also characterised by fluvial processes. This therefore highlights

that the majority of glacial valley fill throughout the NW Caucasus is confined to the middle section of the valleys. It is not unreasonable to assume that there may not be significant volumes of glacial sediments in the lower reaches of the valleys as much of these areas extend beyond the influence of LGM and consequently have not experienced the overdeepening that has allowed for the sediment infilling further up the valley. However, it is known that the heads of the valleys – which are not displaying evidence of sediment fill – were previously glaciated and also one of the most recently deglaciated parts of the mountain range due to their location closest to any existing ice. This presents the question of why these parts of the valleys are not displaying the same postglacial signature as the centre parts of the valleys. This is because such valley morphologies are typically produced by fluvial erosional processes as opposed to glacial ones. Therefore, the presence of these apparent fluvial valleys within a heavily glaciated environment leads to questions regarding the function of glacial erosion within the GCM. More specifically, this suggests that glacial erosion may not have been uniform across these glaciated valleys in the Caucasus, with the middle parts of the valleys experiencing a greater intensity of erosion than elsewhere.

An additional possibility is that there may be processes that have occurred and are still occurring in these valleys that are masking or erasing the glacial sediments, and this is something that could be increasing with glacial retreat. Fluvial and slope processes are both heavily influenced by glacial retreat in mountainous regions. The continued melting of glaciers in a warming climate results in an increase in meltwater and therefore increased stream flow in the rivers that drain these glaciers (Oliva et al., 2019). This can result in an increase in fluvial processes and resulting fluvial reworking of sediments found within the river system through increased valley floor incision and infilling (Knight and Harrison, 2016). The impact of this is that an increase in fluvial processes in the paraglacial landscape has the potential to partially wash away the glacially derived sediments (Rubensdotter and Rosqvist, 2008). Such processes occurring in the GCM could individually or in combination with other processes to be discussed in this chapter, be responsible for the lack of sediment fill identified in some parts of the valleys.

## 5.3.3. Exclusion of tributary valleys

The distribution of glacial valley fill in this thesis is limited to the main valley channels found in the GCM, with most tributary valleys excluded from the approach (see Figure 30). This was

for two main reasons. Firstly, some swaths were plotted in the tributary valleys of the main study catchment but Figure 28 highlights how most of these were excluded from the training data set due to a lack of evidence for glacial valley fill. Similarly, the process outlined in Figure 24 (section 3.6.) highlight how the first step in the application of the model in other valleys was to find areas displaying clear evidence – based on aerial imagery and slope angle – of valley fill. The result of this process was that only the main valley channels were included. However, the reasoning and approaches used to establish the location of glacial sediment fill within these valleys relies solely upon remote methods, and it is likely that there will be some quantity of glacial sediments within these tributary valleys that has been excluded. This is because they are in very close proximity to the remaining glaciation in the GCM (Figure 12b) and so it is incredibly unlikely that they have been above the influence of glacial erosion and deposition. As will be explained later in this chapter, there may be reasons why there is no evidence of glacial sediments being retained and stored in the tributary valley floors. However, despite this, the exclusion of these valleys likely contributes to the reported volume estimate being an underestimate.

#### 5.4. Formation of glacial eroded valleys

From these two observations, there are two main enquiries to explore: firstly, what is the mechanism that controls valley fill as a function of valley width; secondly, is there evidence for a syn- or post-glacial process that limits the maximum amount of fill in an overdeepened glacial valley. The combination of the U-shapes and overdeepened troughs which are responsible for the sediment fill in the GCM seem to be limited to the middle parts of the valleys. As explained in the section 2.3.3., the U-shaped valleys in question are formed through intense erosion at the glacier base resulting in overdeepened troughs that end up being infilled with either water (fjords) or sediments as the ice retreats (e.g. Benn and Evans, 2010). The formation of these troughs can be heavily influenced by factors relating to valley morphology and ice dynamics. Pre-existing valley morphology can have a significant influence on glacial erosion (Benn and Evans, 2010). For example, there may be areas throughout the GCM where past glaciation had left erosional landforms such as overdeepened valleys which were then further exploited and carved by ice during the most recent glaciation. If there were parts of valleys which were already overdeepened, the overrunning ice can then exploit the pre-existing weaknesses in the rock from past erosion. This means that past ice extent – which is unknown for the Caucasus – is likely to have influenced the current valley morphologies by allowing for increased erosion and therefore formation of troughs, which in turn allows for greater sediment

storage capacity. Ice dynamics are the other main influence on glacier erosional processes. Section 2.3.3. highlighted how water is one of the primary agents of erosion at the glacier base as it allows for faster flowing ice and promotes basal water pressure variations. This means that variations in the thermal regime at the base of the ice has significant impacts on the consequent erosional power. Where there are fluctuations in the availability of basal water, there will also therefore be increases or decreases in strength of subglacial erosion. This has implications for the formation of overdeepened valleys as it suggests that this could be limited to places where ice is at its fasted flowing and therefore basal water availability has been high. Glacier ice typically flows the fastest where ice is the thickest – namely around the middle point of the valleys – and where there is the most sliding at the base (Alley et al., 2004). This highlights how the areas at the heads and sides of the valleys where ice does not flow as fast due to thinner, slower moving ice, there is likely to have been far less glacial erosion than towards the centre and middle of the valleys. There will have still been significant erosion but potentially not of the same magnitude as in the middle parts of the valleys where troughs are observed today. The result of this could therefore be glacially eroded U-shaped valleys at the valley head without the capacity to store sediments, flowing down into overdeepened troughs where sediment fill is observed.

Another key part of the results is that there are parts of valleys on a more local scale that do not display evidence of glacial valley fill. The results also highlighted that there are whole valleys that are similarly lacking in this evidence. The valley floor outlines were plotted following the workflow described in section 3.6.. This involved meeting two criteria in order to decide which parts of the valleys to include based on if they showed evidence of sediment fill. These criteria were that the maximum slope values were <14° combined with support from satellite imagery. In Figure 25 which shows the region of the northern Caucasus where the volume calculations were generated from, there are at least 3 whole valleys which have not been included based on these criteria. Figure 30 below shows the location of these valleys:

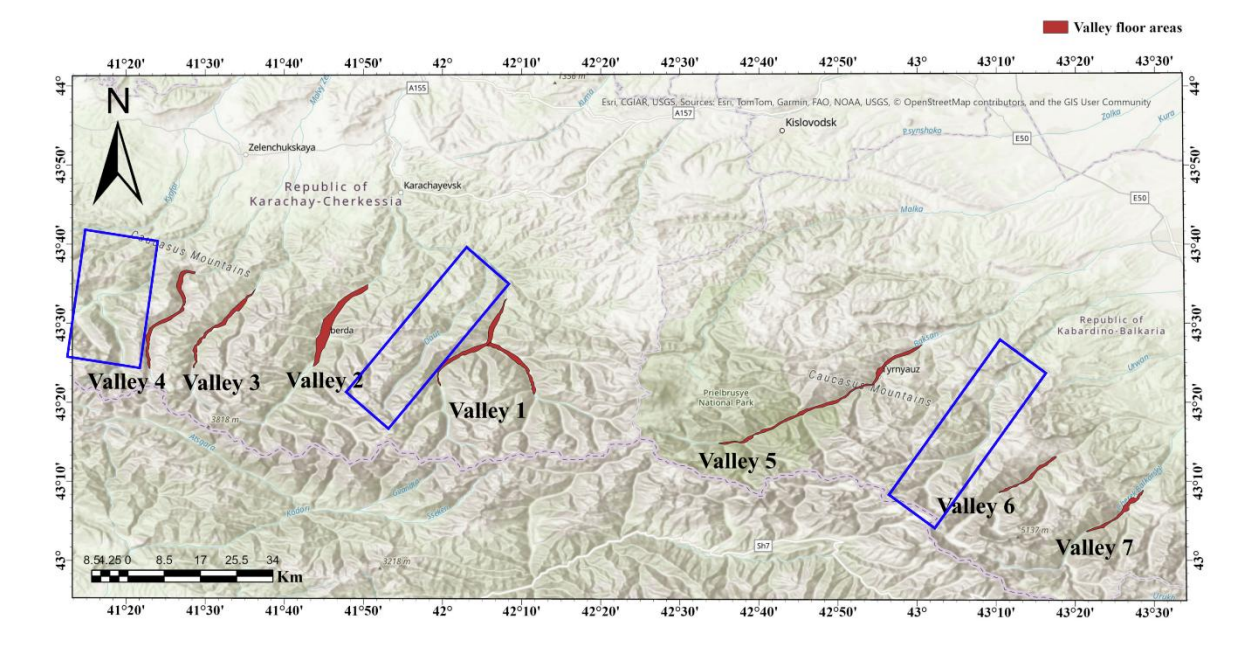


Figure 25 - Map showing valleys used for volume calculation with some valleys not included highlighted by blue boxes.

What is known about the glacial history of the region (see section 2.3.) implies that these valleys experienced glaciation similar to that of the 7 valleys the model was applied to and yet based on the criteria used they do not have sufficient glacial sediment fill to contribute to this study. This contradiction leads to two possible scenarios. The first is that during glaciation something prevented these valleys from experiencing the same levels of erosion and sediment infilling as the others. The second is that a similar volume of sediments were generated but post- or during deglaciation, something caused these sediments to be flushed from the valley to be distributed further downstream beyond valley confinement. This will be discussed further in section 5.5..

In order to establish whether this lack of sediment fill evidence was as a result of a lack of erosion or deposition during glaciation, it is necessary to again reexamine some of the processes which result in overdeepening and trough formation. These processes have been explained previously in this thesis and this chapter in sections 2.3.3 and 5.3.. Variations in local geology in glaciated regions makes it difficult to apply a blanket relationship on the functions that control overdeepened valley width and depth. It has been shown that bedrock lithology has a significant influence on the morphology of glacial valleys due to variations in rock strength causing higher or lower resistance to erosional processes (Brook et al., 2004). For example, the glacially eroded valleys in the Cairngorms, Scotland have been demonstrated to be much

narrower and steeper sided where erosion has been limited due to igneous rocks with a higher rock strength compared to much wider more heavily eroded valleys in An Teallach, Scotland where there is weaker bedrock (Brook et al., 2004). This means that changes in the geology across the region may have influenced the erodibility of the valley floors during glaciation. However, as demonstrated by the geological overview in section 2.1., the NW and NC GCM are characterised by mostly metamorphic rocks with some sedimentary cover. Geological maps do exist for the GCM, but these are limited to a very broad mountain range scale. These maps show little variation in the geology across the study area, with fairly uniform and homogenous lithology across the region (Adamia et al., 2011). From this, it is difficult to establish whether or not lithology may have had a significant and noticeable impact on the levels of subglacial erosion. Geological mapping would indicate not due to there being little variation in the basement rock type (see Figure 3, section 2.1.). However, it is still possible that there may be local variations related to the sedimentary cover or local volcanics from Mt Elbrus responsible for the changes in sediment fill observed. For example, the more extensive overdeepening where glacial valley fill is clearly present could be limited to valleys where the bedrock is dominated by lower strength rocks like sandstones and limestones. Conversely, the parts of valleys where there is no observed fill could be dominated by rocks more resistive to erosion such as schists and gneisses.

#### 5.5. Sediment origin assumption

This study has been underpinned by the assumption that the majority of the sediments stored within the U-shaped overdeepened valleys in the GCM are glacially derived. The variation in sediment fill evidence throughout the length of the glaciated part of the valley could be as a result of other non-glacial processes which are becoming more prevalent in the region. Within the GCM there is significant risk of mudflows which are observed to be increasing in frequency with glacial retreat (Aleinikova et al., 2020). This could have a significant impact on sediment depth variation throughout the valley as during a mudflow, sediment volumes on the order of ~10,000 m³ can be mobilised (Malneva and Kononova, 2011). The source of many of these mudflows are moraines deposited as a result of glacial retreat, many of which can be found laterally at the valley walls (Malneva and Kononova, 2011). The structural integrity of these moraines being broken down as a result of mass transport events could also be a reason for the lack of moraine preservation in some parts of the GCM. The magnitude of these events could therefore be responsible for picking up and redistributing glacial sediments found higher up in

the valleys. However, it is difficult to ascertain why this could have such a profound impact solely in these areas at the heads of the valleys. Mudflows in the GCM occur over a wide range of altitudes, with the majority of flows occurring across an altitude range of 750m – 2230m (Karavaev and Seminozhenko, 2019). Examples from the training catchment area (see Figure 15) show that the valley floors where sediment fill is found are sitting at elevations in excess of 1500m. This would suggest that the influence of mass transport events is not limited to the valley heads where there appears to be an absence of sediment fill. Consequently, although mudflows are likely to have an influence on the volume of sediment fill in these valleys, they cannot be definitively held responsible for the lack of valley fill evidence observed in specific parts of the valleys as this can be better linked to processes outlined in section 5.3.. An additional complication of this follows on from what was discussed in section 5.3.2. concerning fluvial reworking of sediments. As the climate warms and glaciers in the GCM retreat, the greater availability of meltwater contributes to the modification of these sediments (Oliva et al., 2019). This in turn impacts sediment fluxes in that there can be an increase in the redistribution of sediments to further downstream (Knight and Harrison, 2009). As a result of this there can be a change in dominant process from glacial to fluvial which can call into question the origin of the sediments found within these valleys.

#### 5.6. Implications for glacial isostatic adjustment (GIA)

#### 5.6.1. Sediment mass estimate

The second part of the results for this thesis provided a mass estimate for the volume of glacial sediments estimated to be in the NW and NC GCM valley floors of  $8.83 \times 10^{13}$  kg  $\pm$  9.8%. As with the volume estimate, it is important to try to put this sediment mass value into some context by comparing to other similar estimates from other regions. This proves challenging as where there may be many examples of research investigating GIA or sediment loads moving through systems, there is a lack in specific weight estimates for stored sediments. Despite this, such load estimates still provide reasonable validation to the results of this research. This is because they can give insight into whether the mass of sediments in the GCM are within a similar order of magnitude when considering differences in temporal or spatial extent of sediment deposition. Hay et al. (2007) investigated sediment volumes and fluxes into basins surrounding the Alps. Such quantities can be related to the Caucasus sediments as some the volumes estimated in the Alps result from Pleistocene glacial erosion which has been linked to an average sediment thickness. This study found that  $3.3 \times 10^{17}$  kg of sediments in total were

eroded from the Alps during the Pleistocene glaciations which resulted in a total isostatic uplift of 700 m. Comparing to the mass estimate from the Caucasus, there is a significance magnitude difference, with the GCM mass being on the order of 10,000 times smaller than in the Alps. However, this is to be expected for a variety of reasons. Firstly, this mass encompasses all sediments eroded from the mountains throughout all Pleistocene glaciations where at least four major glaciations are recognised (Ochs et al., 2022). Comparatively, the glacial valley fill quantified in this thesis is likely almost entirely comprised of sediments eroded only during the last glaciation. This is because there is minimal evidence of glacial landforms dated prior to the LGM (see section 2.2). Additionally, the volume and mass estimate for the GCM is limited only to valleys in a section of mountain range and also only applies to the sediments stored within the valleys here as opposed to in the basins beyond. Overall, this highlights how when considering the scale differences between these estimates in the Alps and Caucasus, the sediment mass from the Alps helps validate the above mass estimate for the valley fill in these valleys.

#### 5.6.2. Weight distribution

One important aspect when considering the impact of the glaciation and glacial erosion on GIA is the weight distribution on the lithosphere. The above example from the Alps demonstrated the impact of sediments being removed from the alpine valleys resulting in uplift beneath the core of the mountains (Hay et al., 2007). The purpose of this thesis was to establish the quantity of sediments remaining within the past-glaciated valleys, deposited during retreat. This has been successfully done for a section of the GCM with both a volume and mass estimate for these sediments. However, this does not account for the sediments that have been removed from the valley during glacial erosion and deposited more distally from these valleys and from the mountain range in the surrounding basins. Despite this, the results can still be discussed in the context of GIA based on how these sediments are distributed and therefore how this may impact flexure and uplift of the lithosphere.

Section 5.3.2. highlighted how there are many areas throughout GCM where glacial valley fill is expected to be observed but was lacking in enough evidence to be used in the model. This included whole valleys as well as many sections of valleys such as at the valley head even throughout the valleys that have extensive sediment fill further downstream. As previously discussed, this can potentially be attributed to two main reasons. Firstly, as a result of variations in the formation of overdeepened valleys and consequent sediment infilling of these troughs.

Secondly, due to non-glacial processes which have impacted sediment budgets in some areas such as mass transport events like mudflows. Regardless of the reasons behind these discrepancies in sediment fill, the presence and absence of large sediment volumes in areas consequently impacts the overall loading on the lithosphere meaning it could have an impact on the isostatic response. The expectation in the GCM as with other regions experiencing glacial retreat is that there will be rapid isostatic uplift of the land in the region on the scale of over 10 mm per year (Whitehouse, 2018). Such uplift will be the case in the Caucasus but the influence of the location of these sediments can have a quantifiable impact on the amount of uplift as they add a significant weight to the lithosphere as demonstrated by Hay et al. (2007). The concentration of sediment volume in the middle parts of the valleys in the GCM originates from glacial erosion that has stripped sediments from the mountains and deposited it in troughs in the valley floors. This demonstrates that part of the uplift response of the lithosphere will be the adjustment to the transfer of mass from the centre of the mountains to down into the valleys. An interesting dynamic of this is that this will be part of the area where there has been significant ice retreat. This means that as the total load on the valleys from ice has decreased it has subsequently increased again with sediment deposition. Overall, the mass of ice that was present significantly outweighs the mass of the sediments presently estimated but it is likely that the glacial valley fill does in some way moderate the rate or magnitude of uplift. One of the suggestions for the absence of sediments in certain areas is that they have been removed and redistributed further downstream as a result of mudflows. The implications of this for GIA is that it suggests that there will have been removal of sediments from valleys since the LGM. This sediment flux out of the valleys in the GCM would contribute even more to the overall uplift at the core of the mountains being caused only by loss of ice mass.

### 6. Conclusions and Future Work

#### 6.1. Conclusions

The aim of this research was to quantify the volume of sediments stored within valleys in the GCM and consider how this sediment fill varies spatially across these valleys. It was found that there is a total volume of  $42.05 \pm 1.01 \text{ km}^3$  of glacial valley fill across a selection of valleys in the north-western and north-central Caucasus. This volume corresponds to a total sediment mass of  $8.83 \times 10^{13} \pm 8.67 \times 10^{12}$  kg. This sediment fill is found in overdeepened troughs within these valleys formed as a result of intense glacial erosion. The process of estimating these sediment quantities highlighted that there are parts of the studied region of the GCM which are lacking in evidence of glacial sediment fill. More specifically, within each valley, the sediment fill is constrained to the middle section of each valley, with none observed at the valley head and further downstream beyond the direct influence of glaciation. Additionally, there were whole valleys which were not included in the results as they similarly lack evidence of this valley fill. The main reason for this has been attributed to factors that impact the formation of the overdeepened troughs needed for the sediment storage. These troughs are an erosional landform so this can be linked to glacial erosion being variable both throughout these valleys and across the glaciated regions of the Caucasus considered in this study. These variations in erosion can be caused by pre-existing valley morphologies and lithologies, as well as changes in ice dynamics that impact glacier movement and erosional capabilities. The quantity of sediments observed have the capacity to influence GIA in the region as they represent a load on the lithosphere that has been transferred from the core of the mountains out to their margins.

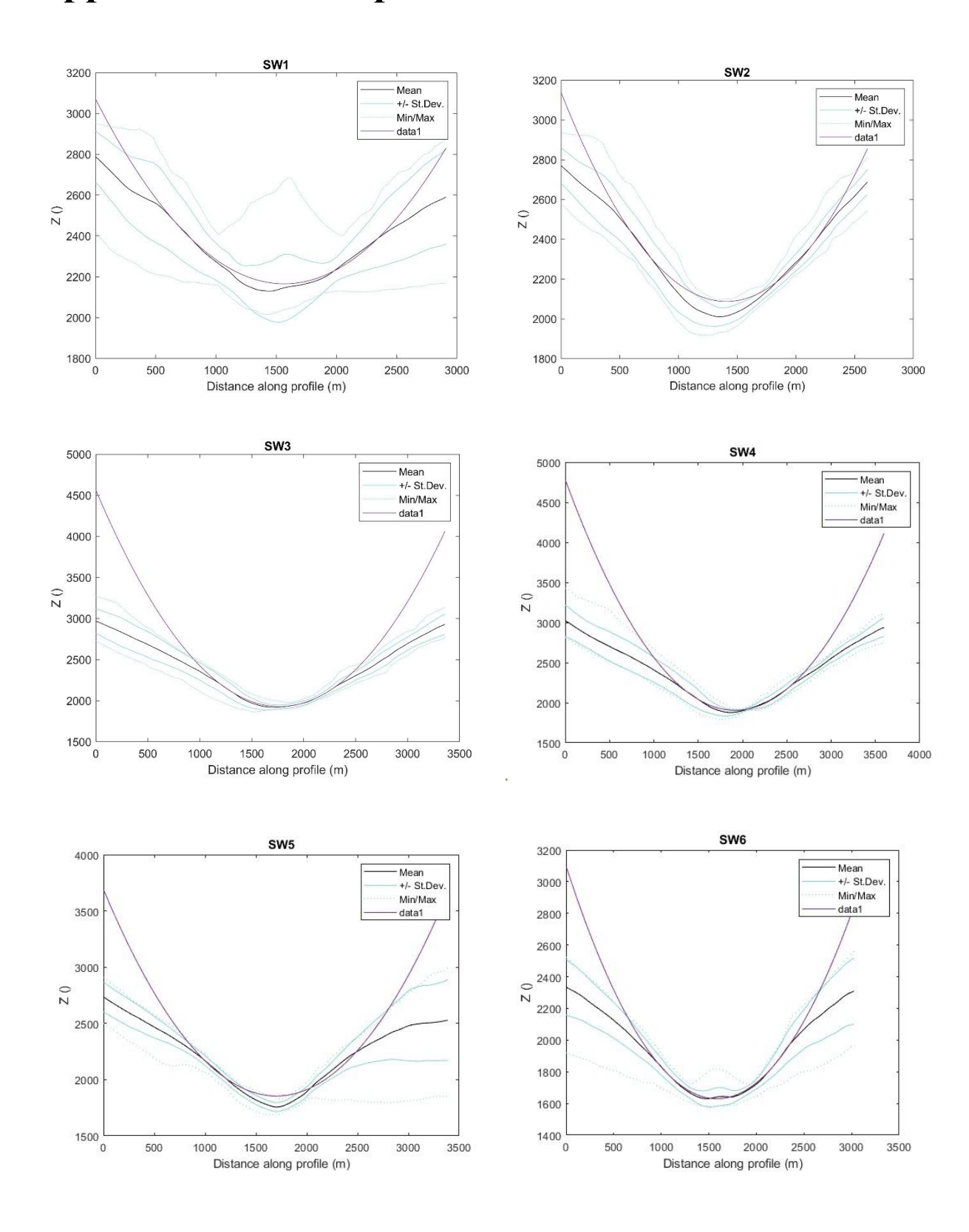
#### **6.2. Future work**

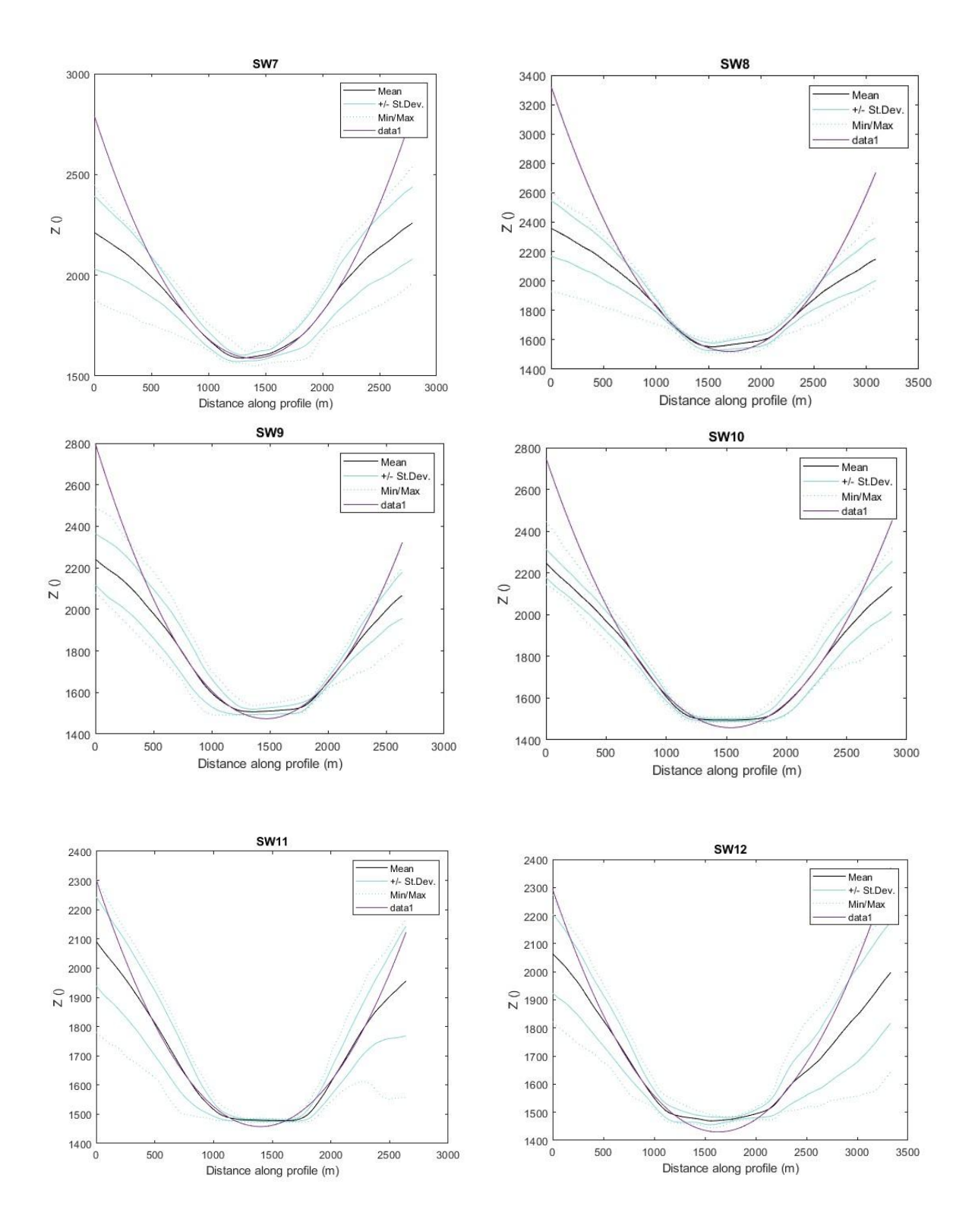
The original rationale behind this study was to support a larger project that would attempt to study the isostatic adjustment associated with glacial retreat in the Caucasus, for which it was necessary to quantify the amount of sediment that has been eroded off the mountains. This research has found that there are  $\sim 9 \times 10^{13}$  kg of sediment filling overdeepened valleys in the GCM which in turn have an influence on the GIA based on their location and provenance as outline in the above section. This figure can be used in further study to attempt to quantify the rate of isostatic adjustment in the Caucasus region as a result of glacial retreat from two perspectives. Firstly, it could be used more broadly to reconstruct the initial size of the GCM before glacial erosion, based on the assumption that these sediments all originated from the mountains. Secondly, the distribution of this sediment mass – namely where it sits within the

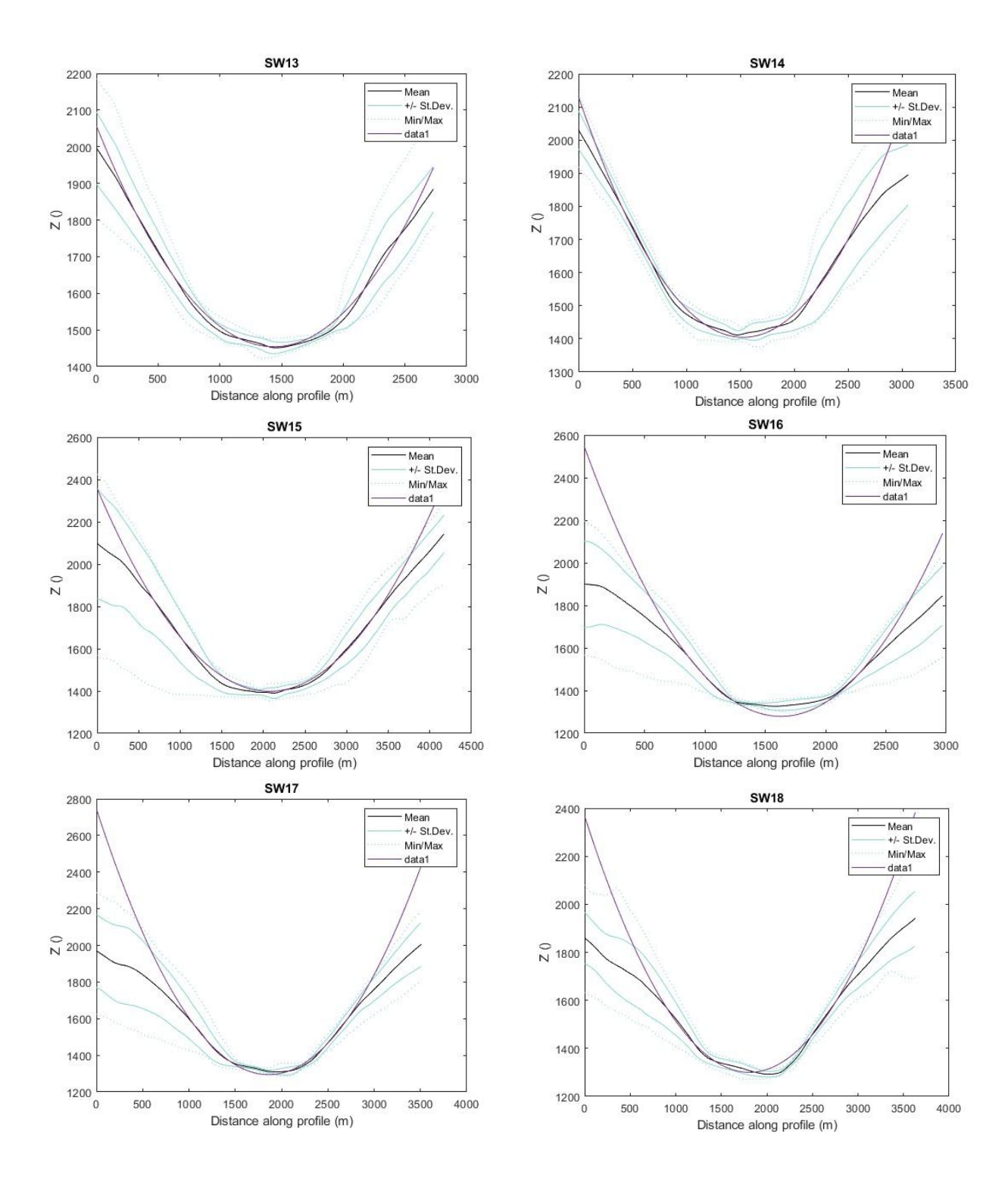
valleys – could be used to inform more detail on the specifics of this isostatic adjustment on the amount of surface uplift across the region based on the transfer of these sediments from the core of the mountains to the margins.

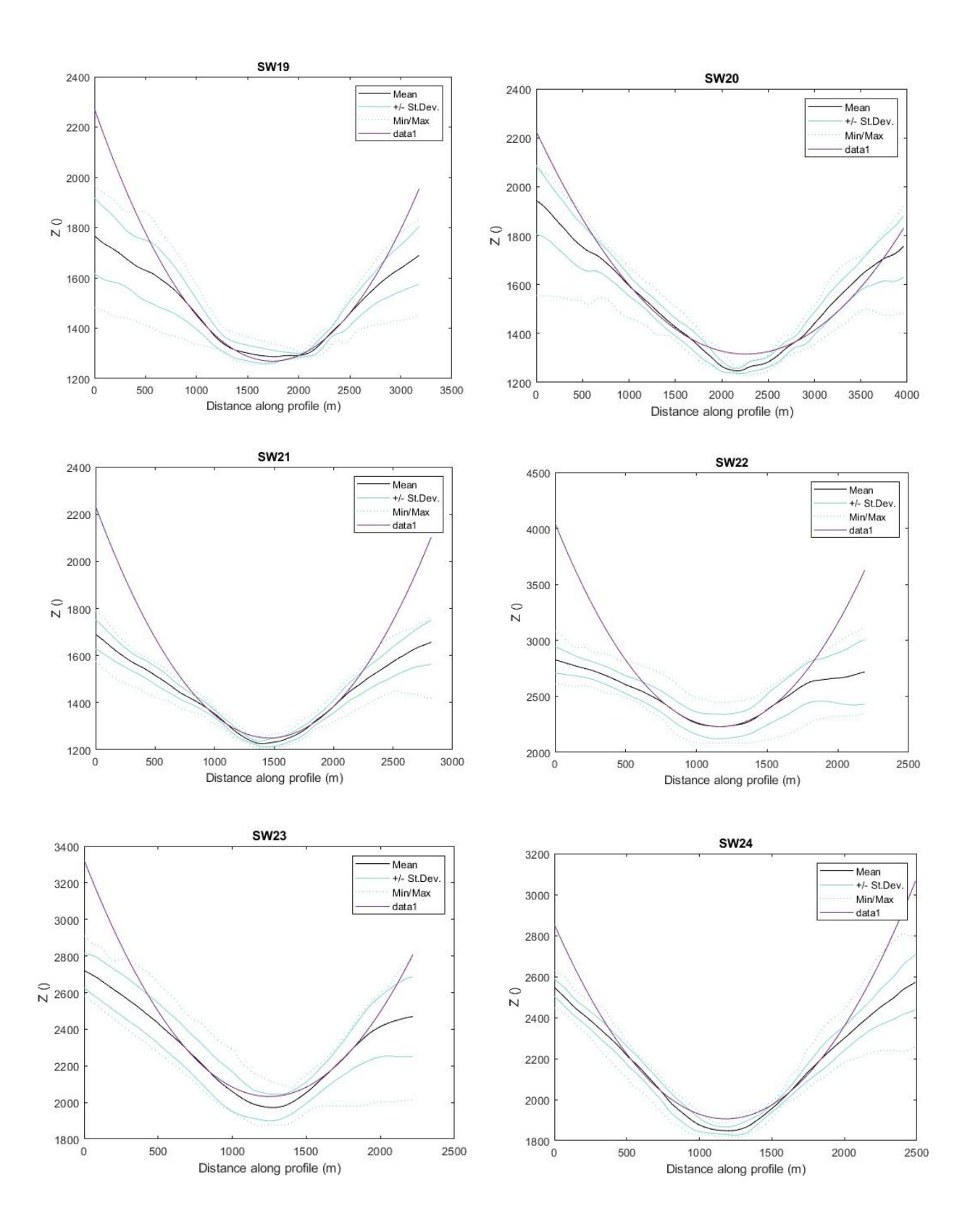
Additionally, beyond the context and rationale behind this research, this study has highlighted other research areas that could be developed relating to the geomorphology of the Caucasus. Assumptions were made in this research as a result of lack of specific and comprehensive detail into the glacial history of the whole region as well as glacial geomorphology within individual valleys. Such assumptions could be addressed in the future if more research was to be done in the Caucasus Mountains. This would help validate and inform the research needed in order to establish the impacts of glacial retreat both locally and in other glaciated mountain regions globally.

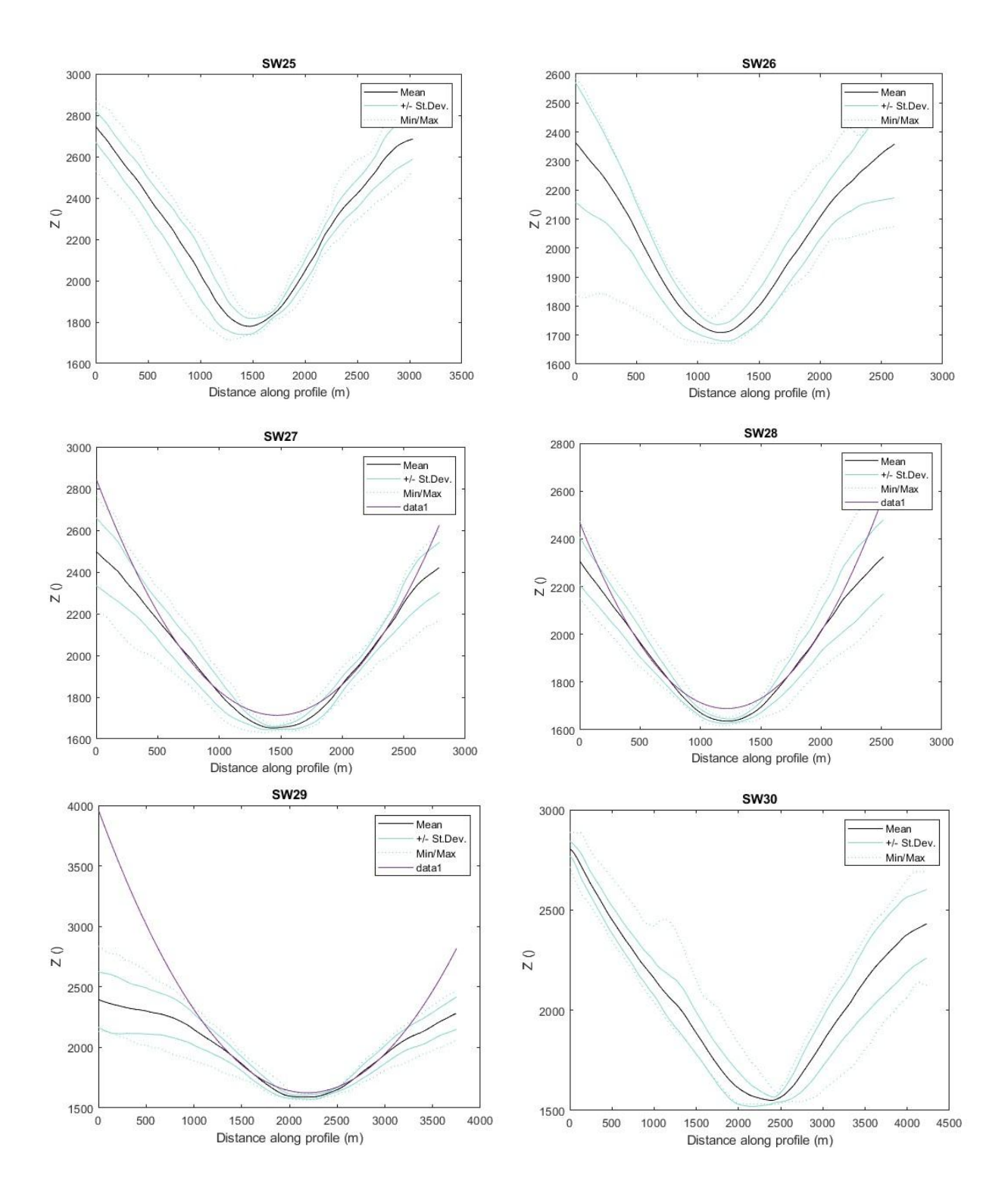
# **Appendix A: Swath profiles**

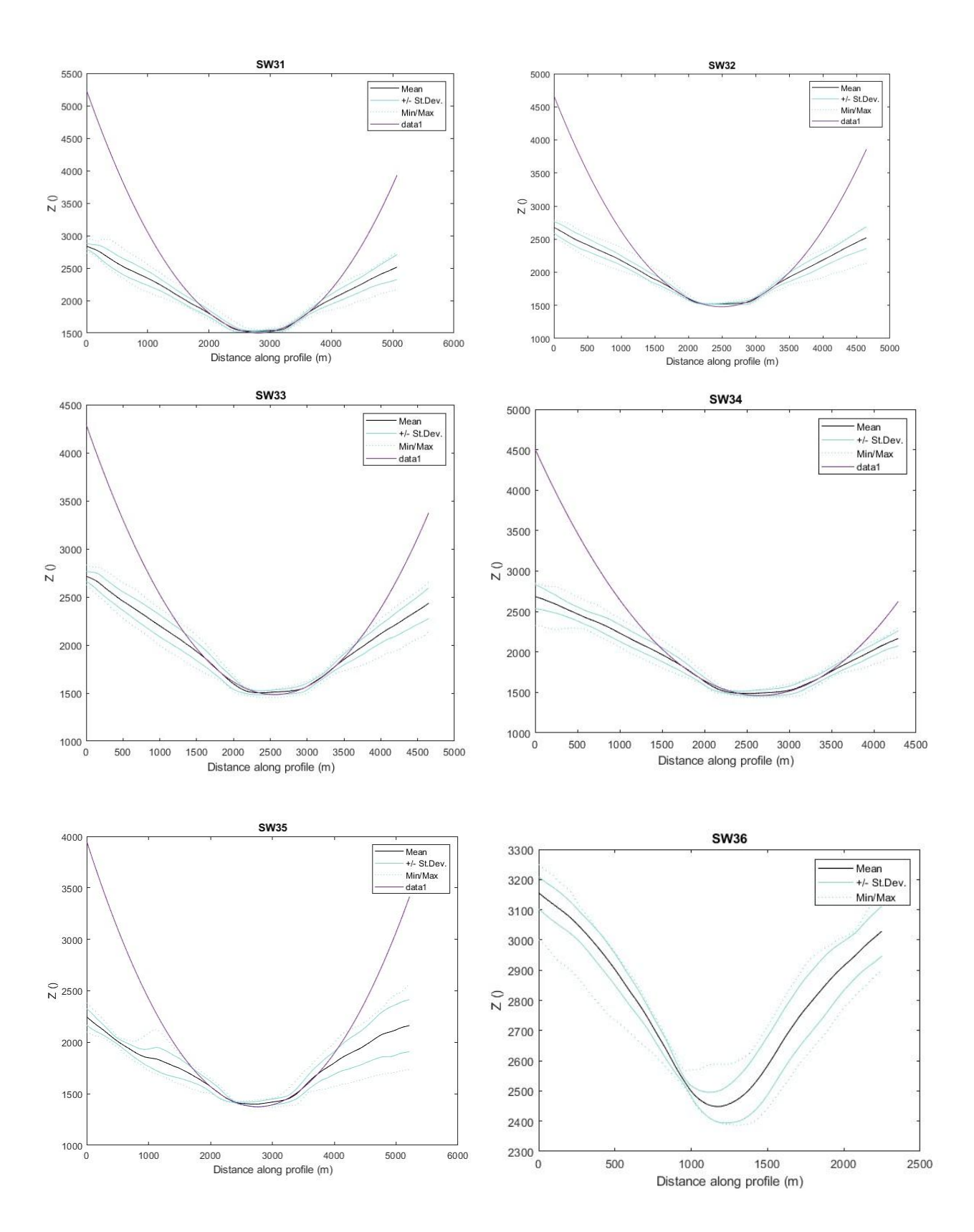


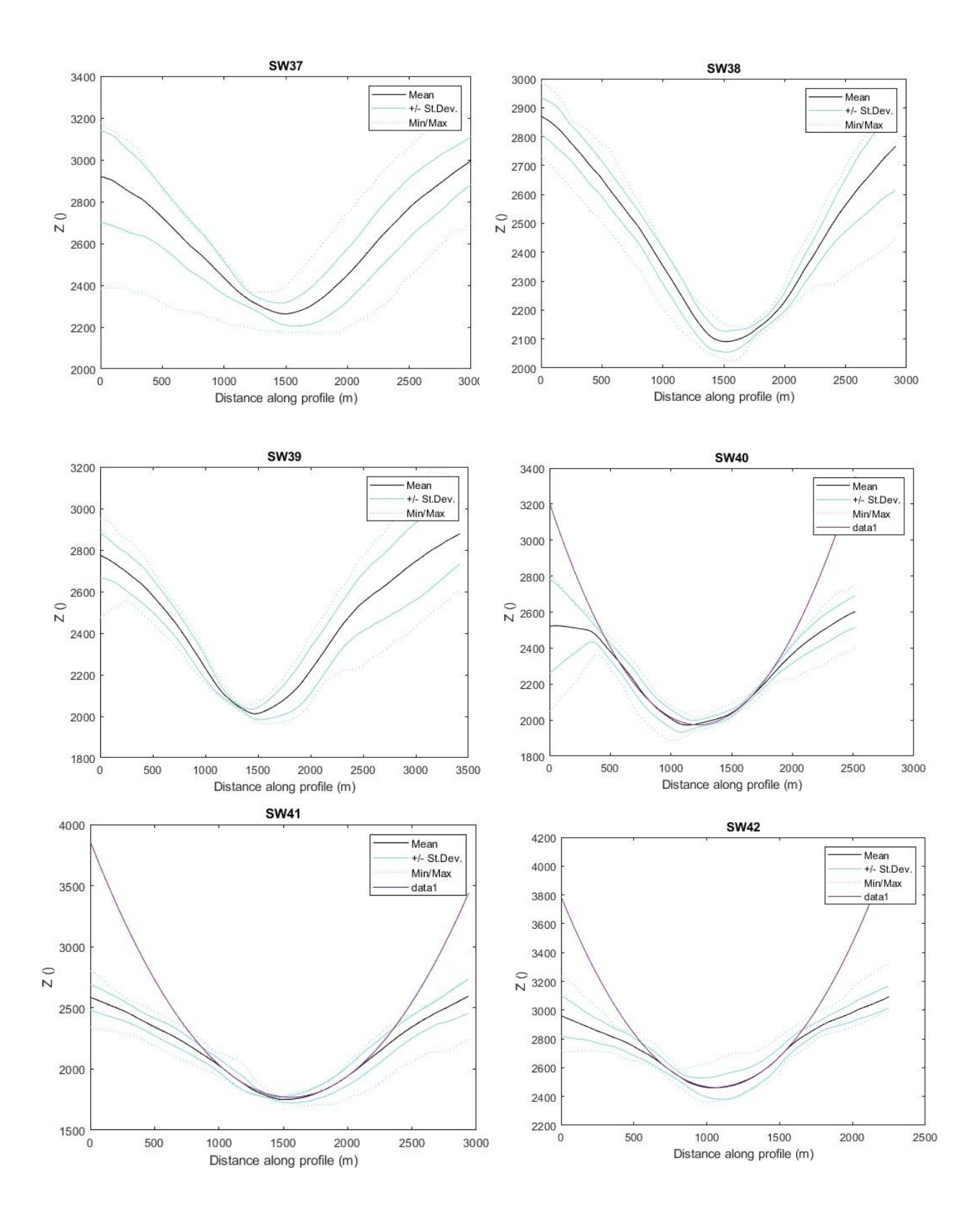


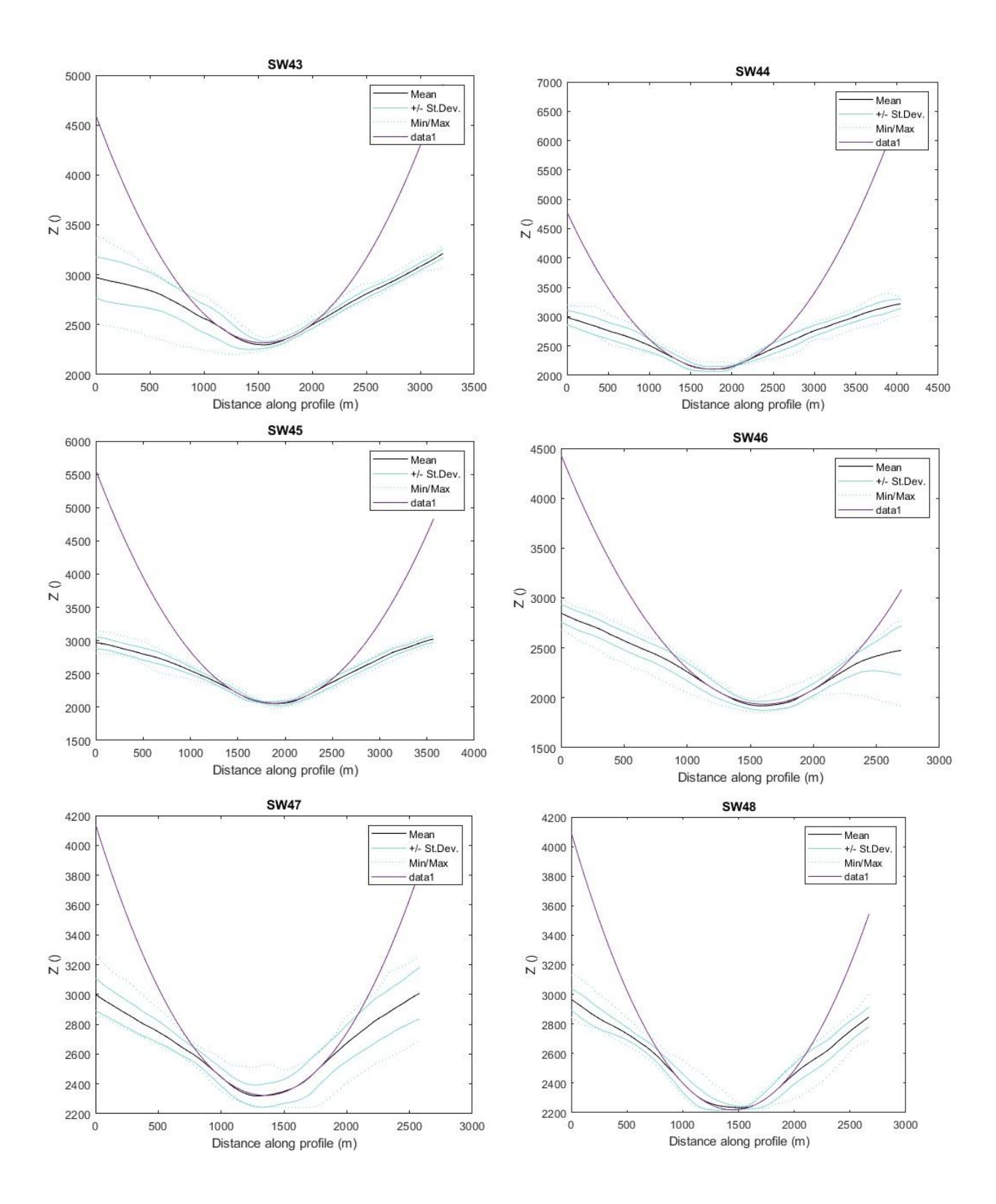


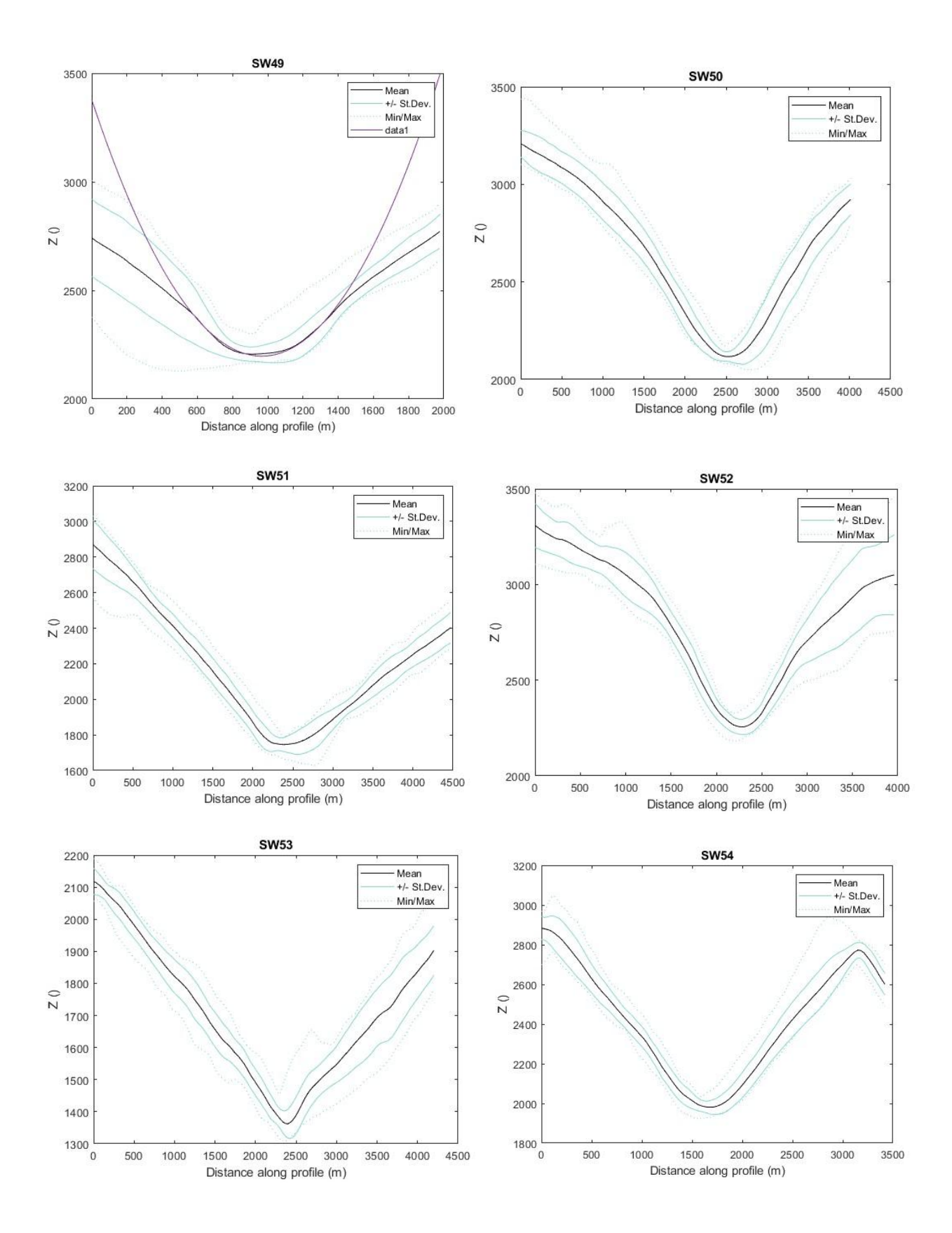


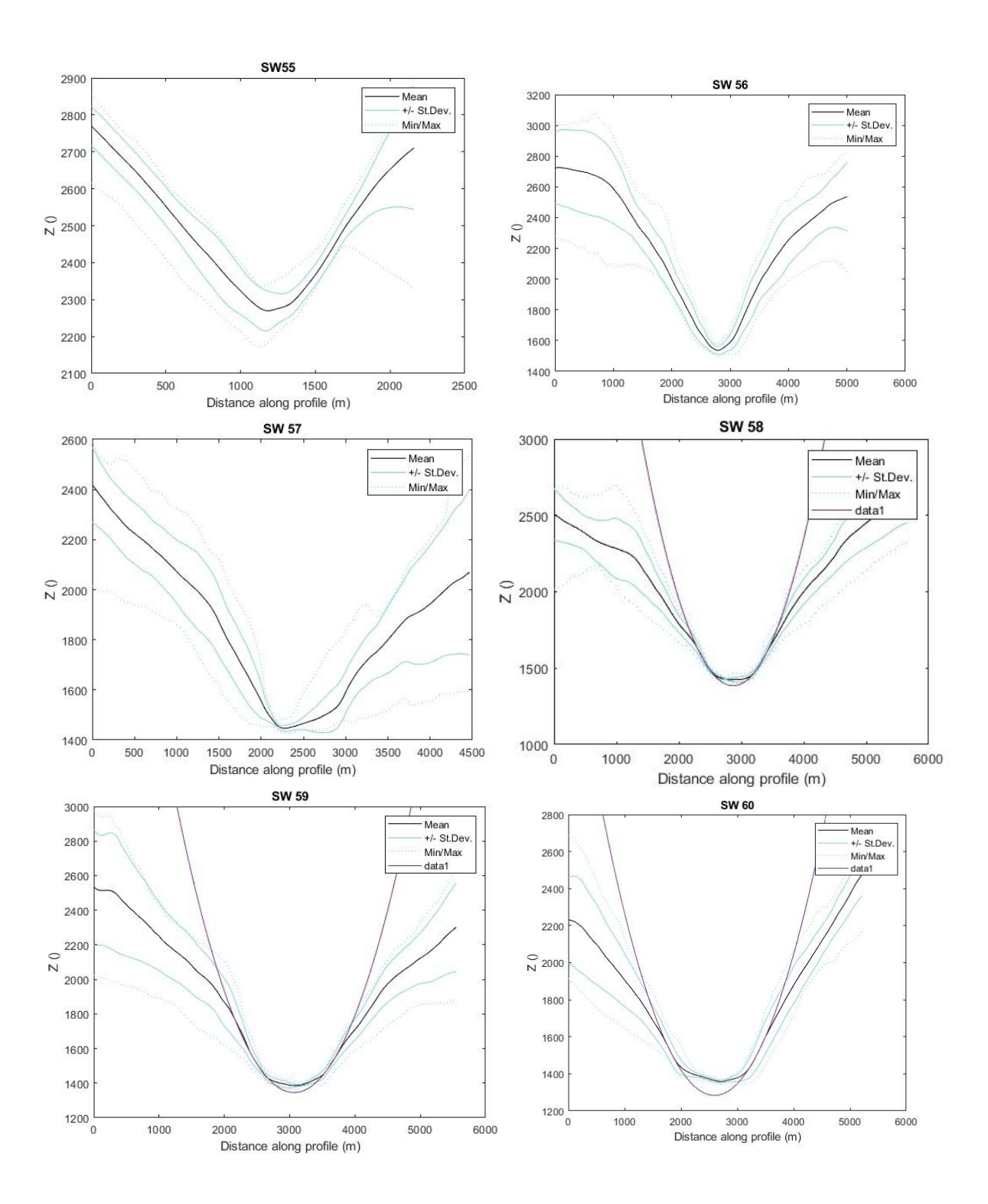


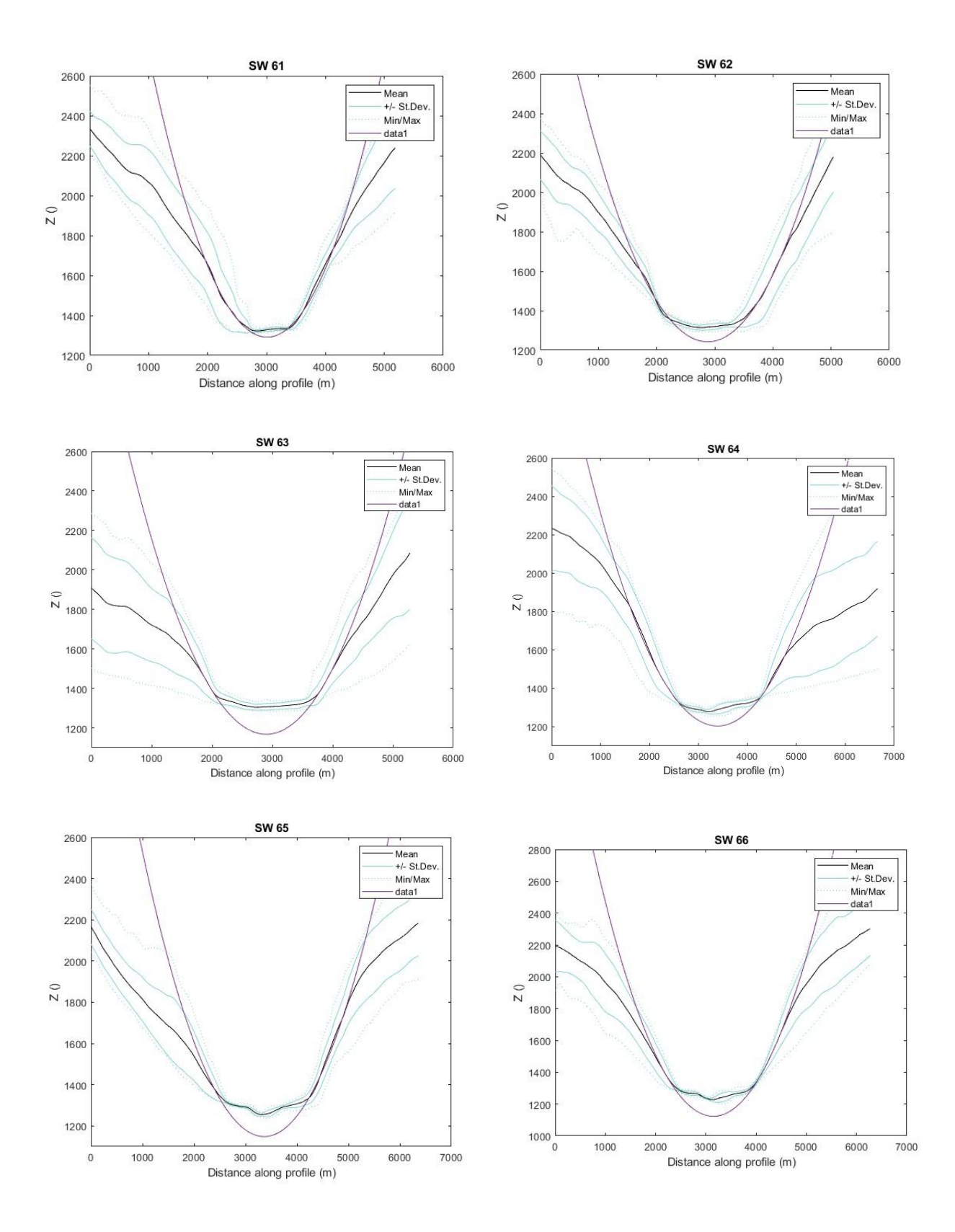


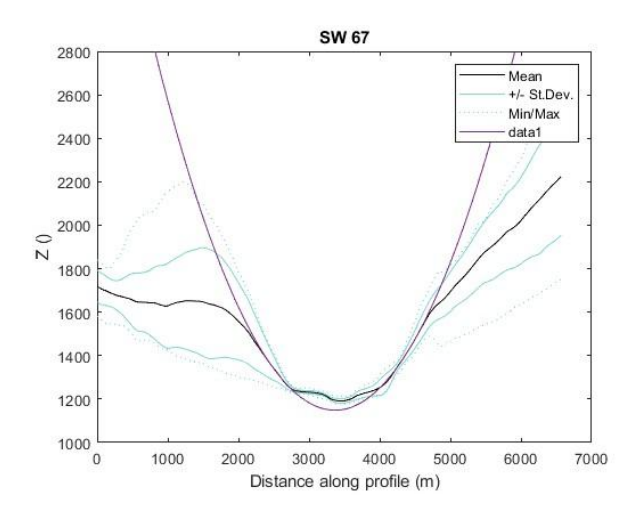












# Appendix B: Hillslope distance and sediment depth tables

Valley 1

a1 (m)	a2 (m)	b1 (m)	b2 (m)	Volume (km^3)
367.3649	469.2437	44.5046	60.91822	0.140306948
469.2437	532.2484	60.91822	73.04892	0.200729283
532.2484	517.5595	73.04892	70.19038	0.220439425
517.5595	391.0964	70.19038	47.83751	0.165931778
391.0964	371.8971	47.83751	45.1192	0.116027925
371.8971	420.5474	45.1192	52.39311	0.125326701
420.5474	469.6766	52.39311	60.99872	0.158294222
469.6766	528.4816	60.99872	72.31752	0.199351431
528.4816	589.5688	72.31752	83.6939	0.250475899
589.5688	630.0678	83.6939	90.21413	0.298121088
630.0678	591.3705	90.21413	84.00548	0.298996371
591.3705	606.7503	84.00548	86.58786	0.287588598
606.7503	435.3593	86.58786	54.86319	0.219151219
435.3593	383.4022	54.86319	46.72519	0.133834324
383.4022	321.8072	46.72519	38.79796	0.099337201
321.8072	375.8469	38.79796	45.66302	0.09716242
375.8469	218.7854	45.66302	26.85491	0.072097036
218.7854	277.2262	26.85491	33.698	0.049253942
277.2262	310.011	33.698	37.42413	0.068775121
310.011	291.1528	37.42413	35.27279	0.072021572
291.1528	295.017	35.27279	35.71075	0.068455053
295.017	229.5538	35.71075	28.16785	0.055115788
229.5538	350.7917	28.16785	42.33718	0.068081901
350.7917	226.7136	42.33718	27.8244	0.067472953
120.6796	130.2676	13.96086	15.21916	0.01253832
130.2676	134.7214	15.21916	15.81064	0.013977871
134.7214	219.11	15.81064	26.89493	0.025414541
219.11	306.6962	26.89493	37.0428	0.055596707
306.6962	323.5667	37.0428	39.00553	0.079150623
323.5667	399.0123	39.00553	49.01513	0.104418446
399.0123	503.3648	49.01513	67.4264	0.163281507
503.3648	549.2266	67.4264	76.31568	0.221744949
549.2266	526.3092	76.31568	71.89503	0.231481419
526.3092	538.5306	71.89503	74.26434	0.226842258
538.5306	518.1574	74.26434	70.30695	0.223373934
518.1574	459.3707	70.30695	59.10184	0.191146624

459.3707	426.8789	59.10184	53.43464	0.156778327
426.8789	411.1685	53.43464	50.89048	0.140054468
411.1685	375.0019	50.89048	45.54602	0.123270096
375.0019	293.7615	45.54602	35.56836	0.089546636
293.7615	368.0004	35.56836	44.59019	0.087614798
368.0004	419.4181	44.59019	52.20962	0.123758873
419.4181	517.9567	52.20962	70.26782	0.176128998
517.9567	622.5317	70.26782	89.08232	0.261119261
622.5317	651.1588	89.08232	93.16808	0.325111915
651.1588	538.661	93.16808	74.2895	0.28432409
538.661	487.2827	74.2895	64.32364	0.210621625
487.2827	511.8738	64.32364	69.08204	0.199553926
511.8738	474.2938	69.08204	61.86133	0.194417604
474.2938	352.6503	61.86133	42.57436	0.137405357
352.6503	423.0785	42.57436	52.80687	0.120272148
423.0785	433.7137	52.80687	54.58303	0.146410815
433.7137	421.2769	54.58303	52.51199	0.145795657
421.2769	465.259	52.51199	60.18056	0.156944116
465.259	488.6188	60.18056	64.57949	0.181748232
488.6188	458.1177	64.57949	58.87413	0.179045604
458.1177	372.2457	58.87413	45.16688	0.138003992
372.2457	272.3952	45.16688	33.15093	0.083461712
272.3952	163.7026	33.15093	19.70671	0.038675645
163.7026	75.45357	19.70671	8.503664	0.011904531
75.45357	100.9793	8.503664	11.46797	0.006233613
100.9793	109.4677	11.46797	12.52408	0.008813723
109.4677	113.0596	12.52408	12.97964	0.009851485
113.0596	146.6617	12.97964	17.41072	0.013501321

Valley 2

a1 (m)	a2 (m)	b1 (m)	b2 (m)	Volume (km^3)
414.1698	525.9243	51.36606	71.82014	0.177353558
525.9243	583.3291	71.82014	82.60123	0.246502386
583.3291	625.1124	82.60123	89.47434	0.292666583
625.1124	592.4656	89.47434	84.19396	0.297081079
592.4656	558.1769	84.19396	78.00856	0.265207855
558.1769	490.2993	78.00856	64.90188	0.220170445
490.2993	546.5799	64.90188	75.81061	0.215201833
546.5799	603.3872	75.81061	86.03542	0.26501867
603.3872	617.3424	86.03542	88.28032	0.29857566
617.3424	691.9157	88.28032	97.97006	0.343755201

691.9157	691.1801	97.97006	97.89379	0.383140123
691.1801	664.0373	97.89379	94.81406	0.367958871
664.0373	688.1334	94.81406	97.57392	0.366304744
688.1334	717.6359	97.57392	100.4097	0.395777379
717.6359	746.5522	100.4097	102.662	0.429095481
746.5522	866.0109	102.662	107.9481	0.520224682
866.0109	995.1833	107.9481	109.8452	0.690569409
995.1833	1050.311	109.8452	110.1679	0.831239415
1050.311	972.8181	110.1679	109.6575	0.813550343
972.8181	930.1172	109.6575	109.1676	0.720535082
930.1172	932.7611	109.1676	109.204	0.690758494
932.7611	964.7017	109.204	109.5789	0.716395274
964.7017	962.1509	109.5789	109.5529	0.738427787
962.1509	1086.983	109.5529	110.3052	0.83497304
1086.983	1047.938	110.3052	110.1572	0.904582077
1047.938	1017.023	110.1572	109.9936	0.846825515
1017.023	831.1376	109.9936	106.9177	0.682171114
831.1376	615.6398	106.9177	88.01324	0.421515689
615.6398	525.3632	88.01324	71.71091	0.261185086
525.3632	517.5753	71.71091	70.19345	0.217531419
517.5753	465.4649	70.19345	60.21854	0.193269536
465.4649	464.6549	60.21854	60.06926	0.172707541
464.6549	308.4005	60.06926	37.23864	0.120832654
308.4005	42.3687	37.23864	5.241281	0.029212057

Valley 3

a1 (m)	a2 (m)	b1 (m)	b2 (m)	Volume (km^3)
147.1024	133.045	17.47004	15.58758	0.015637754
133.045	178.4797	15.58758	21.68262	0.019465552
178.4797	240.9856	21.68262	29.53074	0.035322654
240.9856	239.2991	29.53074	29.33154	0.045973092
239.2991	402.884	29.33154	49.60357	0.083976104
402.884	324.7452	49.60357	39.145	0.105909402
324.7452	203.4704	39.145	24.93587	0.056565914
203.4704	286.6689	24.93587	34.76551	0.04832954
286.6689	377.5372	34.76551	45.89811	0.088449593
377.5372	295.8887	45.89811	35.8097	0.090798836
295.8887	280.6426	35.8097	34.08433	0.066238911
280.6426	233.7022	34.08433	28.66593	0.052863676
233.7022	300.7056	28.66593	36.35765	0.057203698
300.7056	323.5226	36.35765	39.00033	0.07765931

323.5226	277.6319	39.00033	33.74389	0.072136807
277.6319	205.1293	33.74389	25.14667	0.046790755
205.1293	366.9545	25.14667	44.44944	0.06695065
366.9545	385.1323	44.44944	46.97257	0.112725221
385.1323	466.2452	46.97257	60.36258	0.145027169
466.2452	476.6871	60.36258	62.31128	0.177540792
476.6871	401.9152	62.31128	49.45554	0.154399947
401.9152	348.2822	49.45554	42.01916	0.11233961
348.2822	362.6433	42.01916	43.87466	0.100700351
362.6433	385.8432	43.87466	47.07468	0.111661368
385.8432	412.1109	47.07468	51.03928	0.12695811
412.1109	482.5078	51.03928	63.41292	0.160053317
482.5078	725.9418	63.41292	101.1072	0.296025251
725.9418	595.2152	101.1072	84.66419	0.350631853
595.2152	523.8239	84.66419	71.41122	0.251006494
523.8239	434.0776	71.41122	54.64487	0.18383108
434.0776	279.6662	54.64487	33.97394	0.103156858
279.6662	253.5332	33.97394	30.9949	0.056696539
253.5332	201.5755	30.9949	24.69423	0.041456906
201.5755	99.20899	24.69423	11.25166	0.018715376
99.20899	48.36678	11.25166	5.779905	0.004504318
Ni.				

Valley 4

a1 (m)	a2 (m)	<b>b1</b> (m)	b2 (m)	Volume (km^3)
285.594	290.0465	34.64398	35.14756	0.066020469
290.0465	355.803	35.14756	42.97994	0.083387154
355.803	473.2319	42.97994	61.66228	0.138026216
473.2319	458.3884	61.66228	58.92327	0.173284995
458.3884	403.7955	58.92327	49.74331	0.148477798
403.7955	474.2903	49.74331	61.86066	0.154172794
474.2903	544.3415	61.86066	75.38208	0.207765871
544.3415	452.1735	75.38208	57.80313	0.199042498
452.1735	383.636	57.80313	46.75853	0.139627539
383.636	385.482	46.75853	47.02277	0.117876215
385.482	363.8221	47.02277	44.03096	0.111900936
363.8221	345.3507	44.03096	41.65078	0.100213479
345.3507	269.2762	41.65078	32.79699	0.075646407
269.2762	222.996	32.79699	27.3718	0.048434713
222.996	182.5822	27.3718	22.22559	0.03288988
182.5822	272.3586	22.22559	33.14678	0.041776021
272.3586	358.83	33.14678	43.37333	0.079871383

358.83	306.0208	43.37333	36.96531	0.088244233
306.0208	284.0613	36.96531	34.47073	0.069402258
284.0613	312.7461	34.47073	37.74018	0.071013995
312.7461	358.9028	37.74018	43.38283	0.090009361
358.9028	412.5364	43.38283	51.10663	0.118796468
412.5364	431.7196	51.10663	54.24543	0.142155732
431.7196	450.9106	54.24543	57.57761	0.155443437
450.9106	383.8229	57.57761	46.7852	0.139253203
383.8229	331.5684	46.7852	39.95997	0.102147919
331.5684	298.0879	39.95997	36.0596	0.07905518
298.0879	300.0376	36.0596	36.28152	0.071272651
300.0376	341.7466	36.28152	41.20228	0.082168074
341.7466	331.396	41.20228	39.93922	0.090269962
331.396	381.4201	39.93922	46.44369	0.101398254
381.4201	416.8768	46.44369	51.79927	0.127108489
416.8768	369.5967	51.79927	44.80601	0.123432112
369.5967	251.8981	44.80601	30.80574	0.077883209
251.8981	203.0128	30.80574	24.8776	0.041400862
203.0128	264.991	24.8776	32.30936	0.043903112
264.991	239.296	32.30936	29.33118	0.050722567
239.296	277.2688	29.33118	33.70281	0.053269525
277.2688	258.7441	33.70281	31.59492	0.0572731
258.7441	272.3545	31.59492	33.14633	0.056218752
272.3545	243.3751	33.14633	29.81194	0.053058453
243.3751	186.8441	29.81194	22.78636	0.037097673
186.8441	24.22415	22.78636	3.756566	0.01064021

Valley 5

a1 (m)	a2 (m)	<b>b1</b> (m)	b2 (m)	Volume (km^3)
161.4296	272.244	19.40084	33.13379	0.038285955
272.244	293.8615	33.13379	35.57969	0.063883241
293.8615	222.8643	35.57969	27.35571	0.053538452
222.8643	194.088	27.35571	23.73078	0.034702715
194.088	175.0845	23.73078	21.23113	0.02718114
175.0845	126.1005	21.23113	14.66947	0.018224266
126.1005	229.4189	14.66947	28.15158	0.025887997
229.4189	348.4759	28.15158	42.04362	0.067481194
348.4759	388.043	42.04362	47.39233	0.108186674
388.043	422.8803	47.39233	52.77434	0.131170159
422.8803	355.6231	52.77434	42.95668	0.121102894
355.6231	124.5816	42.95668	14.47014	0.049471897

124.5816	213.1552	14.47014	26.15653	0.023243327
213.1552	181.6879	26.15653	22.10749	0.031134368
181.6879	355.4498	22.10749	42.93429	0.059485337
355.4498	416.6729	42.93429	51.76649	0.119069716
416.6729	318.0747	51.76649	38.36007	0.108243049
318.0747	266.2383	38.36007	32.45148	0.068200705
266.2383	254.7701	32.45148	31.1377	0.054101712
254.7701	221.9028	31.1377	27.23805	0.045354773
221.9028	251.356	27.23805	30.74292	0.044694837
251.356	267.8705	30.74292	32.63722	0.053741908
267.8705	245.3975	32.63722	30.04901	0.05253218
245.3975	313.7401	30.04901	37.85538	0.062600757
313.7401	321.2457	37.85538	38.73187	0.080324946
321.2457	327.8861	38.73187	39.51853	0.083941405
327.8861	279.5912	39.51853	33.96546	0.073673545
279.5912	249.197	33.96546	30.49225	0.055779705
249.197	350.0334	30.49225	42.24083	0.072217841
350.0334	517.3854	42.24083	70.15644	0.152100965
517.3854	385.9876	70.15644	47.09545	0.16410173
385.9876	353.0006	47.09545	42.61922	0.108880094
353.0006	303.0723	42.61922	36.62777	0.085913662
303.0723	260.5189	36.62777	31.79839	0.063406863
260.5189	236.8657	31.79839	29.04303	0.049339133
236.8657	291.2403	29.04303	35.2827	0.055769612
291.2403	350.9306	35.2827	42.35487	0.082391296
350.9306	369.1561	42.35487	44.74632	0.10332386
369.1561	381.0528	44.74632	46.39175	0.112148499
381.0528	416.9016	46.39175	51.80326	0.127001188
416.9016	436.1916	51.80326	55.00541	0.145161933
436.1916	409.0051	55.00541	50.55076	0.142501188
409.0051	366.1905	50.55076	44.34694	0.119882706
366.1905	242.298	44.34694	29.68534	0.074794864
242.298	187.9623	29.68534	22.93288	0.037088846
187.9623	257.4381	22.93288	31.44492	0.039853366
257.4381	202.1486	31.44492	24.76742	0.042296361
202.1486	183.0626	24.76742	22.28898	0.029594885
183.0626	182.6507	22.28898	22.23463	0.026650254
182.6507	189.221	22.23463	23.0975	0.027559265
189.221	184.5892	23.0975	22.49011	0.027846211
184.5892	252.7164	22.49011	30.90047	0.038417255
252.7164	239.3823	30.90047	29.34139	0.048272598
239.3823	187.9741	29.34139	22.93443	0.036572239
187.9741	223.5449	22.93443	27.43885	0.033833752

223.5449	166.3379	27.43885	20.06087	0.03050758
166.3379	183.4016	20.06087	22.33368	0.02438932
183.4016	255.0698	22.33368	31.17227	0.038653017
255.0698	279.7806	31.17227	33.98688	0.057042858
279.7806	316.5518	33.98688	38.18231	0.070936649
316.5518	532.5482	38.18231	73.10707	0.147127519
532.5482	639.1164	73.10707	91.52043	0.27563524
639.1164	641.6878	91.52043	91.88102	0.328708306
641.6878	280.2051	91.88102	34.03487	0.178759245
280.2051	279.317	34.03487	33.93445	0.062377319
279.317	409.0625	33.93445	50.55975	0.095565098
409.0625	391.1916	50.55975	47.85148	0.127666534
391.1916	372.3709	47.85148	45.18403	0.116200393
372.3709	381.3889	45.18403	46.43928	0.113210513
381.3889	370.5441	46.43928	44.93468	0.112663875
370.5441	381.0735	44.93468	46.39467	0.112568691
381.0735	408.043	46.39467	50.40051	0.124156111
408.043	435.0155	50.40051	54.80453	0.141777052
435.0155	436.7769	54.80453	55.10564	0.151602109
436.7769	361.278	55.10564	43.69442	0.127351633
361.278	367.5401	43.69442	44.52817	0.105826969
367.5401	297.14	44.52817	35.95183	0.088348103
297.14	193.0181	35.95183	23.59203	0.048589678
193.0181	63.9275	23.59203	7.287471	0.014258514

Valley 6

a1 (m)	a2 (m)	<b>b1</b> (m)	b2 (m)	Volume (km^3)
286.4017	289.9853	34.73529	35.14064	0.066191188
289.9853	260.106	35.14064	31.7511	0.060353224
260.106	315.8784	31.7511	38.10386	0.066304904
315.8784	343.4607	38.10386	41.41499	0.086650739
343.4607	364.2224	41.41499	44.08419	0.099798888
364.2224	346.2522	44.08419	41.76371	0.100580716
346.2522	294.8708	41.76371	35.69417	0.08206049
294.8708	251.4436	35.69417	30.75308	0.059594328
251.4436	312.097	30.75308	37.66506	0.063519328
312.097	362.8754	37.66506	43.90539	0.090932231
362.8754	338.3678	43.90539	40.78605	0.098001618
338.3678	302.9428	40.78605	36.61298	0.08201402
302.9428	240.9232	36.61298	29.52338	0.059192143
240.9232	228.4528	29.52338	28.03494	0.043919328

228.4528	71.88643	28.03494	8.118525	0.01959842
71.88643	244.8512	8.118525	29.98505	0.021972737
244.8512	231.7386	29.98505	28.43069	0.045279841
231.7386	174.6339	28.43069	21.17108	0.033124851
174.6339	259.4982	21.17108	31.68143	0.038033197
259.4982	332.9074	31.68143	40.12149	0.070277445
332.9074	201.3903	40.12149	24.67057	0.058024674
201.3903	134.0606	24.67057	15.72266	0.022717002

Valley 7

a1 (m)	a2 (m)	<b>b1</b> (m)	b2 (m)	Volume (km^3)
180.4711	217.5229	21.94655	26.69903	0.031657588
217.5229	274.1323	26.69903	33.34778	0.048383158
274.1323	295.9043	33.34778	35.81147	0.064772712
295.9043	304.6773	35.81147	36.81136	0.071863597
304.6773	475.4383	36.81136	62.07627	0.123364792
475.4383	343.4274	62.07627	41.41085	0.134931796
343.4274	276.5497	41.41085	33.62145	0.076873305
276.5497	203.3327	33.62145	24.91834	0.046245452
203.3327	196.705	24.91834	24.06905	0.031895963
196.705	267.7806	24.06905	32.62699	0.043328387
267.7806	264.201	32.62699	32.21927	0.056394309
264.201	300.6861	32.21927	36.35543	0.063666219
300.6861	296.7246	36.35543	35.90463	0.071103338
296.7246	425.4073	35.90463	53.19064	0.10505325
425.4073	780.0817	53.19064	104.7121	0.298638447
780.0817	547.621	104.7121	76.00951	0.356127393
547.621	373.3692	76.00951	45.32098	0.171487612
373.3692	514.1	45.32098	69.51594	0.15856915
514.1	722.6779	69.51594	100.8382	0.308949871
722.6779	439.9851	100.8382	55.65813	0.27559528
439.9851	279.9152	55.65813	34.00209	0.105045532
279.9152	289.6211	34.00209	35.09942	0.064634029
289.6211	246.8976	35.09942	30.22434	0.057478551
246.8976	113.4149	30.22434	13.02496	0.027043883

## References

Aarseth, I., (1997). Western Norwegian fjord sediments: age, volume, stratigraphy and role as temporary depository during glacial cycles. *Marine Geology*, 143, pp. 39-53.

Adamia, S., Zakariadze, G., Chkhotua, T., Sadradze, N., and Tsereteli, N., (2011). Geology of the Caucasus: A Review. *Turkish Journal of Earth Sciences*, 20(5).

https://doi.org/10.3906/yer-1005-11

Adamia, S.A., Chkhotua, T., Kekelia, M., Lordkipanidze, M., and Shavishvili, I., (1981). Tectonics of the Caucasus and adjoining regions: implications for the evolution of the Tethys ocean. *Journal of Structural Geology*, 3(4), pp. 437-447.

Aleinikova, A.M., Gaivoron, T.D., Marsheva, N.V., and Mainasheva, G.M., (2020). Risk analysis of mudflows in the Central Caucasus. *IOP Conf. Series: Earth and Environmental Science*, 579 012098.

Alley, R.B., Anandakrishnan, S., Dupont, T.K., and Parizek, B.R., (2004). Ice streams – faster and faster? *Comptes Rendus Physique*, 5, pp. 723-734.

Anderson, R.S., Molnar, P., and Kessler, M.A., (2006). Features of glacial valley profiles simply explained. *Journal of Geophysical Research*, 111.

https://doi.org/10.1029/2005JF000344

Armstrong, T., Roberts, B., and Swithinbank, C., (1973). Illustrated glossary of snow and ice. 2<sup>nd</sup> Edition, Cambridge, Scott Polar Research Institute.

Benn, D.I., and Evans, D.J.A., (2010). Glaciers and Glaciation. 2<sup>nd</sup> Edition, Hodder, London.

Blothe, J.H., and Korup, O., (2013). Millennial lag times in the Himalayan sediment routing system. *Earth and Planetary Science Letters*, 382, pp. 38-46.

http://dx.doi.org/10.1016/j.epsl.2013.08.044

Boulton, G.S., (1979). Processes of glacier erosion on different substrata. *Journal of Glaciology*, 23(89).

Boulton, G.S., and Jones, A.S., (1979). Stability of temperate ice caps and ice sheets resting on beds of deformable sediment. *Journal of Glaciology*, 24(90).

Braithwaite, R.J., and Raper, S.C.B., (2009). Estimating equilibrium-line altitude (ELA) from glacier inventory data. *Annals of Glaciology*, 50(53).

Brook, M.S., Kirkbride, M.P., and Brock, B.W., (2004). Rock strength and development of glacial valley morphology in the Scottish Highlands and northwest Iceland. *Geografiska Annaler*, 86A, pp. 225-234.

Brugnoli, E., Solomina, O., Spaccino, L., and Dolgova, E., (2010). Climate signal in the ring width, density and carbon stable isotopes in pine in central Caucasus. *Geography Environment Sustainability*, 3(4), pp. 4-16.

Buechi, M.W., Rudolf Graf, H., Haldimann, P., Lowick, S.E., and Anselmetti, F.S., (2018). Multiple Quaternary erosion and infill cycles in overdeepened basins of the northern Alpine foreland. *Swiss Journal of Geosciences*, 111, pp. 133-167. <a href="https://doi.org/10.1007/s00015-017-0289-9">https://doi.org/10.1007/s00015-017-0289-9</a>

Chamberlin, T.C., (1888). The rock-scorings of the great ice invasion. US Government Printing Office.

Clarke, B.G., (2018). The engineering properties of glacial tills. *Geotechnical Research*, 5(4), pp. 262-277. <a href="https://doi.org/10.1680/jgere.18.00020">https://doi.org/10.1680/jgere.18.00020</a>

Clarke, G.K., Anslow, F.S., Jarosch, A.H., Radić, V., Menounos, B., Bolch, T., and Berthier, E., (2013). Ice volume and subglacial topography for western Canadian glaciers from mass balance fields, thinning rates, and a bed stress model. *Journal of Climate*, 26, pp. 4282 – 4303. https://doi.org/10.1175/JCLI-D-12-00513.1

Clarke, G.K.C., (2009). Neural networks applied to estimating subglacial topography and glacier volume. *Journal of Climate*, 22, pp. 2146-2160.

Dolgova, E.A., and Solomina, O.N., (2010). First quantitative reconstruction of air temperature for the warm period in the Caucasus based on dendrochronological data. *Doklady Earth Sciences*, 431(1), pp. 371-375.

Dreimanis, A., (1989). Tills: Their genetic terminology and classification. Genetic Classification of Glacigenic Deposits, Blakema, Rotterdam, pp. 17-84.

Fischer, L., Kääb, A., Huggel, C., and Noetzli, J., (2006). Geology, glacier retreat and permafrost degradation as controlling factors of slope instabilities in a high-mountain rock wall: the Monte Rosa east face. *Natural Hazards and Earth System Sciences*, 6, pp. 761-772.

Fitzsimons, S.J., and Veit, H., (2001). Geology and geomorphology of the European Alps and the Southern Alps of New Zealand. *Mountains Research and Development*, 21(4), pp. 340-319. https://doi.org/10.1659/0276-4741(2001)021[0340:GAGOTE]2.0.CO;2

Forbes, J.D., (1846). XIV. Illustrations of the viscous theory of glacier motion.-Part III. *Royal Society*, 136. https://doi.org/10.1098/rstl.1846.0015

Forte, A.M., Whipple, K.X., Bookhagen, B., and Rossi, M.W., (2016). Decoupling of modern shortening rates, climate, and topography in the Caucasus. *Earth and Planetary Science Letters*, 449, pp. 282-294.

Gobejishvili, R., Lomidze, N., and Tielidze, L., (2011). Late Pleistocene (Würmian) glaciations of the Caucasus. *Developments in Quaternary Science*, 15, pp. 141-147. <a href="https://doi.org/10.1016/B978-0-444-53447-7.00012-X">https://doi.org/10.1016/B978-0-444-53447-7.00012-X</a>

Graf, W.L., (1970). The geemorphology of the glacial valley cross section. *Arctic and Alpine Research*, 2(4), pp. 303-312. <a href="https://doi.org/10.1080/00040851.1970.12003589">https://doi.org/10.1080/00040851.1970.12003589</a>

Grotzinger, J., and Jordan, T.H., (2014). Understanding Earth. 7<sup>th</sup> Edition, W.H. Freeman and Company, New York.

Grove, J.M., (2004). The Little Ice Age. 2<sup>nd</sup> Edition, Routledge, London.

Hagg, W., Shahgedanova, M., Mayer, C., Lambrecht, A., and Popovnin, V., (2010). A sensitivity study for water availability in the Northern Caucasus based on climate projections. *Global and Planetary Change*, 73, pp. 161-171.

Hallet, B., (1979). A theoretical model of glacial abrasion. *Journal of Glaciology*, 23(89).

Harbor, J., and Warburton, J., (1993). Relative rates of glacial and nonglacial erosion in alpine environments. *Arctic and Alpine Research*, 25(1), pp. 1-7.

Hay, W.W., Wold, C.N., and Herzog, J.M., (2007). Preliminary mass-balanced 3-D reconstructions of the Alps and surrounding areas during the Miocene. *Lecture Notes in Earth Sciences*, 41, pp. 99-110.

Hinderer, M., (2001). Late Quaternary denudation of the Alps, valley and lake fillings and modern river loads. *Geodinamica Acta*, 14, pp. 231-263.

Hooke, R.L., (1991). Positive feedbacks associated with erosion of glacial circues and overdeepenings. *GSA Bulletin*, 103(8), pp. 1104-1108. <a href="https://doi.org/10.1130/0016-7606(1991)103%3C1104:PFAWEO%3E2.3.CO;2">https://doi.org/10.1130/0016-7606(1991)103%3C1104:PFAWEO%3E2.3.CO;2</a>

Iverson, N.R., (1991). Potential effects of subglacial water-pressure fluctuations on quarrying. *Journal of Glaciology*, 37(125), pp. 27-36.

https://doi.org/10.3189/S0022143000042763

Iverson, N.R., (2002). Processes of glacial erosion. *Modern and Past Glacial Environments*, pp. 131-145. https://doi.org/10.1016/B978-075064226-2/50008-8

Jaboyedoff, M., and Derron, M-H., (2005). A new method to estimate the infilling of alluvial sediment of glacial valleys using a sloping local base level. *Supplementi di Geografica Fisica e Dinamica Quaternaria*, 28, pp. 37-46.

Jordan, P., (2010). Analysis of overdeepened valleys using the digital elevation model of the bedrock surface of Northern Switzerland. *Swiss Journal of Geosciences*, 103, pp. 375-384. https://doi.org/10.1007/s00015-010-0043-z

Karavaev, V.A., and Seminozhenko, S.S., (2019). Terrain morphometry and mudflow features in the northern slope of the Great Caucasus. *Doklady Earth Sciences*, 487(4), pp. 935-938.

Kirkbride, M., and Spedding, N., (1996). The influence of englacial drainage on sediment-transport pathways and till texture of temperate valley glaciers. *Annals of Glaciology*, 22, pp. 160-166. <a href="https://doi.org/10.3189/1996AoG22-1-160-166">https://doi.org/10.3189/1996AoG22-1-160-166</a>

Knight, J., and Harrison, S., (2016). Mountain glacial and paraglacial environments under global climate change: lessons from the past, future directions and policy implications. *Geografiska Annaler: Series A, Physical Geography*, 96, pp. 245-264. <a href="https://doi.org/10.1111/geoa.12051">https://doi.org/10.1111/geoa.12051</a>

Koronovskii, N.V., (2016). Stages of recent volcanism and problems of their correlation with landscape formation in the central Caucasus. *Geotectonics*, 50, pp. 491-508.

Kos, A., Amann, F., Strozzi, T., Delaloye, R., von Ruette, J., and Springman, S., (2016). Contemporary glacier retreat triggers a rapid landslide response, Great Aletsch Glacier, Switzerland. *Geophysical Research Letters*, 43(24), pp. 12466 – 12474. https://doi.org/10.1002/2016GL071708

Kutsov, S., Shahgedanova, M., Mikhalenko, V., Ginot, P., Lavrentiev, L., and Kemp, S., (2013). High-resolution provenance of desert dust deposited on Mt. Elbrus, Caucasus in 2009-2012 using snow pit and firn core records. *The Cryosphere*, 7, pp. 1481-1498.

Liebl, M., Robl, J., Egholm, D.L., Prasicek, G., Stüwe, K., Gradwohl, G., and Hergarten, S., (2021). Topographic signatures of progressive glacial landscape transformation. *Earth Surface Processes and Landforms*, 46, pp. 1964-1980. <a href="https://doi.org/10.1002/esp.5139">https://doi.org/10.1002/esp.5139</a>

Linsbauer, A., Paul, F., and Haeberli, W., (2012). Modelling glacier thickness distribution and bed topography over entire mountain ranges with GlabTop: Application of a fast and robust approach. *Journal of Geophysical Research*, 117. https://doi.org/10.1029/2011JF002313

Malneva, I.V., and Kononova, N.K., (2011), Assessment of a mudflow hazard on the Black Sea coast of Caucasus and in the adjacent mountainous areas. *Italian Journal of Engineering Geology and Environment*, pp. 965-971. <a href="https://doi.org/10.4408/IJEGE.2011-03.B-105">https://doi.org/10.4408/IJEGE.2011-03.B-105</a>

Margat, J., and van der Gun, J., (2013), Groundwater Around the World: A Geographic Synopsis, Taylor and Francis Ltd., London.

Matskovsky, V.V., Dolgova, E.A., and Solomina, O.N., (2010). Terbeda Valley runoff variability (AS 1850-2005) based on tree-ring reconstruction. *IOP Conference Series: Earth and Environmental Science*, 9.

Menzies, J., van der Meer, J.J.M., and Rose, J., (2006). Till – as a glacial 'tectomict', its internal architecture, and the development of a 'typing' method for till differentiation. *Geomorphology*, 75, pp. 172-200.

Mey, J., Scherler, D., Zeilinger, G., and Strecker, M.R., (2015). Estimating the fill thickness and bedrock topography in intermontane valleys and artificial neural networks. *Journal of Geophysical Research: Earth Surface*, 120, pp. 1301-1320.

https://doi.org/10.1002/2014JF003270

Mikhalenko, V., Sokratov, S., Kutuzov, S., Ginot, P., Legrand, M., Preunkert, S., Lavrentiev, L., Kozachek, A., Ekaykin, A., Faïn, X., Lim, S., Schotterer, U., Lipenkov, V., and Toropov, P., (2015). Investigation of a deep ice core from the Elbrus western plateau, the Caucasus, Russia. *The Cryosphere*, 9, pp. 2253-2270. https://doi.org/10.5194/tc-9-2253-2015

Montgomery, D.R., (2002). Valley formation by fluvial and glacial erosion. *Geology*, 30(11), pp. 1047-1050.

Moser, J., Mauvilly, J., Koiava, K., Gamkrelidze, I., Enna, N., Lavrishev, V., and Kalberguenova, V., (2022). Tectonics in the Greater Caucasus (Georgia – Russia): From an intracontinental rifted basin to a doubly verging fold-and-thrust belt. *Marine and Petroleum Geology*, 140. https://doi.org/10.1016/j.marpetgeo.2022.105630

Nabney, I., (2025). Netlab (https://www.mathworks.com/matlabcentral/fileexchange/2654-netlab), MATLAB Central File Exchange.

Ochs, S.I., Monegato, G., and Reitner, J.M., (2022). Chapter 39 – The Alps: glacial landforms prior to the Last Glacial Maximum. *European Glacial Landscapes*, pp. 283-294. https://doi.org/10.1016/B978-0-12-823498-3.00008-X

Oliva, M., Mercier, D., Fernandez, J.R., and McColl, S.T., (2019). Paraglacial processes in recently deglaciated environments. *Land Degradation & Development*, 31(15), 1871-1876. https://doi.org/10.1002/ldr.3283

Otto, J.C., Goetz, J., and Schrott, L., (2008). Sediment storage in Alpine sedimentary systems – quantification and scaling issues. *Sediment Dynamics in Changing Environments* (*Proceedings of a symposium held in Christchurch, New Zealand, Dec 2008*).

Otto, J-C., Schrott, L., Jaboyedoff, M., and Dikau, R., (2009). Quantifying sediment storage in a high alpine valley (Turtmanntal, Switzerland). *Earth Surface Processes and Landforms*, 34, pp. 1726-1742. <a href="https://doi.org/10.1002/esp.1856">https://doi.org/10.1002/esp.1856</a>

Patton, H., Swift, D.A., Clark, C.D., Livingstone, S.J., and Cook, S.J., (2016). Distribution and characteristics of overdeepenings beneath the Greenland and Antarctic ice sheets: Implications for overdeepening origin and evolution. *Quaternary Science Reviews*, 148, pp. 128-145. http://dx.doi.org/10.1016/j.quascirev.2016.07.012

Pomper, J., Salcher, B.C., Eichkitz, C., Prasicek, G., Lang, A., Lindner, M., and Götz, J., (2017). The glacially overdeepened trough of the Salzach Valley, Austria: Bedrock geometry and sedimentary fill of a major Alpine subglacial basin. *Geomorphology*, 295, pp. 147-158. http://dx.doi.org/10.1016/j.geomorph.2017.07.009

Popovnin, V.V., (1999). Annual mass-balance series of a temperate glacier in the Caucasus, reconstructed from an ice core. *Geografiska Annaler: Series A, Physical Geography*, 81(4), pp. 713-724. <a href="https://doi.org/10.1111/1468-0459.00099">https://doi.org/10.1111/1468-0459.00099</a>

Preusser, F., Reitner, J.M., and Schlüchter, C., (2010), Distribution, geometry, age and origin of overdeepened valleys and basins in the Alps and their foreland. *Swiss Journal of Geoscience*, 103, pp. 407-426. https://doi.org/10.1007/s00015-010-0044-y

Robin, G. de Q., (1976). Is the basal ice of a temperate glacier at the pressure melting point? *Journal of Glaciology*, 16(74), pp. 183-196. https://doi.org/10.3189/S002214300003152X

Rubensdotter, L., and Rosqvist, G., (2009). Influence of geomorphological setting, fluvial-, glaciofluvial- and mass-movement processes on sedimentation in alpine lakes. *The Holocene*, 19(4), pp. 665-678. https://doi.org/10.1177/0959683609104042

Schlunegger, F., and Norton, K.P., (2013). Water versus ice: The competing roles of modern climate and Pleistocene glacial erosion in the Central Alps of Switzerland. *Tectonophysics*, 602, pp. 370-381. http://dx.doi.org/10.1016/j.tecto.2013.03.027

Schrott, L., Hufschmidt, G., Hankammer, M., Hoffmann, T., and Dikau, R., (2003). Spatial distribution of sediment storage types and quantification of valley dill deposits in an alpine basin, Reintal, Bavarian Alps, Germany. *Geomorphology*, 55, pp. 45-63. https://doi.org/10.1016/S0169-555X(03)00131-4

Schwanghart, W., and Scherler, D., (2014). Short Communication: TopoToolbox 2 – MATLAB-Based Software for Topographic Analysis and Modeling in Earth Surface Sciences. *Earth Surface Dynamics*, 2(1), pp. 1-7. https://doi.org/10.5194/esurf-2-1-2014.

Schwenk, M.A., Schläfli, P., Bandou, D., Gribenski, N., Douillet, G.A., and Schlunegger, F., (2022). From glacial erosion to basin overfill: a 240m-thick overdeepening-fill sequence in Bern, Switzerland. *Scientific Drilling*, 30, pp. 17-42.

Seinova, I.B., Sidorova, T.L., and Chernomorets, S.S., (2007). Processes of debris flow formation and the dynamics of glaciers in the Central Caucasus. *Debris-Flow Hazards Mitigation: Mechanics, Prediction, and Assessment*, Chen & Major.

Serebryanny, L.R., Golodkovskaya, N.A., & Orlov, A.V., (1985). Glacier fluctuations and moraine accumulation processes in the Central Caucasus. *Nauka*, pp. 216.

Shahgedanova, M., Hagg, W., Hassell, D., Stokes, C.R., and Popovnin, V., (2009), Climate change, glacier retreat, and water availability in the Caucasus region. *Threats to Global Water Security*, pp. 131-143.

Shahgedanova, M., Nosenko, G., Kutuzov, S., Rototaeva, O., and Khromova, T., (2014). Deglaciation of the Caucasus Mountains, Russia/Georgia, in the 21<sup>st</sup> century observed with ASTER satellite imagery and aerial photography. *The Cryosphere*, 8, pp. 2367-2379. https://doi.org/10.5194/tc-8-2367-2014

Smith, M.J., Rose, J., and Booth, S., (2006). Geomorphological mapping of glacial landforms from remotely sensed data: An evaluation of the principal data sources and an assessment of their quality. *Geomorphology*, 76, pp. 148-165.

Solomina, O.N., (2000). Retreat of mountain glaciers of northern Eurasia since the Little Ice Age maximum. *Annals of Glaciology*, 31. https://doi.org/10.3189/172756400781820499

Solomina, O.N., Bradley, R.S., Jomelli, V., Geirsdottir, A., Kaufman, D.S., Koch, J., McKay, N.P., Masiokas, M., Miller, G., Nesje, A., Nicolussi, K., Owen, L.A., Putnam, A.E., Wanner, H., Wiles, G., and Yang, B., (2016). Glaciers fluctuations during the past 2000 years. *Quaternary Science Reviews*, 149, pp. 61-90.

http://dx.doi.org/10.1016/j.quascirev.2016.04.008

Solomina, O.N., Alexandrovskiy, A.L., Zazovskaya, E.P., Konstantinov, E.A., Shishkov, V.A., Kuderina, T.M., and Bushueva, I.S., (2022). Late-Holocene advances of the Greater Azau Glacier (Elbrus area, Northern Caucasus) revealed by 14C dating of palaeosols. *The Holocene*, 32(5), pp. 468-481. <a href="https://doi.org/10.1177/09596836221074029">https://doi.org/10.1177/09596836221074029</a>

Solomina, O.N., Jomelli, V., and Bushueva, I.S., (2024). Holocene glacier variations in the Northern Caucasus, Russia. *European Glacial Landscapes: The Holocene*, pp. 353-365. https://doi.org/10.1016/B978-0-323-99712-6.00005-2

Stokes, C.R., Gurney, S.D., Shahgedanova, M., and Popovnin, V., (2006). Late-20<sup>th</sup>-century changes in glacier extent in the Caucasus Mountains, Russia/Georgia. *Journal of Glaciology*, 52(176), pp. 99-109.

Stokes, C.R., Popovnin, V., Aleynikov, A., Gurney, S.D., and Shahgedanova, M., (2007). Recent glacier retreat in the Caucasus Mountains, Russia, and associated increase in supraglacial debris cover and supra-/proglacial lake development. *Annals of Glaciology*, 46, pp. 195-203. <a href="https://doi.org/10.3189/172756407782871468">https://doi.org/10.3189/172756407782871468</a>

Straumann, R.K., and Korup, O., (2009), Quantifying postglacial sediment storage at the mountain-belt scale. *Geology*, 37(12), pp. 1079-1082. <a href="https://doi.org/10.1130/G30113A.1">https://doi.org/10.1130/G30113A.1</a>

Sutherland, J.L., Carrivick, J.L., Gandy, N., Shulmeister, J., Quincey, D.J., and Cornford, S.L., (2020). Proglacial lakes control glacier geometry and behaviour during recession. *Geophysical Research Letters*, 47. https://doi.org/10.1029/2020GL088865

Svensson, H., (1959). Is the cross-section of a glacial valley a parabola? *Journal of Glaciology*, 3(25), pp. 362-363. https://doi.org/10.3189/S0022143000017032

Syvitski, J., Andrews, J.T., Schafer, C.T., and Stravers, J.A., (2022). Sediment fill of Baffin Island fjords: Architecture and rates. *Quaternary Science Reviews*, 284. https://doi.org/10.1016/j.quascirev.2022.107474

Tashilova, A.A., Ashabokov, B.A., Kesheva, L.A., and Teunova, N.V., (2019). Analysis of climate change in the Caucasus region: End of the 20<sup>th</sup>-beginning of the 21<sup>st</sup> century. *Climate*, 7(11). <a href="https://doi.org/10.3390/cli7010011">https://doi.org/10.3390/cli7010011</a>

The MathWorks Inc., (2024). MATLAB version: 24.2.0.2712019 (R2024b), Natick, Massachusetts. https://www.mathworks.com

Tielidze, L.G., (2016). Glacier change over the last century, Caucasus Mountains, Georgia, observed from old topographical maps, Landsat and ASTER satellite imagery. *The Cryosphere*, 10, pp. 713-725. <a href="https://doi.org/10.5194/tc-10-713-2016">https://doi.org/10.5194/tc-10-713-2016</a>

Tielidze, L.G., (2017). Late Pleistocene and Holocene glaciation. *Glaciers of Georgia, Geography of the Physical Environment*. <a href="https://doi.org/10.1007/978-3-319-50571-8\_6">https://doi.org/10.1007/978-3-319-50571-8\_6</a>

Tielidze, L.G., Gadrani, L., and Kumladze, R., (2015). A one century record of changes at Nenskra and Nakra River basins glaciers, Caucasus Mountains, Georgia. *Natural Science*, 7, pp. 151-157. <a href="http://dx.doi.org/10.4236/ns.2015.73017">http://dx.doi.org/10.4236/ns.2015.73017</a>

Tielidze, L.G., Nosenko, G.A., Khromova, T.E., and Paul, F., (2022). Strong acceleration of glacier area loss in the Greater Caucasus between 2000 and 2020. *The Crysophere*, 16, pp. 489-504. https://doi.org/10.5194/tc-16-489-2022

Tielidze, L.G., Mackintosh, A.N., Gavashelishvili, A., Gadrani, L., Nadaraia, A., and Elashvili, M., (2025). Post-Little Ice Age equilibrium-line altitude and temperature changes in the Greater Caucasus based on small glaciers. *Remote Sensing*, 17(1486). https://doi.org/10.3390/rs17091486

Toropov, P.A., Aleshina, M.A., and Grachev, A.M., (2019). Large-scale climatic factors driving glacier recession in the Greater Caucasus, 20<sup>th</sup>-21<sup>st</sup> century. *International Journal of Climatology*, 2019, pp. 1-18. <a href="https://doi.org/10.1002/joc.6101">https://doi.org/10.1002/joc.6101</a>

Tsypelnkov, A., Vanmaercke, M., Collins, A.L., Kharchenko, S., and Golosov. V., (2021), Elucidating suspended sediment dynamics in a glacierized catchment after an exceptional erosion event: The Djankuat catchment, Caucasus Mountains, Russia. *Catena*, 203. <a href="https://doi.org/10.1016/j.catena.2021.105285">https://doi.org/10.1016/j.catena.2021.105285</a>

Vezzoli, G., Garzanti, E., Vincent, S.J., Andò, S., Carter, A., and Resentini, A., (2014). Tracking sediment provenance and erosional evolution of the western Greater Caucasus. *Earth Surface Processes and Landforms*, 39, pp. 1101-1114. https://doi.org/10.1002/esp.3567

Vezzoli, G., Garzanti, E., Limonata, M., and Radeff, G., (2020). Focused erosion at the core of the Greater Caucasus: Sediment generation and dispersal from Mt. Elbrus to the Caspian Sea. *Earth Science Reviews*, 200. https://doi.org/10.1016/j.earscirev.2019.102987

Walczak, S., and Cerpa, N., (2003). Artificial neural networks. *Enclycopedia of Physical Science and Technology, 3<sup>rd</sup> Ed,* pp. 603-645. <a href="https://doi.org/10.1016/B0-12-227410-5/00837-1">https://doi.org/10.1016/B0-12-227410-5/00837-1</a>

Walker, J.D., and Geissman, J.W., (2022). Geological Time Scale v. 6.0. *Geological Society of America*. <a href="https://doi.org/10.1130/2022.CTS006C">https://doi.org/10.1130/2022.CTS006C</a>.

Wanner, H., Beer, J., Bütikofer, J., Crowley, T.J., Cubasch, U., Flückiger, J., Goosse, H., Grosjean, M., Joos, F., Kaplan, J.O., Küttel, M., Müller, S.A., Prentice, C., Solomina, O., Stocker, T.F., Tarasov, P., Wagner, M., and Widmann, M., (2008). Mid- to Late Holocene climate change: An overview. *Quaternary Science Reviews*, 27, pp. 1791-1828. https://doi.org/10.1016/j.quascirev.2008.06.013

Watts, A.B., (2023). Isostasy and flexure of the lithosphere. 2<sup>nd</sup> Edition, Cambridge University Press.

Whitehouse, P.L., (2018). Glacial isostatic adjustment modelling: historical perspectives, recent advances, and future directions. *Earth Surface Dynamics*, 6, pp. 401-429. https://doi.org/10.5194/esurf-6-401-2018

Whiteman, C.A., (2002). Processes of terrestrial glacial deposition. *Modern and Past Glacial Environments*, pp. 171-181. https://doi.org/10.1016/B978-075064226-2/50010-6

Wilson, D.S., Jamieson, S.S.R., Barrett, P.J., Leitchenkov, G., Gohl, K., and Larter, R.D., (2012). Antarctic topography at the Eocene-Oligocene boundary. *Palaeogeography, Palaeoclimatology, Palaeoecology*, 335-336, pp. 24-34. https://doi.org/10.1016/j.palaeo.2011.05.028

WWF - Caucasus., (2006). Climate Zones of the Caucasus Ecoregion. https://www.grida.no/resources/7894. Accessed on 14/10/2025

Zimmer, P.D., and Gabet, E.J., (2018). Assessing glacial modification of bedrock valleys using a novel approach. *Geomorphology*, 318, pp. 336-347.

https://doi.org/10.1016/j.geomorph.2018.06.021